GRANT
IN-18-CR
84448
P. 133

SLEW MANEUVERS OF SPACECRAFT CONTROL LABORATORY EXPERIMENT (SCOLE)

By

Yogendra P. Kakad

Associate Professor
Dept. of Electrical Engineering
University of North Carolina at Charlotte
Charlotte, NC 28223

Final Report for NASA Grant NAG-1-535

Spacecraft Control Branch
NASA Langley Research Center
Hampton, Virginia 23665-5225

April 1992

(NASA-CR-190228) SLEW MANEUVERS OF SPACECRAFT CONTROL LABORATORY EXPERIMENT (SCOLE) Final Report (North Carolina Univ.) 133 p CSCL 22B

N92-24198

Unclas

G3/18 0084448

Table of Contents

SUMMARY 1
INTRODUCTION 2
LIST OF SYMBOLS 4
ANALYTICS 7
NUMERICAL DATA 46
TABLE 1 48
REFERENCES 52
APPENDIX I 58
APPENDIX II 59
APPENDIX III 61

INTENTIONALLY BLANK

PRECEDING PAGE BLANK NOT FILMED

SLEW MANEUVERS OF SPACECRAFT CONTROL LABORATORY EXPERIMENT (SCOLE)

Y. P. Kakad

Dept. of Electrical Engineering
University of North Carolina at Charlotte
Charlotte, NC 28223

SUMMARY

This is the final report on the dynamics and control of slew maneuvers of the Spacecraft COntrol Laboratory Experiment (SCOLE) test facility initiated and developed by the Spacecraft Controls Branch at NASA Langley Research Center. The report includes the work done under grant period from November 1st., 1984 through April 30th, 1992. Although the final experimental work to be performed on the test facility is scheduled to be done in May 1992, the report includes all theoretical and numerical work upto the closing date of the grant. A supplementary report will be issued on the experimental work after the remaining work is completed. In the appendix, two current publications on the grant work are included and the other publications based on the grant work are cited in the references.

The report documents the basic dynamical equation derivations for an arbitrary large angle slew maneuver as well as the basic decentralized slew maneuver control algorithm.

The dynamics and control of slew maneuver of NASA Spacecraft COntrol Laboratory Experiment (SCOLE) test facility are developed in terms of an arbitrary maneuver about any given axis. The set of dynamical equations incorporate rigid-body slew maneuver and three-dimensional vibrations of the complete assembly comprising the rigid shuttle, the flexible beam, and the reflector with an offset mass. The analysis also includes kinematic nonlinearities of the entire assembly during the maneuver and the dynamics of the interaction between the rigid shuttle and the flexible appendage. The final set of dynamical equations obtained for slewing maneuvers are highly nonlinear and coupled in terms of the flexible modes and the rigid-body modes.

The equations are further simplified and evaluated numerically to include the first ten flexible modes and the SCOLE data to yield a model for designing control systems to perform slew maneuvers.

The control problem formulation incorporates the nonlinear dynamical equations and is expressed in terms of a two-point boundary value problem utilizing a quadratic type of performance index.

The two-point boundary value problem is solved as hierarchical control problem with the overall system being split in terms of two subsystems, namely the slewing of the entire assembly and the vibration suppression of the flexible antenna. The coupling variables between the two dynamical subsystems are identified and these two subsystems for control purposes are treated

independently in parallel at the first level. Then the state-space trajectory of the combined problem is optimized at the second level.

1. INTRODUCTION

The primary control objective of the Spacecraft Control Laboratory Experiment (SCOLE) is to direct the RF Line-Of-Sight (LOS) of the antenna-like configuration towards a fixed target under the conditions of minimum time and limited control authority [1]. This problem of directing the LOS of antenna- like configuration involves both the slewing maneuver of the entire assembly and the vibration suppression of the flexible antenna-like beam. The study of ordinary rigid-body slew maneuvers has received considerable attention in the literature [2,3] due to the fact that any arbitrary large-angle slew maneuver involves kinematic nonlinearities. This is further complicated in the case of SCOLE by virtue of a flexible appendage deployed from the rigid space shuttle. The dynamics of arbitrary large-angle slew maneuvers of SCOLE model are derived in this report as a set of coupled equations with the rigid-body motions including the nonlinear kinematics and the vibratory equations of the flexible appendage.

The dynamical equations of slewing maneuvers of this large flexible spacecraft are developed by writing the total kinetic and potential energy expressions for the entire system. The energy expressions are further utilized in formulating Lagrange's equations which are expressed in terms of non-generalized co-ordinates using an inertial co-ordinate system and a body-fixed co-ordinate system at the point of attachment of the flexible beam to the shuttle. The generic model used for this analysis consists of a distributed parameter beam with two end masses. The three dimensional linear vibration analysis of this free-free beam model with end masses [4] is incorporated together with rigid-slewing maneuver dynamics which are written in terms of four Euler parameters [5] and angular

rotation about an arbitrary axis of rotation to yield the final set of highly nonlinear and coupled equations. In the derivation of the equations, it is assumed that the vibratory analysis is for small motions. These nonlinear and coupled dynamical equations are used in this article to study the slew maneuver control in terms of a hierarchical feedback control scheme.

The control problem of slewing maneuvers of this large flexible spacecraft is developed by using the two-point boundary value problem in terms of the rigid-body slewing and the vibration suppression of the flexible appendage as two separate dynamical subsystems. A decentralized optimal control scheme is utilized in order to solve individual boundary-value problem for each of the two subsystems by defining their state variable models and incorporating the coupling variables between the two subsystems in these models. Also, the boundary conditions of the overall system are reworked in terms of boundary conditions of each subsystem. A quadratic performance index is utilized for the overall system and is subsequently expressed in terms of a sum of two individual performance indices of the subsystems.

The basic algorithm for obtaining an optimal closed-loop state feedback sceme involves using a trajectory in terms of a vector of Lagrange multipliers as an initial guess at level two. This is used at level one in quasilinearization application.

The two-point boundary value problem for each subsystem is solved at level one by using a quasilinearization technique as a trajectory optimization problem. In the quasilinearization procedure, starting from an initial guessed state trajectory, successive linearizations are performed of state equations in such a way that the final solution of the state trajectory is within an acceptable degree subject to boundary conditions. The state vector definition at this level is an augmented state vector which includes both system states and costates.

These optimum solutions of the system trajectories are utilized at level two to yield the updated trajectory of the vector of Lagrange multipliers of the overall system to be used for quasilinearization process at level one. The basic steps of the algorithm are repeated to optimize this second level trajectory with respect to prespecified error criterion to obtain an optimal feedback law.

2. LIST OF SYMBOLS

$\underline{a}(z)$ Position vector of mass element on the beam from the point of attachment

B Damping matrix

C Inertial frame to body-fixed frame transformation

$\underline{c}$ Position vector from the point of attachment to the mass center of the beam

D Mass density of the beam

$\underline{d}(z,t)$ Displacement vector of mass element in the body-fixed frame

E Modulus of Elasticity

$\underline{F}_o(t)$ Force applied at the orbiter mass center

$\underline{F}_2(t)$ Force applied at the reflector mass center

$\underline{G}_o(t)$ Moment applied about the orbiter mass center

G_ψ Modulus of rigidity for the beam

I Beam cross section moment of inertia

I_x Beam cross section moment of inertia, roll bending

I_y Beam cross section moment of inertia, pitch bending

I_o Equivalent mass moment of inertia

I_1 Mass moment of inertia matrix of the shuttle

I_2 Mass moment of inertia matrix of the reflector

J Mass moment of inertia matrix of the beam

K Stiffness matrix

L The Length of the beam

M Angular velocity vector transformation

M_ψ Effective moment applied at the reflector c.g.

m Total mass of the flexible beam

m_1 Mass of the orbiter

m_2 Mass of the reflector

N The total number of subsystems

n The maximum number of modes considered

$\underline{Q}$ The generalized force vector

q_i Generalized coordinates

$\underline{R}$ Position vector of the mass center of the orbiter in the inertial frame

$\underline{r}$ Position vector from the orbiter mass center to the point of attachment

r_x x co-ordinate of the reflector mass center in the body-fixed frame

r_y y co-ordinate of the reflector mass center in the body-fixed frame

T Total Kinetic Energy

U Total Potential Energy

$u_x(z,t)$ The beam deflection in x direction referred to the body-fixed frame

$u_y(z,t)$ The beam deflection in y direction referred to the body-fixed frame

$u_\psi(z,t)$ The torsional deflection about z axis in the body-fixed frame

$\underline{u_i}$ Control vector of ith system

$\underline{V}$ Velocity vector of the mass center of the orbiter in the body-fixed frame

$\underline{V_o}$ Velocity vector of the point of attachment in the body-fixed frame

$\underline{x_i}$ State vector of ith system

$\underline{z_i}$ Vector of interconnecting variables

ρ Mass per unit length of the flexible beam

$\underline{\gamma}$ Vector representing the axis rotation during the slew maneuver

ϕ_{xi} i th Eigenfunction corresponding to u_x

ϕ_{yi} i th Eigenfunction corresponding to u_y

$\phi_{\psi i}$ i th Eigenfunction corrsponding to u_ψ

$\underline{\theta}$ The attitude of the orbiter in the inertial frame

ξ Slew Angle

$\underline{\omega}$ The angular velocity of the orbiter in the inertial frame

$\underline{\Omega}$ The angular velocity of the reflector in the inertial frame

$\underline{\varepsilon}$ Vector of Euler parameters

$\delta(z-z_j)$ Direc delta function

$\Phi(\underline{\lambda})$ Dual functional for two-point boundary value problem

$\underline{\lambda}$ Vector of Lagrange multipliers

ζ Damping ratio

3. ANALYTICS

Co-ordinate Systems

The motion of SCOLE assembly when considered as a rigid body in space has six dynamic degrees of freedom: three of these define the location of the mass center, and three define the orientation (attitude) of the body. The motion of this rigid body is goverened by newtonion laws of motion expressed in terms of changes in linear momentum and angular momentum. These relationships are valid only when the axes along which the motion is resolved are an inertial frame of reference [9,10]. To define the orientation of the orbiter in space, a set of orthogonal axes fixed in the body is utilized. Then the attitude of the orbiter is defined in terms of the angles $(\theta_1,\theta_2,\theta_3)$ between the body- fixed axes and the inertial co-ordinate axes. The body-fixed frame origin is located at the point of attachment of the flexible appendage with the rigid shuttle for this analysis (Fig. 1).

The transformation from the inertial frame to the body-fixed frame is given by the matrix, C as developed in figure 2 where if $\vec{i}, \vec{j}, \vec{k}$ represent the dexteral set of orthogonal unit vectors fixed in the body- fixed frame and θ_1 is the rotation about $\vec{i}$, θ_2 is the rotation about $\vec{j}$ and θ_3 is the rotation about $\vec{k}$. These rotations are carried out successively as shown in figure 1 and the matrix C is given as

$$C = \begin{bmatrix} \cos\theta_3 & \sin\theta_3 & 0 \\ -\sin\theta_3 & \cos\theta_3 & 0 \\ 0 & 0 & 1 \end{bmatrix} \begin{bmatrix} \cos\theta_2 & 0 & -\sin\theta_2 \\ 0 & 1 & 0 \\ \sin\theta_2 & 0 & \cos\theta_2 \end{bmatrix} \begin{bmatrix} 1 & 0 & 0 \\ 0 & \cos\theta_1 & \sin\theta_1 \\ 0 & -\sin\theta_1 & \cos\theta_1 \end{bmatrix} \qquad (1)$$

Thus C^T is obtained as

$$C^T = \begin{bmatrix} \cos\theta_2\cos\theta_3 & -\cos\theta_2\sin\theta_3 & \sin\theta_2 \\ \sin\theta_1\sin\theta_2\cos\theta_3+\sin\theta_3\cos\theta_1 & -\sin\theta_1\sin\theta_2\sin\theta_3+\cos\theta_3\cos\theta_1 & -\sin\theta_1\cos\theta_2 \\ -\cos\theta_1\sin\theta_2\cos\theta_3+\sin\theta_3\sin\theta_1 & \cos\theta_1\sin\theta_2\sin\theta_3+\cos\theta_3\sin\theta_1 & \cos\theta_1\cos\theta_2 \end{bmatrix}$$

(2)

In order to completely define the attitude (orientation), it is needed to relate the rotation angles θ_1, θ_2, and θ_3 to the angular velocity components (ω_1, ω_2, ω_3) of the orbiter. One way of obtaining the required relations is via body-three angles method [5] which was utilized in developing C matrix in equation (1) and these relations are

$$\begin{aligned} \dot{\theta}_1 &= (\omega_1 \cos\theta_3 - \omega_2 \sin\theta_3)/\cos\theta_2 \\ \dot{\theta}_2 &= (\omega_1 \sin\theta_3 + \omega_2 \cos\theta_3) \\ \dot{\theta}_3 &= (-\omega_1 \cos\theta_3 + \omega_2 \sin\theta_3)\tan\theta_2 + \omega_3 \end{aligned} \tag{3}$$

Thus, the angular velocity of the orbiter can be obtained in the inertial frame by means of the following transformation

$$\underline{\omega} = M^T \underline{\dot{\theta}} \tag{4}$$

where the transformation M^T is given as

$$M^T = \begin{bmatrix} \cos\theta_2 \cos\theta_3 & \sin\theta_3 & 0 \\ -\cos\theta_2 \sin\theta_3 & \cos\theta_3 & 0 \\ \sin\theta_2 & 0 & 1 \end{bmatrix} \tag{5}$$

Although the body-three angles method is used here for obtaining the transformations C and M, there are three other methods which can be used to obtain the same transformations. A detailed discussion of all the methods is given in reference [5] and a summary of the transformations using the remaining three methods is given in the Appendix.

Kinetic Energy

If the position vector of the mass center of the orbiter in the inertial frame (Fig. 3), $\underline{R}$, is given as

$$\underline{R} = \begin{bmatrix} R_X \\ R_Y \\ R_Z \end{bmatrix} \tag{6}$$

then the velocity of the mass center in the inertial frame is

$$\underline{V}^I(t) = \begin{bmatrix} \dot{R}_X \\ \dot{R}_Y \\ \dot{R}_Z \end{bmatrix} \tag{7}$$

This velocity can be transformed in the body-fixed frame as

$$\underline{V}(t) = C \begin{bmatrix} \dot{R}_X \\ \dot{R}_Y \\ \dot{R}_Z \end{bmatrix} \tag{8}$$

The velocity of the point of attachment in the body-fixed frame is

$$\underline{V}_o = \underline{V} + \underline{\omega} \times \underline{r} \tag{9}$$

where $\underline{r}$ is the vector from orbiter mass center to the point of attachment.

Defining the position vector (Fig. 4), $\underline{a}$, of a mass element on the beam from the point of attachment (origin of the body-fixed frame) before deformation as

$$\underline{a} = \begin{bmatrix} 0 \\ 0 \\ z \end{bmatrix} \tag{10}$$

and the displacement vector of this mass element as

$$\underline{d}(z,t) = \begin{bmatrix} u_x(z,t) \\ u_y(z,t) \\ 0 \end{bmatrix} \tag{11}$$

the position vector after deflection is given as $\underline{a}+\underline{d}$. The kinetic energy in the

beam [6] is

$$T_1 = (1/2)\, m\underline{V}_o^T\underline{V}_o + (1/2)\,\underline{\omega}^T[J]\underline{\omega} - m\underline{V}o^T[\tilde{\underline{c}}]\underline{\omega} + (1/2)\int \underline{\dot{d}}^T\underline{\dot{d}}dm$$

$$+ \underline{V}_o^T\int \underline{\dot{d}}dm + \underline{\omega}^T\int \tilde{\underline{a}}\underline{\dot{d}}dm + (1/2)\int \begin{bmatrix} \dot{u}_x' & \dot{u}_y' & \dot{u}_\psi \end{bmatrix} dl \begin{bmatrix} \dot{u}_x' \\ \dot{u}_y' \\ \dot{u}_\psi \end{bmatrix} \qquad (12)$$

where the vector $\underline{c}$ is from the point of attachment to the mass center of the beam and if it is assumed that the beam is a thin rod, then it is given as

$$\underline{c} = \begin{bmatrix} c_x \\ c_y \\ c_z \end{bmatrix}$$

$$= (1/m)\int \underline{a}dm = \begin{bmatrix} 0 \\ 0 \\ -L/2 \end{bmatrix} \qquad (13)$$

and using the skew symmetric form for the vector cross product for any two vectors $\underline{c}$ and $\underline{\omega}$ (in the same reference frame) as

$$\underline{c}\times\underline{\omega} = [\,\tilde{\underline{c}}\,]\,\underline{\omega}$$

$$\tilde{\underline{c}} = \begin{bmatrix} 0 & -c_z & c_y \\ c_z & 0 & -c_x \\ -c_y & c_x & 0 \end{bmatrix} \qquad (14)$$

also, the moment of inertia matrix is given as

$$J = (1/3)\,\rho L^3 \begin{bmatrix} 1 & 0 & 0 \\ 0 & 1 & 0 \\ 0 & 0 & 0 \end{bmatrix} \qquad (15)$$

where ρ is the mass per unit length of the beam. The last term in the equation (12) corresponding to torsional motion is given as

$$(1/2)\int \begin{bmatrix} \dot{u}_x' & \dot{u}_y' & \dot{u}_\psi \end{bmatrix} dl \begin{bmatrix} \dot{u}_x' \\ \dot{u}_y' \\ \dot{u}_\psi \end{bmatrix}$$

$$= (1/2)\int \begin{bmatrix} \dot{u}_x' & \dot{u}_y' & \dot{u}_\psi \end{bmatrix} \begin{bmatrix} 1/2(\rho ds)s^2 & 0 & 0 \\ 0 & 1/2(\rho ds)s^2 & 0 \\ 0 & 0 & 0 \end{bmatrix} \begin{bmatrix} \dot{u}_x' \\ \dot{u}_y' \\ \dot{u}_\psi \end{bmatrix} . \qquad (16)$$

The kinetic energy equation (12) can be simplified as

$$T_1 = (1/2)\,\rho L \underline{V}_o^T \underline{V}_o + (1/6)\,\rho L^3 \left[\omega_1^2 + \omega_2^2 \right] - \rho L \underline{V}_o^T \underline{\tilde{c}}\,\underline{\omega} + \rho L \sum_{i=1}^{n} \dot{q}_i^2$$
$$+ \underline{V}_o^T \underline{\dot{\alpha}} + \underline{\omega}^T \underline{\dot{\beta}} + (1/4)\,\rho \left[\sum_{i=1}^{n} p_{5i} \dot{q}_i^2 + \sum_{i=1}^{n} p_{6i} \dot{q}_i^2 \right] \qquad (17)$$

where

$$u_x = \sum_{i=1}^{n} \phi_{xi}(s) q_i(t)$$
$$u_y = \sum_{i=1}^{n} \phi_{yi}(s) q_i(t)$$
$$u_x' = \sum_{i=1}^{n} \phi_{xi}'(s) q_i(t)$$
$$u_y' = \sum_{i=1}^{n} \phi_{yi}'(s) q_i(t)$$
$$u_\psi = \sum_{i=1}^{n} \phi_{\psi i}(s) q_i(t)$$
$$p_{1i} = \int_0^L \phi_{xi}(s) ds$$
$$p_{2i} = \int_0^L \phi_{yi}(s) ds$$
$$p_{3i} = \int_0^L s \phi_{xi}(s) ds$$
$$p_{4i} = \int_0^L s \phi_{yi}(s) ds \qquad (18)$$
$$p_{5i} = \int_0^L \left[s \phi_{xi}' \right]^2 ds$$
$$p_{6i} = \int_0^L \left[s \phi_{yi}' \right]^2 ds$$

and

$$\underline{\dot{\alpha}}(t) = \rho \begin{bmatrix} \sum_{i=1}^{n} p_{1i}\dot{q}_i \\ \sum_{i=1}^{n} p_{2i}\dot{q}_i \\ 0 \end{bmatrix} \tag{19}$$

$$\underline{\dot{\beta}}(t) = \rho \begin{bmatrix} \sum_{i=1}^{n} p_{4i}\dot{q}_i \\ \sum_{i=1}^{n} p_{3i}\dot{q}_i \\ 0 \end{bmatrix} \tag{20}$$

The expressions for $p_{1i}, p_{2i}, p_{3i}, p_{4i}, p_{5i}$, and p_{6i} are developed as follows. Note that

$$\phi_{xi}(s) = A_{xi}\sin\beta_i s + B_{xi}\cos\beta_i s + C_{xi}\sinh\beta_i s + D_{xi}\cosh\beta_i s$$

where $\beta_i = \left[\frac{\omega_i^2 \rho}{EI} \right]^{1/4}$.

Since for SCOLE configuration $EI_x = EI_y$ and $\beta_{ix} = \beta_{iy}$, EI and β_i are used for both $\phi_{xi}(s)$ and $\phi_{yi}(s)$. However, this may not be true for other configurations.

$$p_{1i} = \int_0^L \phi_{xi}(s)ds$$

$$p_{2i} = \int_0^L \phi_{yi}(s)ds$$

$$p_{1i} = \frac{1}{\beta_i L^2}\left[-A_{xi}\cos\beta_i L + B_{xi}\sin\alpha_i + C_{xi}\cosh\beta_i L + D_{xi}\sinh\beta_i L + A_{xi} - C_{xi} \right] \tag{21A}$$

Defining $\alpha_i = \beta_i L$

$$p_{1i} = \frac{1}{\alpha_i L}\left[-A_{xi}\cos\alpha_i + B_{xi}\sin\alpha_i + C_{xi}\cosh\alpha_i + D_{xi}\sinh\alpha_i + A_{xi} - C_{xi}\right] \tag{21B}$$

similarly,

$$p_{2i} = \frac{1}{\beta_i L^2}\left[-A_{yi}\cos\beta_i L + B_{yi}\sin\beta_i L + C_{yi}\cosh\beta_i L + D_{yi}\sinh\beta_i L + A_{yi} - C_{yi}\right] \tag{22A}$$

$$p_{2i} = \frac{1}{\alpha_i L}\left[-A_{yi}\cos\alpha_i + B_{yi}\sin\alpha_i + C_{yi}\cosh\alpha_i + D_{yi}\sinh\alpha_i + A_{yi} - C_{yi}\right] \tag{22B}$$

$$p_{3i} = \int_0^L s\,\phi_{xi}(s)\,ds$$

$$p_{4i} = \int_0^L s\,\phi_{yi}(s)\,ds$$

and these can be given as

$$p_{3i} = A_{xi}\left[\frac{\sin\beta_i L}{\beta_i^2} - \frac{L\cos\beta_i L}{\beta_i}\right] + B_{xi}\left[\frac{\cos\beta_i L}{\beta_i^2} + \frac{L\sin\beta_i L}{\beta_i} - \frac{1}{\beta_i^2}\right] + C_{xi}\left[\frac{L\cosh\beta_i L}{\beta_i} - \frac{\sinh\beta_i L}{\beta_i^2}\right] + D_{xi}\left[\frac{L\sinh\beta_i L}{\beta_i} - \frac{\cosh\beta_i L}{\beta_i^2} + \frac{1}{\beta_i^2}\right] \tag{23A}$$

$$p_{3i} = A_{xi}\left[\frac{L^2\sin\alpha_i}{\alpha_i^2} - \frac{L^2\cos\alpha_i}{\alpha_i}\right] + B_{xi}\left[\frac{L^2\cos\alpha_i}{\alpha_i^2} + \frac{L^2\sin\alpha_i}{\alpha_i} - \frac{L^2}{\alpha_i^2}\right] + C_{xi}\left[\frac{L^2\cosh\alpha_i}{\alpha_i} - \frac{L^2\sinh\alpha_i}{\alpha_i^2}\right] + D_{xi}\left[\frac{L^2\sinh\alpha_i}{\alpha_i} - \frac{L^2\cosh\alpha_i}{\alpha_i^2} + \frac{L^2}{\alpha_i^2}\right] \tag{23B}$$

Similarly,

$$p_{4i} = A_{yi}\left[\frac{\sin\beta_i L}{\beta_i^2} - \frac{L\cos\beta_i L}{\beta_i}\right] + B_{yi}\left[\frac{\cos\beta_i L}{\beta_i^2} + \frac{L\sin\beta_i L}{\beta_i} - \frac{1}{\beta_i^2}\right] + C_{yi}\left[\frac{L\cosh\beta_i L}{\beta_i} - \frac{\sin\beta_i L}{\beta_i^2}\right] + D_{yi}\left[\frac{L\sinh\beta_i L}{\beta_i} - \frac{\cosh\beta_i L}{\beta_i^2} + \frac{1}{\beta_i^2}\right] \tag{24A}$$

$$p_{4i} = A_{yi}\left[\frac{L^2\sin\alpha_i}{\alpha_i^2} - \frac{L^2\cos\alpha_i}{\alpha_i}\right] + B_{yi}\left[\frac{L^2\cos\alpha_i}{\alpha_i^2} + \frac{L^2\sin\alpha_i}{\alpha_i} - \frac{L^2}{\alpha_i^2}\right] +$$

$$C_{yi}\left[\frac{L^2\cosh\alpha_i}{\alpha_i}-\frac{L^2\sinh\alpha_i}{\alpha_i^2}\right]+D_{yi}\left[\frac{L^2\sinh\alpha_i}{\alpha_i}-\frac{L^2\cosh\alpha_i}{\alpha_i^2}+\frac{L^2}{\alpha_i^2}\right] \quad (24B)$$

$$p_{5i}=\int_0^L\left\{s\phi_{xi}'(s)\right\}^2 ds$$

$$p_{6i}=\int_0^L\left\{s\phi_{yi}'(s)\right\}^2 ds$$

and these can be shown to be

$$\begin{aligned}
p_{5i}=A_{xi}^2&\left[\frac{\beta_i^2L^3}{6}+\frac{1}{2}\left\{\frac{L}{2}\cos2\beta_iL+(\frac{L^2\beta_i}{2}-\frac{1}{4\beta_i})\sin2\beta_iL\right\}\right]\\
&-A_{xi}B_{xi}\left[\frac{L}{2}\sin2\beta_iL+\left\{\frac{1}{4\beta_i}-\frac{L^2\beta_i}{2}\right\}\cos2\beta_iL-\frac{1}{4\beta_i}\right]\\
&+A_{xi}C_{xi}\left[\beta_iL^2\left\{(\cos\beta_iL\sinh\beta_iL)+(\sin\beta_iL\cosh\beta_iL)\right\}\right.\\
&\left.-2L\left\{\sin\beta_iL\sinh\beta_iL\right\}-\frac{1}{\beta_i}\left\{(\cos\beta_iL\sinh\beta_iL)-(\sin\beta_iL\cosh\beta_iL)\right\}\right]\\
&+A_{xi}D_{xi}\left[\beta_iL^2\left\{(\cos\beta_iL\cosh\beta_iL)+(\sin\beta_iL\sinh\beta_iL)\right\}\right.\\
&\left.-2L\left\{\sin\beta_iL\cosh\beta_iL\right\}-\frac{1}{\beta_i}\left\{(\cos\beta_iL\cosh\beta_iL)-(\sin\beta_iL\sinh\beta_iL)\right\}+\frac{1}{\beta_i}\right]\\
&+B_{xi}^2\left[\frac{\beta_i^2L^3}{6}-\frac{1}{2}\left\{\frac{L}{2}\cos2\beta_iL+(\frac{L^2\beta_i}{2}-\frac{1}{4\beta_i})\sin2\beta_iL\right\}\right]\\
&-B_{xi}C_{xi}\left[\beta_iL^2\left\{(\sin\beta_iL\sinh\beta_iL)-(\cos\beta_iL\cosh\beta_iL)\right\}\right.\\
&\left.+2L\left\{\cos\beta_iL\sinh\beta_iL\right\}-\frac{1}{\beta_i}\left\{(\cos\beta_iL\cosh\beta_iL)\right\}\right.\\
&\left.\left\{+(\sin\beta_iL\sinh\beta_iL)\right\}+\frac{1}{\beta_i}\right]\\
&-B_{xi}D_{xi}\left[\beta_iL^2\left\{(\sin\beta_iL\cosh\beta_iL)-(\cos\beta_iL\sinh\beta_iL)\right\}\right.\\
&\left.+2L\left\{\cos\beta_iL\cosh\beta_iL\right\}-\frac{1}{\beta_i}\left\{(\cos\beta_iL\sinh\beta_iL)\right\}\right.
\end{aligned}$$

$$\left\{-(\sin\beta_i L\cosh\beta_i L)\right\}\Bigg]$$

$$+C_{xi}^2\left[\frac{1}{2}\left\{\beta_i L\cosh 2\beta_i L+(\frac{\beta_i L^2}{2}+\frac{1}{4\beta_i})\sinh^2\beta_i L-\frac{\beta_i^2 L^3}{3}\right\}\right]$$

$$+C_{xi}D_{xi}\left[\frac{\beta_i L^2}{2}\cos 2\beta_i L-\frac{L}{2}\sinh 2\beta_i L+\frac{1}{4\beta_i}\cosh 2\beta_i L-\frac{1}{4\beta_i}\right]$$

$$+D_{xi}^2\left[\frac{1}{2}\left\{\beta_i L\cos 2\beta_i L+(\frac{\beta_i L^2}{2}+\frac{1}{4\beta_i})\sinh^2\beta_i L+\frac{\beta_i^2 L^3}{3}\right\}\right] \qquad (25)$$

$$p_{6i}=A_{yi}^2\left[\frac{\beta_i^2 L^3}{6}+\frac{1}{2}\left\{\frac{L}{2}\cos 2\beta_i L+(\frac{L^2\beta_i}{2}-\frac{1}{4\beta_i})\sin 2\beta_i L\right\}\right]$$

$$-A_{yi}B_{yi}\left[\frac{L}{2}\sin 2\beta_i L+(\frac{1}{4\beta_i}-\frac{L^2\beta_i}{2})\cos 2\beta_i L-\frac{1}{4\beta_i}\right]$$

$$+A_{yi}C_{yi}\left[\beta_i L^2\left\{(\cos\beta_i L\sinh\beta_i L)+(\sin\beta_i L\cosh\beta_i L)\right\}-2L\left\{\sin\beta_i L\sinh\beta_i L\right\}\right.$$

$$\left.-\frac{1}{\beta_i}\left\{(\cos\beta_i L\sinh\beta_i L)-(\sin\beta_i L\cosh\beta_i L)\right\}\right]$$

$$+A_{yi}D_{yi}\left[\beta_i L^2\left\{(\cos\beta_i L\cosh\beta_i L)+(\sin\beta_i L\sinh\beta_i L)\right\}-2L\left\{\sin\beta_i L\cosh\beta_i L\right\}\right.$$

$$\left.-\frac{1}{\beta_i}\left\{(\cos\beta_i L\cosh\beta_i L)-(\sin\beta_i L\sinh\beta_i L)\right\}+\frac{1}{\beta_i}\right]$$

$$+B_{yi}{}^2\left[\frac{\beta_i^2 L^3}{6}-\frac{1}{2}\left\{\frac{L}{2}\cos 2\beta_i L+(\frac{L^2\beta_i}{2}-\frac{1}{4\beta_i})\sin 2\beta_i L\right\}\right]$$

$$-B_{yi}C_{yi}\left[\beta_i L^2\left\{(\sin\beta_i L\sinh\beta_i L)-(\cos\beta_i L\cosh\beta_i L)\right\}+2L\left\{\cos\beta_i L\sinh\beta_i L\right\}\right.$$

$$\left.-\frac{1}{\beta_i}\left\{(\cos\beta_i L\cosh\beta_i L)+(\sin\beta_i L\sinh\beta_i L)\right\}+\frac{1}{\beta_i}\right]$$

$$-B_{yi}D_{yi}\left[\beta_i L^2\left\{(\sin\beta_i L\cosh\beta_i L)-(\cos\beta_i L\sinh\beta_i L)\right\}+2L\left\{\cos\beta_i L\cosh\beta_i L\right\}\right.$$

$$\left.-\frac{1}{\beta_i}\left\{(\cos\beta_i L\sinh\beta_i L)-(\sin\beta_i L\cosh\beta_i L)\right\}\right]$$

$$C_{yi}^2\left[\frac{1}{2}\left\{\beta_i L\cosh 2\beta_i L+(\frac{\beta_i L^2}{2}+\frac{1}{4\beta_i})\sinh^2\beta_i L-\frac{\beta_i^2 L^3}{3}\right\}\right]$$

$$C_{yi}D_{yi}\left[\frac{\beta_i L^2}{2}\cos 2\beta_i L-\frac{L}{2}\sinh 2\beta_i L+\frac{1}{4\beta_i}\cos 2\beta_i L-\frac{1}{4\beta_i}\right]$$

$$D_{yi}^2\left[\frac{1}{2}\left\{\beta_i L\cos 2\beta_i L+(\frac{\beta_i L^2}{2}+\frac{1}{4\beta_i})\sinh^2\beta_i L+\frac{\beta_i^2 L^3}{3}\right\}\right] . \qquad (26)$$

The equations (25) and (26) can alternatively be derived by replacing $\beta_i = \frac{\alpha_i}{L}$.

The kinetic energy of the reflector is

$$T_2 = (1/2)\, m_2 \underline{V}_o^T \underline{V}_o - m_2 \underline{V}_o^T \underline{\tilde{a}}(L)\underline{\omega} + m_2 \underline{V}_o^T \underline{\dot{d}}(L) - (1/2)\, m_2 \underline{\omega}^T \underline{\tilde{a}}^T(L)\underline{\tilde{a}}(L)\underline{\omega} + m_2 \underline{\omega}^T \underline{\tilde{a}}(L)\underline{\dot{d}}(L) + (1/2)\, m_2 \underline{\dot{d}}^T(L)\underline{\dot{d}}(L) + (1/2)\, \underline{\Omega}^T I_2 \underline{\Omega} \qquad (27)$$

where m_2 is the mass of the reflector and I_2 is the mass moment of inertia matrix of the reflector. The deflection vector $\underline{d}(L)$ at the mass center of the reflector is given as

$$\underline{d}(L) = \begin{bmatrix} u_x(L) - r_y u_\psi(L) \\ u_y(L) + r_x u_\psi \\ u_x'(L) r_x + u_y'(L) r_y \end{bmatrix} \qquad (28)$$

and the position vector from the point of attachment to the reflector mass center is given by

$$\underline{a}(L) = \begin{bmatrix} r_x \\ r_y \\ -L \end{bmatrix} . \qquad (29)$$

Thus,

$$\underline{\dot{d}}(L) = \begin{bmatrix} \dot{u}_x(L) - r_y \dot{u}_\psi(L) \\ \dot{u}_y(L) + r_x \dot{u}_\psi(L) \\ \dot{u}_x'(L) r_x + \dot{u}_y'(L) r_y \end{bmatrix} . \qquad (30)$$

The angular velocity of the reflector in the inertial co-ordinate system $\underline{\Omega}$ can be shown to be

$$\underline{\Omega} = \underline{\omega} + \begin{bmatrix} \dot{u}_x' \\ \dot{u}_y' \\ \dot{u}_\psi \end{bmatrix}_L \qquad (31)$$

The equation (27) can be simplified as

$$T_2 = (1/2)\, m_2 \underline{V}_o^T \underline{V}_o - m_2 \underline{V}_o^T \tilde{\underline{a}}(L)\underline{\omega} + m_2 \underline{V}_o^T \dot{\underline{d}}(L) + (1/2)\, m_2 L^2 \left[\omega_1^2 + \omega_2^2\right] + m_2 \underline{\omega}^T \tilde{\underline{a}}(L)\dot{\underline{d}}(L) + (1/2)\, m_2 \left\{ \sum_{i=1}^{n}\sum_{j=1}^{n} \phi_{xi}(L)\phi_{xj}(L)\dot{q}_i\dot{q}_j + \sum_{i=1}^{n}\sum_{j=1}^{n} \phi_{yi}(L)\phi_{yj}(L)\dot{q}_i\dot{q}_j \right\} + (1/2)\, \dot{\underline{P}}^T I_2 \dot{\underline{P}} + (1/2)\, \underline{\omega}^T I_2 \underline{\omega} \qquad (32)$$

where

$$\dot{\underline{P}}^T = \left[\dot{u}_x \;\; \dot{u}_y \;\; \dot{u}_\psi \right]_L = \left[\sum_{i=1}^{n} \phi_{xi}'(L)\dot{q}_i(t) \;\; \sum_{i=1}^{n} \phi_{yi}'(L)\dot{q}_i \;\; \sum_{i=1}^{n} \phi_{\psi i}(L)\dot{q}_i(t) \right] . \qquad (33)$$

The kinetic energy of the shuttle, T_o , is given as

$$T_o = (1/2)\, m_1 \underline{V}^T \underline{V} + (1/2)\, \underline{\omega}^T \left[I_1 \right] \underline{\omega} \qquad (34)$$

where m_1 is the mass of the shuttle and I_1 is the mass moment of inertia matrix of the shuttle.

The total kinetic energy is given as

$$T = T_o + T_1 + T_2 \qquad (35)$$

This can be simplified as

$$T = (1/2)\, m_o \underline{V}^T \underline{V} + \underline{\omega}^T \left[H \right] \underline{V} + (1/2)\, \underline{\omega}^T \left[I_o \right] \underline{\omega} + \rho L \sum_{i=1}^{n} \dot{q}_i^2 + \underline{V}^T \dot{\underline{\alpha}} + \underline{\omega}^T \tilde{\underline{r}} \dot{\underline{\alpha}} + \underline{\omega}^T \dot{\underline{\beta}} + m_2 \underline{V}^T \dot{\underline{d}}(L) + m_2 \underline{\omega}^T \tilde{\underline{r}} \dot{\underline{d}}(L) + m_2 \underline{\omega}^T \tilde{\underline{a}}(L)\dot{\underline{d}}(L) + (1/2)\, m_2 \left[\sum_{i=1}^{n} \left\{ \phi_{xi}^2(L) + \phi_{yi}^2(L) \right\} \dot{q}_i^2 \right] + (1/2)\, \dot{\underline{P}}^T I_2 \dot{\underline{P}} + (1/4)\, \rho \left[\sum_{i=1}^{n} p_{5i}\dot{q}_i^2 + \sum_{i=1}^{n} p_{6i}\dot{q}_i^2 \right] \qquad (36)$$

where

$$m_o = m_1+\rho L+m_2$$

$$H = \left[\rho L+m_2\right]\tilde{\underline{r}}+m_2\tilde{\underline{a}}(L)+\rho L\tilde{\underline{c}}$$

$$I_o = I_1+(1/3)\,\rho L^3\begin{bmatrix}1&0&0\\0&1&0\\0&0&0\end{bmatrix}+I_2+J_2-\rho L\tilde{\underline{r}}\tilde{\underline{r}}-\rho L\tilde{\underline{r}}\tilde{\underline{c}}-m_2\tilde{\underline{r}}\tilde{\underline{r}}-m_2\tilde{\underline{r}}\tilde{\underline{a}}(L)$$

The term J_2 in this equation can be shown to be:

$$J_2 = m_2\begin{bmatrix}(r_y^2+L^2) & -r_xr_y & r_xL\\ -r_xr_y & (r_x^2+L^2) & r_yL\\ r_xL & r_yL & (r_x^2+r_y^2)\end{bmatrix} .$$

The total kinetic energy expression can be further simplified as

$$T = (1/2)\,m_o\underline{V}^T\underline{V}+\underline{\omega}^T\left[H\right]\underline{V}+(1/2)\,\underline{\omega}^T\left[I_o\right]\underline{\omega}+\underline{V}^T\left[A_1\right]\dot{\underline{q}} \qquad (37)$$
$$+\underline{\omega}^T\left[A_2\right]\dot{\underline{q}}+(1/2)\,\dot{\underline{q}}^T\left[A_3\right]\dot{\underline{q}}$$

where

$$\left[A_1\right]\dot{\underline{q}} = \dot{\underline{\alpha}}+m_2\dot{\underline{d}}(L)$$

$$\left[A_2\right]\dot{\underline{q}} = \tilde{\underline{r}}\dot{\underline{\alpha}}+\dot{\underline{\beta}}+m_2\tilde{\underline{r}}\dot{\underline{d}}(L)+m_2\tilde{\underline{a}}(L)\dot{\underline{d}}(L)$$

$$\left[A_3\right] = \begin{bmatrix}0\\ \rho L+m_2+p_{5i}+p_{6i}\\ 0\end{bmatrix}+\left[\left[\phi'(L)\right]^T I_2\left[\phi'(L)\right]\right] .$$

In this equation

$$\left[\phi'(L)\right]^T = \begin{bmatrix}\phi_{1x}'(L) & 0 & 0\\ 0 & \phi_{1y}'(L) & 0\\ 0 & 0 & \phi_{1\psi}(L)\\ \cdot & \cdot & \cdot\\ \cdot & \cdot & \cdot\\ \phi_{ix}'(L) & 0 & 0\\ 0 & \phi_{iy}'(L) & 0\\ 0 & 0 & \phi_{i\psi}(L)\end{bmatrix}$$

Here i=2,3,.....,n. The number n indicates the total number of flexible modes considered.

Equations of motion

Lagrange's equations of motion for the case of independent generalized co-ordinates q_k are

$$\frac{d}{dt}\frac{\partial T}{\partial \dot{q}_k} - \frac{\partial T}{\partial q_k} = Q_k - \frac{\partial U}{\partial q_k} \qquad (k=1,2,.....,n) \tag{38}$$

where, $T = T(\underline{q},\underline{\dot{q}})$ is the kinetic energy

$U = U(\underline{q})$ is the potential energy, and

Q_k are the generalized forces arising from nonconservative sources.

The generalized co-ordinates are:

R_X, R_Y, R_Z – position of orbiter mass center relative to inertial frame origin.

$\theta_1, \theta_2, \theta_3$ – roll, pitch and yaw angles of orbiter.

$q_1, q_2, ..., q_n$ – modal deformation co-ordinates for the beam.

The previous kinetic energy expression developed in equation (37) is given in terms of nonholonomic velocities $\underline{V}$ and $\underline{\omega}$, and generalized velocities $\underline{\dot{q}}$. Using the notation $\bar{T}(\underline{V},\underline{\omega},\underline{\dot{q}})$ for this kinetic energy expression and T for kinetic energy expression in terms of generalized velocities, the equations of motion are developed. Thus, equation (37) is rewritten as

$$\bar{T} = (1/2)\, m_o \underline{V}^T \underline{V} + \underline{\omega}^T \left[H\right] \underline{V} + (1/2)\underline{\omega}^T \left[I_o\right] \underline{\omega} + \underline{V}^T \left[A_1\right] \underline{\dot{q}} + \underline{\omega}^T \left[A_2\right] \underline{\dot{q}} + (1/2)\underline{\dot{q}}^T \left[A_3\right] \underline{\dot{q}} \tag{37}$$

(a) Translational Equations

From the chain rule applied to equation (37) using equation (8), one gets

$$\begin{bmatrix} \frac{\partial T}{\partial \dot{R}_X} \\ \frac{\partial T}{\partial \dot{R}_Y} \\ \frac{\partial T}{\partial \dot{R}_Z} \end{bmatrix} = C^T \begin{bmatrix} \frac{\partial \bar{T}}{\partial V_1} \\ \frac{\partial \bar{T}}{\partial V_2} \\ \frac{\partial \bar{T}}{\partial V_3} \end{bmatrix} \quad . \tag{39}$$

Also, the generalized forces are $C\underline{F}(t)$ where

$$\underline{F}(t) = \underline{F}_o(t) + \underline{F}_2(t) \tag{40}$$

$\underline{F}_o(t)$ represents the force applied at the orbiter mass center and $\underline{F}_2(t)$ represents the force applied at the reflector mass center. From Lagrange's equations

$$\frac{d}{dt}\left[\frac{\partial \bar{T}}{\partial \underline{V}}\right] + C\dot{C}^T \left[\frac{\partial \bar{T}}{\partial \underline{V}}\right] = \underline{F}(t) \tag{41}$$

and from equation (37)

$$\left[\frac{\partial \bar{T}}{\partial \underline{V}}\right] = m_o \underline{V} - H\underline{\omega} + A_1 \dot{\underline{q}} \tag{42}$$

Substituting equation (42) in (41),

$$m_o \dot{\underline{V}} - H\dot{\underline{\omega}} + A_1 \ddot{\underline{q}} = -C\dot{C}^T (m_o \underline{V} - H\underline{\omega} + A_1 \dot{\underline{q}}) + \underline{F}(t) \tag{43}$$

This can be rewritten as

$$m_o \dot{\underline{V}} - H\dot{\underline{\omega}} + A_1 \ddot{\underline{q}} = \underline{N}_1 + \underline{F}(t) \tag{44}$$

where the nonlinear term $\underline{N}_1$ is given as

$$\begin{aligned} \underline{N}_1 &= -C\dot{C}^T (m_o \underline{V} - H\underline{\omega} + A_1 \dot{\underline{q}}) \\ &= -\tilde{\underline{\omega}} (m_o \underline{V} - H\underline{\omega} + A_1 \dot{\underline{q}}) \end{aligned} \tag{45}$$

Here, $\tilde{\underline{\omega}} = C\dot{C}^T$.

(b) Rotational Equations :

From equation (4)

$$\underline{\omega} = M^T \underline{\dot{\theta}}$$

Again using the chain rule

$$\left[\frac{\partial T}{\partial \underline{\theta}}\right] = M \left[\frac{\partial \bar{T}}{\partial \underline{\omega}}\right] \tag{46}$$

Also

$$\begin{bmatrix} \frac{\partial T}{\partial \theta_1} \\ \frac{\partial T}{\partial \theta_2} \\ \frac{\partial T}{\partial \theta_3} \end{bmatrix} = \begin{bmatrix} \frac{\partial V^T}{\partial \theta_1} \\ \frac{\partial V^T}{\partial \theta_2} \\ \frac{\partial V^T}{\partial \theta_3} \end{bmatrix} \left[\frac{\partial \bar{T}}{\partial \underline{V}}\right] + \begin{bmatrix} \frac{\partial \omega^T}{\partial \theta_1} \\ \frac{\partial \omega^T}{\partial \theta_2} \\ \frac{\partial \omega^T}{\partial \theta_3} \end{bmatrix} \left[\frac{\partial \bar{T}}{\partial \underline{\omega}}\right] \quad . \tag{47}$$

It can be shown that

$$\frac{\partial V^T}{\partial \theta_i} = \underline{V}^T C \frac{\partial C^T}{\partial \theta_i} \ldots\ldots i = 1,2,3,\ldots\ldots \tag{48A}$$

and

$$\frac{\partial \omega^T}{\partial \theta_i} = \underline{\omega}^T M^{-1} \frac{\partial M}{\partial \theta_i} \ldots\ldots i = 1,2,3,\ldots\ldots \tag{48B}$$

and

$$\left[\frac{\partial T}{\partial \underline{\theta}}\right] = \begin{bmatrix} \underline{V}^T C \frac{\partial C^T}{\partial \theta_1} \\ \underline{V}^T C \frac{\partial C^T}{\partial \theta_2} \\ \underline{V}^T C \frac{\partial C^T}{\partial \theta_3} \end{bmatrix} \left[\frac{\partial \bar{T}}{\partial \underline{V}}\right] + \begin{bmatrix} \underline{\omega}^T M^{-1} \frac{\partial M}{\partial \theta_1} \\ \underline{\omega}^T M^{-1} \frac{\partial M}{\partial \theta_2} \\ \underline{\omega}^T M^{-1} \frac{\partial M}{\partial \theta_3} \end{bmatrix} \left[\frac{\partial \bar{T}}{\partial \underline{\omega}}\right] \quad . \tag{49}$$

From equation (37),

$$\left[\frac{\partial \bar{T}}{\partial \underline{\omega}}\right] = H\underline{V} + I_o\underline{\omega} + A_2\dot{\underline{q}} \tag{50}$$

and as before

$$\left[\frac{\partial \bar{T}}{\partial \underline{V}}\right] = m_o\underline{V} - H\underline{\omega} + A_1\dot{\underline{q}} \tag{42}$$

Using the Lagrange's equations

$$\frac{d}{dt}\left[\frac{\partial T}{\partial \underline{\theta}}\right] - \frac{\partial T}{\partial \underline{\theta}} = M\underline{G} \tag{51}$$

where $\underline{G}$ is the net moment about the mass center of the orbiter with respect to the body-fixed frame. It is given as

$$\underline{G} = \underline{G}_o + (\underline{r}+\underline{a})\times\underline{F}_2 \tag{52}$$

$\underline{G}_o$ is the external moment applied about the mass center. Eqation (51) can be simpified by substituting equations (42),(49), and (50) together with the relation-ship developed in (46) as

$$H\dot{\underline{V}} + I_o\dot{\underline{\omega}} + A_2\ddot{\underline{q}} = \underline{G} + \underline{N}_2 \tag{53}$$

where the nonlinear term $\underline{N}_2$ is given as

$$\underline{N}_2 = M^{-1}\begin{bmatrix} \underline{V}^T C\dfrac{\partial C^T}{\partial \theta_1} \\ \underline{V}^T C\dfrac{\partial C^T}{\partial \theta_2} \\ \underline{V}^T C\dfrac{\partial C^T}{\partial \theta_3} \end{bmatrix}\left[\frac{\partial \bar{T}}{\partial \underline{V}}\right] + M^{-1}\left(\begin{bmatrix} \underline{\omega}^T M^{-1}\dfrac{\partial M}{\partial \theta_1} \\ \underline{\omega}^T M^{-1}\dfrac{\partial M}{\partial \theta_2} \\ \underline{\omega}^T M^{-1}\dfrac{\partial M}{\partial \theta_3} \end{bmatrix} - \dot{M}\right)\left[\frac{\partial \bar{T}}{\partial \underline{\omega}}\right], \tag{54}$$

(c) Vibration Equations of the Beam

Since $\bar{T}$ in equation (37) is given in terms of $\underline{\dot{q}}$ which is a vector of generalized velocities,

$$\frac{\partial \bar{T}}{\partial \underline{\dot{q}}} = \frac{\partial T}{\partial \underline{\dot{q}}}$$

and

$$\left[\frac{\partial T}{\partial \underline{\dot{q}}}\right] = A_1^T \underline{V} + A_2^T \underline{\omega} + A_3 \underline{\dot{q}} \tag{55}$$

The potential energy in the beam is given by

$$U = (1/2)\underline{q}^T K \underline{q} \tag{56}$$

where the stiffness matrix K is given as

$$K = \begin{bmatrix} \diagdown & 0 & \\ & k_{ii} & \\ 0 & & \diagdown \end{bmatrix} \tag{57}$$

and

$$k_{ii} = EI\beta_i^4 \left[\int_0^L \phi_{xi}^2(s)ds + \int_0^L \phi_{yi}^2(s)ds\right] + G_\psi \beta_{\psi i}^2 \int_0^L \phi_{\psi i}^2(s)ds$$

G_ψ represents the modulus of rigidity of the beam and $\beta_{\psi i} = \left[\frac{D\omega_i^2}{G_\psi}\right]^{\frac{1}{2}}$ where D is the mass per unit volume (mass density) of the beam. Thus,

$$\left[\frac{\partial U}{\partial \underline{q}}\right] = K\underline{q} \quad . \tag{58}$$

Using the Lagrangian Equations (38) and assuming that $\underline{F}_2 = \underline{0}$,

$$A_1^T \dot{\underline{V}} + A_2^T \dot{\underline{\omega}} + A_3 \ddot{\underline{q}} = -K\underline{q} \quad . \tag{59}$$

(d) Motion Stiffness

As noted in references (27,28), generalized active forces associated with motion stiffness must be taken into account in order to obtain dynamical equations for performing large arbitrary maneuvers. This provides the mechanism of compensating errors caused by premature linearization during the modal analysis for an arbitrary flexible body undergoing the most general large rotation and translation.

For a mass element on the beam from the point of attachment (origin of the body-fixed frame) before deformation, the translational velocity in the inertial frame is as given as

$$\underline{V}^a = \underline{V}_o + \omega \times (\underline{a} + \underline{d}) + \dot{\underline{d}}(z,t) \tag{60}$$

where $\underline{V}_o$ is given by equation (9). The corresponding angular velocity in the inertial frame of the mass element is given as

$$\underline{\omega}^a = \underline{\omega} + \dot{\underline{\beta}}(z,t) \tag{61}$$

where

$$\underline{\beta} = \begin{bmatrix} 0 \\ 0 \\ u_\psi(z,t) \end{bmatrix}$$

and $u_\psi(z,t)$ is the torsional displacement of the beam.

Differentiation of the right-hand side of equation (61) with respect to t yields the acceleration of mass element in the inertial frame as

$$\underline{a}^a = \dot{\underline{V}}_o + \dot{\underline{\omega}} \times (\underline{a} + \underline{d}) + \ddot{\underline{d}}(z,t) + \underline{\omega} \times \left[\underline{V}_o + \omega \times (\underline{a} + \underline{d}) + 2\underline{d}(z,t) \right] \tag{62}$$

Similarly the angular acceleration of the mass center in the inertial frame follows from equation (4).

$$\underline{\alpha}^a = \dot{\underline{\omega}} + \underline{\omega} \times \dot{\underline{\beta}}(z,t) + \ddot{\underline{\beta}}(z,t) \tag{63}$$

Equation (62) can be simplified as

$$\underline{a}^a = \dot{\underline{V}} + \underline{\omega} \times (\underline{\omega} \times \underline{r}) + \dot{\underline{\omega}} \times (\underline{a} + \underline{d}) + \ddot{\underline{d}}(z,t)$$

$$+ \underline{\omega} \times \left[\underline{V} + \underline{\omega} \times \underline{r} + \underline{\omega} \times (\underline{a} + \underline{d}) + 2\underline{d}(z,t)\right] \tag{64}$$

The inertia forces associated with acceleration in equation (64) can be given as

$$\underline{F}^* = -\int_0^L (\rho dz)\underline{a}^a - m_2 \underline{a}^a(L) \tag{65}$$

and the inertia moment associated with angular acceleration is

$$\underline{G}^* = -\int_0^L (dl)\underline{\alpha}^a - I_2 \underline{\alpha}^a(L) - \int_0^L \left\{\underline{\omega}^a \times \left[(dl)\underline{\omega}^a\right]\right\} - \underline{\omega}^a(L) \times \left[I_2 \underline{\omega}\right] \tag{66}$$

The inertia force obtained in equation (65) is added to the right hand side of equation (44) and the inertia moment of equation (66) is similarly added to equation (53).

(e) Slewing Equations

If it is considered to perform a slew maneuver about an arbitrary axis $\underline{\gamma}$ and the slew angle to be ξ, then the slew maneuver can be expressed in terms of four Euler parameters. These four Euler parameters are defined as

$$\underline{\varepsilon} = \begin{bmatrix} \varepsilon_1 \\ \varepsilon_2 \\ \varepsilon_3 \end{bmatrix} = \underline{\lambda} \sin\frac{\xi}{2} \tag{67}$$

$$\varepsilon_4 = \cos\frac{\xi}{2} \tag{68}$$

and their derivatives with respect to time are given as

$$\frac{d\underline{\varepsilon}}{dt} = \frac{1}{2}\left(\varepsilon_4\underline{\omega} + \underline{\varepsilon}\times\underline{\omega}\right) \tag{69}$$

$$\frac{d\varepsilon_4}{dt} = -\frac{1}{2}\underline{\omega}\cdot\underline{\varepsilon} \quad . \tag{70}$$

The four Euler parameters can be related to the angular velocity components of the rigid assembly as

$$\begin{bmatrix} \dot{\varepsilon}_1 \\ \dot{\varepsilon}_2 \\ \dot{\varepsilon}_3 \\ \dot{\varepsilon}_4 \end{bmatrix} = \begin{bmatrix} \varepsilon_1 & \varepsilon_4 & -\varepsilon_3 & \varepsilon_2 \\ \varepsilon_2 & \varepsilon_3 & \varepsilon_4 & -\varepsilon_1 \\ \varepsilon_3 & -\varepsilon_2 & \varepsilon_1 & \varepsilon_4 \\ \varepsilon_4 & -\varepsilon_1 & -\varepsilon_2 & -\varepsilon_3 \end{bmatrix} \begin{bmatrix} 0 \\ \omega_1 \\ \omega_2 \\ \omega_3 \end{bmatrix} \quad . \tag{71}$$

If a slew maneuver is considered to be purely rotational, then the translational velocity and acceleration can be shown to be negligible during the slew maneuver and only the rotational and vibration equations are reqired for the analysis and they are simplified by setting $\dot{\underline{V}} \equiv \underline{0}$ in both (53) and (59) and are written as follows

$$I_o\dot{\underline{\omega}} + A_2\ddot{\underline{q}} = \underline{G}(t) + \underline{N}_2(\underline{\omega}) \tag{72}$$

$$A_2^T\dot{\underline{\omega}} + \bar{A}_3\ddot{\underline{q}} + K\underline{q} = \underline{Q}(t) \quad , \tag{73}$$

where,

$\underline{G}(t)$ is the net moment applied about the mass center of the orbiter and is given by the following equations (figs. 3 & 4)

$$\underline{G}(t) = \underline{G}_0(t) + (\underline{r} + \underline{a})\times\underline{F}_2 \quad . \tag{74}$$

Also, $\underline{Q}(t)$ represents the generalized force vector which is given by the following equation

$$\underline{Q}(t) = \begin{bmatrix} \sum_{j=1}^{m} (Q_{jx_1}(t) + Q_{jy_1}(t)) + Q_{x_1} + Q_{y_1} + Q_{\psi_1} \\ \sum_{j=1}^{m} (Q_{jx_2}(t) + Q_{jy_2}(t)) + Q_{x_2} + Q_{y_2} + Q_{\psi_2} \\ \cdots \\ \cdots \\ \cdots \\ \sum_{j=1}^{m} (Q_{jx_i}(t) + Q_{jy_i}(t)) + Q_{xi} + Q_{yi} + Q_{\psi i} \\ \cdots \\ \cdots \end{bmatrix} \tag{75}$$

where, the generalized force components are given as

$$Q_{jx_i} = \int_0^L F_{jx}(z,t)\delta(z-z_j)\phi_{xi}(z)dz \tag{76}$$

$$Q_{jy_i} = \int_0^L F_{jy}(z,t)\delta(z-z_j)\phi_{yi}(z)dz \tag{77}$$

and

$$Q_{j\psi_i}(t) = 0 \quad . \tag{78}$$

Here, $F_{jx}(z,t)$ is the x component of the concentrated force applied at location j on the flexible antenna and F_{jy} is the y component of that force.

Also,

$$\begin{aligned} Q_{xi}(t) &= F_{2x}(t)\phi_{xi}(L) \\ Q_{yi}(t) &= F_{2y}(t)\phi_{yi}(L) \\ Q_{\psi}(t) &= M_{\psi}(t)\phi_{\psi i}(L) \end{aligned} \tag{79}$$

Here, $\underline{F}_2$ is the force applied at the reflector C. G.

Thus,

$$M_\psi(t) = F_{2x} r_y + F_{2y} r_x + M_{2\psi} \tag{80}$$

The location of reflector C. G. is given by coordinates (r_x, r_y) and $M_{2\psi}$ represents the external moment applied at the reflector C. G.

Thus equations (79) - (80) completely represent the dynamics of the slew maneuver. These equations are nonlinear and coupled including both the rigid-body dynamics and the dynamics of the flexible appendage with kinematic nonlinearities. It is important to note that the nonlinear term $N_2(\underline{\omega})$ is dependent on the rotational velocity and as a result determined by the slew maneuver rate. Thus the basic slew maneuver stretegy has to be developed before this term can be linearized.

(f) Vibration Equations of the Beam with Damping

If damping is included in the derivation of vibration equations of the beam, then the damping effect can be expressed in terms of frictional forces. These are nonconservative, retarding forces and are assumed to be proportional to the generalized velocities. In deriving the vibration equations by means of Lagrange's equations, the following function is introduced

$$F_d = \frac{1}{2} \sum_{i=1}^{n} \sum_{j=1}^{n} b_{ij} \dot{q}_i \dot{q}_j \quad . \tag{81}$$

It also has a positive definite quadratic form similar to the kinetic and potential energy expressions.

With this definition, Lagrange's equations assume the form

$$\frac{d}{dt} \frac{\partial T}{\partial \dot{q}_k} - \frac{\partial T}{\partial q_k} \frac{\partial F_d}{\partial \dot{q}_k} = Q_k - \frac{\partial U}{\partial q_k} \qquad (k=1,2,.....,n) \tag{82}$$

Again, as before

$$\left[\frac{\partial T}{\partial \underline{\dot{q}}}\right] = A_1^T \underline{V} + A_2^T \underline{\omega} + A_3 \underline{\dot{q}} \tag{55}$$

and

$$\left[\frac{\partial U}{\partial \underline{q}}\right] = K\,\underline{q} \tag{58}$$

and it can be seen from (81) that

$$\left[\frac{\partial F_d}{\partial \underline{\dot{q}}}\right] = B\,\underline{\dot{q}} \tag{83}$$

where the damping matrix B is symmetrical and is given as

$$B = \begin{bmatrix} b_{11} & b_{12} & . & . & b_{1n} \\ b_{21} & b_{22} & . & . & b_{2n} \\ . & . & . & . & . \\ . & . & . & . & . \\ b_{n1} & b_{n2} & . & . & b_{nn} \end{bmatrix} \quad . \tag{84}$$

The vibration equations are given as

$$A_1^T \underline{\dot{V}} + A_2^T \underline{\dot{\omega}} + A_3 \underline{\ddot{q}} + B\underline{\dot{q}} = -K\underline{q} + \underline{Q}(t) \quad . \tag{85}$$

The slewing equations (72) and (73) would be modified as

$$I_2 \underline{\dot{\omega}} + A_2 \underline{\ddot{q}} = \underline{G}(t) + \underline{N}_2(\underline{\omega}, \underline{\dot{q}}) \tag{86}$$

$$A_2^T \underline{\dot{\omega}} + A_3 \underline{\ddot{q}} + B\underline{\dot{q}} = -K\underline{q} + \underline{Q}(t) \quad . \tag{87}$$

Nonlinear Term in the Rotational Equations

The nonlinear term $\underline{N}_2$ in the rotational equations (72) and (86) during the slewing maneuver is simplified as

$$\underline{N}_2 = M^{-1}\left(\begin{bmatrix} \underline{\omega}^T M^{-1}\frac{\partial M}{\partial \theta_1} \\ \underline{\omega}^T M^{-1}\frac{\partial M}{\partial \theta_2} \\ \underline{\omega}^T M^{-1}\frac{\partial M}{\partial \theta_3} \end{bmatrix} - \dot{M}\right)\left[I_o\underline{\omega} + A_2\dot{\underline{q}}\right] \tag{88}$$

where

$$\underline{\omega}^T M^{-1}\frac{\partial M}{\partial \theta_1} = \begin{bmatrix} 0 & 0 & 0 \end{bmatrix} \tag{89}$$

$$\underline{\omega}^T M^{-1}\frac{\partial M}{\partial \theta_2} = \frac{1}{\cos\theta_2}\Big[(-\omega_1\sin\theta_2\cos^2\theta_3+\omega_2\sin\theta_2\sin\theta_3\cos\theta_3) \quad (\omega_1\sin\theta_2\sin\theta_3\cos\theta_3$$

$$-\omega_2\sin\theta_2\sin^2\theta_3) \quad (\omega_1\cos\theta_2\cos\theta_3-\omega_2\cos\theta_2\sin\theta_3)\Big] \tag{90}$$

$$\underline{\omega}^T M^{-1}\frac{\partial M}{\partial \theta_3} = \frac{1}{\cos\theta_2}\begin{bmatrix} (\omega_2\cos\theta_2) & (-\omega_1\cos\theta_2) & 0 \end{bmatrix} \tag{91}$$

Since the transformation matrix, M , is a function of θ_2 and θ_3, the time derivative of M can be expressed by the chain rule as

$$\dot{M} = \frac{\partial M}{\partial \theta_2}\dot{\theta}_2 + \frac{\partial M}{\partial \theta_3}\dot{\theta}_3 \tag{92}$$

From equation (5)

$$\frac{\partial M}{\partial \theta_2}\dot{\theta}_2 = \begin{bmatrix} (-\sin\theta_2\cos\theta_3)\dot{\theta}_2 & (\sin\theta_2\sin\theta_3)\dot{\theta}_2 & (\cos\theta_2)\dot{\theta}_2 \\ 0 & 0 & 0 \\ 0 & 0 & 0 \end{bmatrix} \tag{93}$$

$$\frac{\partial M}{\partial \theta_3}\dot{\theta}_3 = \begin{bmatrix} (-\cos\theta_2\sin\theta_3)\dot{\theta}_3 & (-\cos\theta_2\cos\theta_3)\dot{\theta}_3 & 0 \\ (\cos\theta_3)\dot{\theta}_3 & (-\sin\theta_3)\dot{\theta}_3 & 0 \\ 0 & 0 & 0 \end{bmatrix} \tag{94}$$

Substituting these equations (93) and (94) in (92)

$$\dot{M} = \begin{bmatrix} (-\sin\theta_2\cos\theta_3)\dot{\theta}_2+(-cos\,\theta_2\sin\theta_3)\dot{\theta}_3 & (\sin\theta_2\sin\theta_3)\dot{\theta}_2+(-\cos\theta_2\cos\theta_3)\dot{\theta}_3 & (\cos\theta_2)\dot{\theta}_2 \\ (\cos\theta_3)\dot{\theta}_3 & (-\sin\theta_3)\dot{\theta}_3 & 0 \\ 0 & 0 & 0 \end{bmatrix} \tag{95}$$

From equation (4), this can also be expressed as

$$\dot{M} = \frac{1}{\cos\theta_2} \begin{bmatrix} \begin{matrix}(-\sin\theta_2\cos\theta_3)(\omega_1\cos\theta_2\sin\theta_3 \\ +\omega_2\cos\theta_2\cos\theta_3)+(-\cos\theta_2\sin\theta_3) \\ (-\omega_1\sin\theta_2\cos\theta_3+\omega_2\sin\theta_2\sin\theta_3 \\ +\omega_3\cos\theta_2)\end{matrix} & \begin{matrix}(\sin\theta_2\sin\theta_3)(\omega_1\cos\theta_2\sin\theta_3 \\ +\omega_2\cos\theta_2\cos\theta_3)+(-\cos\theta_2\cos\theta_3) \\ (-\omega_1\sin\theta_2\cos\theta_3+\omega_2\sin\theta_2\sin\theta_3 \\ +\omega_3\cos\theta_2)\end{matrix} \\ \begin{matrix}(cos\,\theta_3)(-\omega_1\sin\theta_2\cos\theta_3 \\ +\omega_2\sin\theta_2\sin\theta_3+\omega_3\cos\theta_2)\end{matrix} & \begin{matrix}(-\sin\theta_3)(-\omega_1\sin\theta_2\cos\theta_3 \\ +\omega_2\sin\theta_2\sin\theta_3+\omega_3\cos\theta_2)\end{matrix} \\ 0 & 0 \end{bmatrix}$$

$$\begin{bmatrix} \cos\theta_2(\omega_1\cos\theta_2\sin\theta_3+\omega_2\cos\theta_2\cos\theta_3) \\ 0 \\ 0 \end{bmatrix} \tag{96}$$

Also, M^{-1} is given as

$$M^{-1} = \frac{1}{\cos\theta_2} \begin{bmatrix} \cos\theta_3 & \cos\theta_2\sin\theta_3 & -\sin\theta_2\cos\theta_3 \\ -\sin\theta_3 & \cos\theta_2\cos\theta_3 & \sin\theta_2\sin\theta_3 \\ 0 & 0 & \cos\theta_2 \end{bmatrix} . \tag{97}$$

Thus, the nonlinear term N_2 can be rewritten as

$$N_2 = A'_3(\underline{\omega},\underline{\theta}) \left[I_o\underline{\omega}+A_2\dot{\underline{q}} \right]$$

Where the term A'_3 is

$$A'_3(\underline{\omega},\underline{\theta}) = M^{-1}\left[\begin{bmatrix} 0 \\ \underline{\omega}^T M^{-1}\dfrac{\partial M}{\partial \theta_2} \\ \underline{\omega}^T M^{-1}\dfrac{\partial M}{\partial \theta_3} \end{bmatrix} - \dot{M}\right]$$

$$N_2 = A'_3(\underline{\omega},\underline{\theta})I_o\underline{\omega} + A'_3(\underline{\omega},\underline{\theta})A_2\dot{\underline{q}}$$

$$= A_4(\underline{\omega},\underline{\theta}) + A_5(\underline{\omega},\underline{\theta})\dot{\underline{q}} \qquad (98)$$

where A_4 depends on the rigid-body slewing and is nonlinear in terms of $\underline{\omega}$ and $\underline{\theta}$. The second term relates the coupling between the rigid-body slewing and the flexible modes. This equation can be further simplified in terms of Euler parameters by relationships developed in appendix II as

$$\underline{N}_2 = A_6(\underline{\omega},\underline{\varepsilon}) + A_7(\underline{\omega},\underline{\varepsilon})\dot{\underline{q}} \qquad (99)$$

where $\underline{\varepsilon}$ is the Euler vector comprising all four Euler parameters,

From equations (72) and (73) and by defining $A = A_2{}^T I_o{}^{-1} A_2 + A_3$, the following equations are obtained

$$\dot{\underline{\omega}} = I_o{}^{-1}\left[A_2A^{-1}B\dot{\underline{q}} + A_2A^{-1}K\underline{q} + \left\{A_2A^{-1}A_2{}^TI_o{}^{-1} + I_3\right\}\underline{G}(t) + \left\{A_2^{-1}A_2{}^TI_o{}^{-1} + I_3\right\}\underline{N}_2(\underline{\omega},\underline{\varepsilon})\right] \qquad (100)$$

$$\ddot{\underline{q}} = A^{-1}B\dot{\underline{q}} - A^{-1}K\underline{q} - A^{-1}A_2{}^TI_o{}^{-1}\underline{G}(t) + A^{-1}A_2{}^TI_o{}^{-1}\underline{N}_2(\underline{\omega},\underline{\varepsilon}) + A^{-1}\underline{Q}(t) \qquad (101)$$

It is assumed that control forces applied for vibration suppression has negligible effect on rotational maneuver of the spacecraft in developing equations (100) and (101). Also, I_3 represents 3x3 identity matrix in these equations.

Subsystems and State Variable Models

The two dynamical subsystems considered for decentralized control are the dynamics of the slewing of the rigidized SCOLE assembly and the vibration dynamics of the flexible antenna. These subsystems are represented by subscripts I and II respectively for subsequent analysis.

The following are the definitions of state variables and control variables for subsystem I.

$$x_{I1} \triangleq \varepsilon_1; \quad x_{I2} \triangleq \varepsilon_2; \quad x_{I3} \triangleq \varepsilon_3; \quad x_{I4} \triangleq \varepsilon_4;$$

$$x_{I5} \triangleq \omega_1; \quad x_{I6} \triangleq \omega_2; \quad x_{I7} \triangleq \omega_3;$$

$$x_{I8} \triangleq G_1; \quad x_{I9} \triangleq G_2; \quad x_{I10} \triangleq G_3;$$

$$u_{I1} \triangleq \dot{G}_1; \quad u_{I2} \triangleq \dot{G}_2; \quad u_{I3} \triangleq \dot{G}_3 \ .$$

The interconnecting variables from the second subsystem to reflect the coupling between the subsystems are defined as

$$z_{I1} \triangleq x_{II1}; \quad z_{I2} \triangleq x_{II2}; \quad z_{I3} \triangleq x_{II3}; \quad z_{I4} \triangleq x_{II4}; \quad z_{I5} \triangleq 0;$$
$$z_{I6} \triangleq 0 \ ; \quad z_{I7} \triangleq 0; \quad z_{I8} \triangleq 0 \ ; \quad z_{I9} \triangleq 0 \ ; \quad z_{I10} \triangleq 0 .$$

The following state equations are obtained for subsystem I using these definitions

$$\begin{bmatrix} \dot{x}_{I1} \\ \dot{x}_{I2} \\ \dot{x}_{I3} \\ \dot{x}_{I4} \\ \dot{x}_{I5} \\ \dot{x}_{I6} \\ \dot{x}_{I7} \\ \dot{x}_{I8} \\ \dot{x}_{I9} \\ \dot{x}_{I10} \end{bmatrix} = \begin{bmatrix} 0 & D & 0 \\ 0 & 0 & H \\ 0 & 0 & 0 \end{bmatrix} \begin{bmatrix} x_{I1} \\ x_{I2} \\ x_{I3} \\ x_{I4} \\ x_{I5} \\ x_{I6} \\ x_{I7} \\ x_{I8} \\ x_{I9} \\ x_{I10} \end{bmatrix} + \begin{bmatrix} 0 & 0 & 0 \\ 0 & B_2 & B_3 \\ I & 0 & 0 \end{bmatrix} \begin{bmatrix} u_{I1} \\ u_{I2} \\ u_{I3} \\ z_{I1} \\ z_{I2} \\ z_{I3} \\ z_{I4} \end{bmatrix}$$

$$+ \begin{bmatrix} 0 \\ \hline H \\ \hline 0 \end{bmatrix} \underline{N}_2 \left(x_{I1}, x_{I2}, x_{I3}, x_{I4}, x_{I5}, x_{I6}, x_{I7} \right) \qquad (102)$$

Here, $H = I_o^{-1} \left[A_2 A^{-1} A_2{}^T I_o^{-1} + I_3 \right]$,

$$B_2 = I_o^{-1} A_2 A^{-1} K ,$$

$$B_3 = I_o^{-1} A_2 A^{-1} B ,$$

$$D = \begin{bmatrix} x_{I4} & -x_{I3} & x_{I2} \\ x_{I3} & x_{I4} & -x_{I1} \\ -x_{I2} & x_{I1} & x_{I4} \\ -x_{I1} & -x_{I2} & -x_{I3} \end{bmatrix} .$$

For the second subsystem which is the flexible appendage of the entire system, the first two flexible modes are considered and the corresponding state variables and control variables are defined as

$x_{II1} \underline{\Delta} q_1$; $x_{II2} \underline{\Delta} q_2$;

$x_{II3} \underline{\Delta} \dot{q}_1$; $x_{II4} \underline{\Delta} \dot{q}_2$;

$u_{II1} \underline{\Delta} Q_1$; $u_{II2} \underline{\Delta} Q_2$; .

As in the previous case, the coupling between the two subsystems is derived in terms of the following interconnecting variables from the first subsystem.

$z_{II1} \underline{\Delta} x_{I1}$; $z_{II2} \underline{\Delta} x_{I2}$; $z_{II3} \underline{\Delta} x_{I3}$;
$z_{II4} \underline{\Delta} x_{I4}$;

$z_{II5} \underline{\Delta} x_{I5}$; $z_{II6} \underline{\Delta} x_{I6}$; $z_{II7} \underline{\Delta} x_{I7}$;

$z_{II7} \underline{\Delta} x_{I8}$; $z_{II9} \underline{\Delta} x_{I9}$; $z_{II10} \underline{\Delta} x_{I10}$.

The following are the state equations of this subsystem.

$$\begin{bmatrix} \dot{x}_{II1} \\ \dot{x}_{II2} \\ \dot{x}_{II3} \\ \dot{x}_{II4} \end{bmatrix} = \left[\begin{array}{c|c} 0 & I \\ \hline -A^{-1}K & -A^{-1}B \end{array}\right] \begin{bmatrix} x_{II1} \\ x_{II2} \\ x_{II3} \\ x_{II4} \end{bmatrix} + \left[\begin{array}{c|c} 0 & 0 \\ \hline A^{-1} & -A^{-1}A_2{}^T I_o{}^{-1} \end{array}\right] \begin{bmatrix} u_{II1} \\ u_{II2} \\ z_{II8} \\ z_{II9} \\ z_{II10} \end{bmatrix}$$

$$+ \left[\begin{array}{c} 0 \\ \hline -A^{-1}A_2{}^T I_o{}^{-1} \end{array}\right] \underline{N}_2(z_{II1}, z_{II2}, z_{II3}, z_{II4}, z_{II5}, z_{II6}, z_{II7}) \qquad (103)$$

The Optimal Control Problem

A general problem for the optimal control of interconnected dynamical systems like large flexible spacecrafts can be formulated as

$$\textit{Minimize} \quad J(\underline{x}_i, \underline{u}_i, \underline{z}_i) \quad i = 1,2,...,N \qquad (104)$$
$$\textit{w.r.t.} \ \underline{u}_i$$

where $\underline{x}_i$ is the n_i dimensional state vector of the ith subsystem, $\underline{u}_i$ is the corresponding m_i dimensional control vector and $\underline{z}_i$ is the r_i dimensional vector of interconnection inputs from the other subsystem. The integer N represents the total number of subsystems and the scalar functional J is defined by

$$J = \sum_{i=1}^{N} \left\{ P_i(\underline{x}_i(t_f)) + \int_{t_o}^{t_f} L_i \left[\underline{x}_i(t), \underline{u}_i(t), \underline{z}_i(t) \right] dt \right\} \qquad (105)$$

where $L_i \left[\underline{x}_i(t), \underline{u}_i(t), \underline{z}_i(t) \right]$ is the performance index at time t for i = 1,2,..,N subsystems. The functional J defined in equation (105) is to be minimized subject to the constraints which define the subsystem dynamics, i.e.

$$\dot{\underline{x}}_i = \underline{f}_i \left[\underline{x}_i(t), \underline{u}_i(t), \underline{z}_i(t), t \right], \ t_o \le t \le t_f$$

$$\underline{x}_i(t_o) = \underline{x}_{io} \ , \quad i = 1,2...,N \ . \tag{106}$$

Also, the minimum of J must satisfy the interconnection relationship

$$\sum_{i=1}^{N} \underline{G}_i^{*}(\underline{x}_i,\underline{z}_j) = \underline{0} \ . \tag{107}$$

The Open-loop Hierarchical Control

Using the method of Goal Coordination or infeasible method [17,22], we consider another problem which is obtained by maximizing the dual function $\Phi(\underline{\lambda})$ with respect to $\underline{\lambda}(t)$ $(t_o \leq t \leq t_f)$, where

$$\Phi(\underline{\lambda}) = \underset{\underline{x},\underline{u},\underline{z}}{Min} \left\{ \tilde{J}(\underline{x},\underline{u},\underline{z},\underline{\lambda}) \right\} \tag{108}$$

subject to constraints in equations (106) and (107). Here

$$\underline{x} = \begin{bmatrix} \underline{x}_1 \\ . \\ . \\ . \\ \underline{x}_N \end{bmatrix} \quad \underline{u} = \begin{bmatrix} \underline{u}_1 \\ . \\ . \\ . \\ \underline{u}_N \end{bmatrix} \quad \underline{z} = \begin{bmatrix} \underline{z}_1 \\ . \\ . \\ . \\ \underline{z}_N \end{bmatrix} \tag{109}$$

Also, $\underline{\lambda}$ in equation (108) is a vector of Lagrange multipliers which is given as

$$\underline{\lambda} = \begin{bmatrix} \underline{\lambda}_1 \\ . \\ . \\ . \\ \underline{\lambda}_N \end{bmatrix} . \tag{110}$$

$$\tilde{J} = \sum_{i=1}^{N} \left\{ P_i(\underline{x}_i(t_f)) + \int_{t_o}^{t_f} L_i(\underline{x}_i,\underline{u}_i,\underline{z}_i,t)\, dt + \int_{t_o}^{t_f} \underline{\lambda}^T \underline{G}_i^{*}(\underline{x}_i,\underline{z}_j,t)\, dt \right\} \tag{111}$$

$$j = 1,2,...,N$$

Rewriting this functional $\tilde{J}$ as

$$\tilde{J} = \sum_{i=1}^{N} J_i$$

$$= \sum_{i=1}^{N} \left\{ P_i(\underline{x}_i(t_f)) + \int_{t_o}^{t_f} \left[L_i(\underline{x}_i,\underline{u}_i,\underline{z}_i,t) + \underline{\lambda}^T \underline{G}_i(\underline{x}_i,\underline{z}_i,t) \right] dt \right\} \qquad (112)$$

where,

$$J_i = P_i(\underline{x}_i(t_f)) + \int_{t_o}^{t_f} \left[L_i(\underline{x}_i,\underline{u}_i,\underline{z}_i,t) + \underline{\lambda}^T \underline{G}_i(\underline{x}_i,\underline{z}_i,t) \right] dt \qquad (113)$$

and where $\underline{\lambda}^T \underline{G}_i^*(\underline{x}_i,\underline{z}_j,t)$ has been refactored into the form $\underline{\lambda}^T \underline{G}_i(\underline{x}_i,\underline{z}_i,t)$, i.e. into a form separable in the index i.

Thus,

$$\tilde{J} = J + \int_{t_o}^{t_f} \underline{\lambda}^T \sum_{i=1}^{N} \underline{G}_i(\underline{x}_i,\underline{z}_i)\, dt \qquad (114)$$

Then by the fundamental theorem of strong Lagrange duality [25]

$$\min_{\underline{u}_i} J = \max_{\underline{\lambda}} \Phi(\underline{\lambda}), \quad i = 1,2,...,N. \qquad (115)$$

Thus an alternative way of optimizing J is to maximize $\Phi(\underline{\lambda})$.

From equation (112), for a given $\underline{\lambda}(t)$, $t_o \le t \le t_f$, the functional $\tilde{J}$ is separable into N independent minimization problems, the ith of which is given by

$$Min \quad J_i = P_i(\underline{x}_i(t_f)) + \int_{t_o}^{t_f} \left[L_i(\underline{x}_i,\underline{u}_i,\underline{z}_i) + \underline{\lambda}^T \underline{G}_i(\underline{x}_i,\underline{z}_i) \right] dt \qquad (116)$$

$\underline{x}_i, \underline{u}_i, \underline{z}_i$

subject to

$$\dot{\underline{x}}_i = \underline{f}_i\,(\underline{x}_i, \underline{u}_i, \underline{z}_i)\,, \quad t_o \le t \le t_f$$
$$\underline{x}_i\,(t_o) = \underline{x}_{io} \tag{117}$$

This leads to a two-level optimization structure where on the first level, for given $\underline{\lambda}$, the N independent minimization problems described in equations (116) and (117) are solved and on the second level, the $\underline{\lambda}\,(t)$ ($t_o \le t \le t_f$) trajectory is improved by an optimization scheme like the steepest ascent method, i.e. from iteration j to $j+1$

$$\underline{\lambda}\,(t)^{j+1} = \underline{\lambda}\,(t)^j + \alpha^j + \underline{d}^j\,(t) \quad t_o \le t \le t_f \tag{118}$$

where

$$\underline{d}^j = \nabla\,\Phi(\underline{\lambda}(t)) = \sum_{i=1}^{N} \underline{G}_i\,(\underline{x}_i, \underline{z}_i)\,, \tag{119}$$

$\nabla\,\Phi\,(\underline{\lambda})$ is the gradient of $\Phi\,(\underline{\lambda})$, $\alpha_j > 0$ is the step length and $\underline{d}^j$ is the steepest ascent search direction. At the optimum $\underline{d}^j \rightarrow 0$ and the appropriate Lagrange multipier, $\underline{\lambda}$, is the optimum one.

The development of this algorithm depends on the assertion Max $\Phi(\underline{\lambda})$ = min J and this may not be valid for all nonlinear systems. Consequently, linearization of $\underline{G}_i$, and linearized equations for $\underline{f}_i$ may be required for constraints to be convex and convexity of the constraints is necessary to prove this assertion. Nevertheless, the method is attractive from the standpoint of simplicity and that the dual function is concave for this nonlinear case. This ensures that if the duality assertion is valid, the optimum obtained is the Global Optimum.

On the first level, since equation (116) is to be minimized subject to equation (117), the necessary conditions lead to a two point boundary value problem from which an open loop optimum control could be calculated. However, it is desirable to calculate a closed loop control and for this the quasilinearization approach can be utilized at level one for all subsystems. Thus an iterative scheme can be set up whereby an initial trajectory of $\underline{\lambda}(t)^*$, $t_o \le t \le t_f$ is guessed at level two and provided to level one. At level one the two-point boundary value problems of the subsystems are solved by quasilinearization. The state and control trajectories of all the subsystems obtained at level one are sent to level two. The test for optimality based on equation (119) is conducted at level two and if this is not satisfied, equation (118) is used to obtain the new $\underline{\lambda}(t)$ for the next iteration.

Subsystem Closed Loop Controllers

The closed loop controllers are obtained at the first level by solving the two-point boundary value problems of the subsystems utilizing the quasilinearization procedure. As noted in equations (116) and (117), the first level problem for the ith subsystem is

For given $\underline{\lambda}(t)$, $t_o \le t \le t_f$,

$$\min_{\underline{x}_i,\underline{u}_i,\underline{z}_i} \left\{ P_i\left[\underline{x}_i(t_f)\right] + \int_{t_o}^{t_f} \left[L_i(\underline{x}_i,\underline{u}_i,\underline{z}_i) + \underline{\lambda}^T \underline{G}_i(\underline{x}_i,\underline{z}_i) \right] dt \right\} \tag{116}$$

subject to

$$\begin{aligned} \dot{\underline{x}}_i &= \underline{f}_i(\underline{x}_i,\underline{u}_i,\underline{z}_i), \quad t_o \le t \le t_f \\ \underline{x}_i(t_o) &= \underline{x}_{io} \ . \end{aligned} \tag{117}$$

For this problem, the Hamiltonian H_i can be written as

$$H_i = L_i (\underline{x}_i, \underline{u}_i, \underline{z}_i) + \underline{\lambda}^T \underline{G}_i (\underline{x}_i, \underline{z}_i) + \underline{\eta}_i{}^T \underline{f}_i (\underline{x}_i, \underline{u}_i, \underline{z}_i) \ . \tag{120}$$

For a given $\underline{\lambda}$, the state and costate equations become

$$\dot{\underline{x}}_i (t) = \underline{f}_i (\underline{x}_i, \underline{u}_i, \underline{z}_i) \tag{121}$$

$$\dot{\underline{\eta}}_i (t) = - \frac{\partial H_i}{\partial \underline{x}_i} = - \left[\frac{\partial L_i}{\partial \underline{x}_i} + \frac{\partial \underline{G}_i{}^T}{\partial \underline{x}_i} \underline{\lambda} + \frac{\partial \underline{f}_i{}^T}{\partial \underline{x}_i} \underline{\eta}_i \right] \tag{122}$$

with

$$\frac{\partial H_i}{\partial \underline{u}_i} = \underline{0} ; \qquad \frac{\partial H_i}{\partial \underline{z}_i} = \underline{0} \tag{123}$$

It is assumed here that using the equations (122) and (123), it is possible to obtain the control $\underline{u}_i$ and the interconnect variable vector $\underline{z}_i$ which is an explicit function of $\underline{\eta}_i$ and $\underline{x}_i$, i.e.

$$\begin{aligned} \underline{u}_i &= \underline{c}_i (\underline{x}_i, \underline{\eta}_i) \\ \underline{z}_i &= \underline{d}_i (\underline{x}_i, \underline{\eta}_i) \end{aligned} \tag{124}$$

Using these relationships for $\underline{u}_i$ and $\underline{z}_i$ in equations (121) and (122), the following equations are obtained

$$\dot{\underline{x}}_i = \underline{a}_i (\underline{x}_i, \underline{\eta}_i) , \qquad t_o \le t \le t_f \tag{125}$$

$$\dot{\underline{\eta}}_i = \underline{b}_i (\underline{x}_i, \underline{\eta}_i) , \qquad t_o \le t \le t_f \tag{126}$$

with the boundary conditions

$$\underline{x}_i (t_o) = \underline{x}_{io} \tag{127}$$

and from the transversality conditions

$$\underline{\eta}_i(t_f) = \frac{\partial P_i\left[\underline{x}_i(t_f)\right]}{\partial \underline{x}_i} \quad . \tag{128}$$

Quasilinearization Procedure

The two-point boundary value problem of ith subsystem is given by equations (125) and (126) subject to boundary conditions of equations (127) and (128). This problem is solved by quasilinearization technique as follows.

Defining $\underline{y} = \begin{bmatrix} \underline{x}_i \\ \underline{\eta}_i \end{bmatrix}$,

equations (125) and (126) can be rewritten as

$$\dot{\underline{y}}(t) = \underline{F}\left[\underline{y}(t)\right] \quad . \tag{129}$$

In the quasilinearization procedure, starting from an initial guessed trajectory for $\underline{y} = \underline{y}^j(t)$, successive linearizations are performed of equation (129) in such a way that the final linear equation for $\underline{y}$ solves equation (129) to an acceptable degree subject to boundary conditions (127) and (128) which could be expressed in a more general form as

$$\underline{y}(t_o)^T A_o = \underline{b_o}^T \tag{130}$$

$$\underline{y}(t_f)^T A_f = \underline{b_f}^T \tag{131}$$

where A_o , A_f are $2n$ x n matrices.

The linearized equation of (129) about a trajectory $\underline{y} = \underline{y}^j(t)$ is obtained by Taylor series expansion as

$$\dot{\underline{y}} = \underline{F}(\underline{y}^j) + J(\underline{y}^j)(\underline{y} - \underline{y}^j) + \underline{\Psi} \tag{132}$$

where $J(\underline{y}^j)$ is the Jacobian of $\underline{F}\left[\underline{y}(t)\right]$, $t_o \le t \le t_f$, at $\underline{y}^j$ and $\underline{\Psi}$ represents the

contribution of the higher order terms. Neglecting these higher order terms, the following linear equation is obtained

$$\dot{\underline{y}} = \underline{F}(\underline{y}^j) + J(\underline{y}^j)(\underline{y} - \underline{y}^j) \quad . \tag{133}$$

If the initial guessed trajectory $\underline{y}^j$ while satisfying equations (130),(131) and (133) does not satisfy equation (129), then an iterative search can be utilized to obtain a better linearizing trajectory by various methods discussed in references 19, 20, and 21. This iterative search is given by noting that equation (133) can be written by expanding individual equations (118) and (119) by Taylor series expansion about a known trajectory $\underline{x}_i^j(t)$, $\underline{\eta}_i^j(t)$, $t \in [t_o, t_f]$, and retaining terms of up to first order. The linearized reduced differential equations are

$$\dot{\underline{x}}_i^{(j+1)} = \underline{a}_i\left[\underline{x}_i^j(t), \underline{\eta}_i^j(t)\right] + \left[\frac{\partial \underline{a}_i}{\partial \underline{x}_i}(\underline{x}_i^j(t), \underline{\eta}_i^j(t))\right]\left[\underline{x}_i^{(j+1)}(t) - \underline{x}_i^j(t)\right] + \left[\frac{\partial \underline{a}_i}{\partial \underline{\eta}_i}(\underline{x}_i^j(t), \underline{\eta}_i^j(t))\right]\left[\underline{\eta}_i^{(j+1)}(t) - \underline{\eta}_i^j(t)\right] \tag{134}$$

$$\dot{\underline{\eta}}_i^{(j+1)} = \underline{b}_i\left[\underline{x}_i^j(t), \underline{\eta}_i^j(t)\right] + \left[\frac{\partial \underline{b}_i}{\partial \underline{x}_i}(\underline{x}_i^j(t), \underline{\eta}_i^j(t))\right]\left[\underline{x}_i^{(j+1)}(t) - \underline{x}_i^j(t)\right] + \left[\frac{\partial \underline{b}_i}{\partial \underline{\eta}_i}(\underline{x}_i^j(t), \underline{\eta}_i^j(t))\right]\left[\underline{\eta}_i^{(j+1)}(t) - \underline{\eta}_i^j(t)\right] \tag{135}$$

These differential equations can be rewritten as

$$\dot{\underline{x}}_i^{(j+1)} = A_{11}(t)\underline{x}_i^{(j+1)}(t) + A_{12}(t)\underline{\eta}_i^{(j+1)}(t) + \underline{e}_1{}^j(t) \tag{136}$$

$$\dot{\underline{\eta}}_i^{(j+1)} = A_{21}(t)\underline{x}_i^{(j+1)}(t) + A_{22}(t)\underline{\eta}_i^{(j+1)}(t) + \underline{e}_2{}^j(t) \tag{137}$$

or, in the partitioned matrix form,

$$\begin{bmatrix} \dot{\underline{x}}_i^{(j+1)}(t) \\ \dot{\underline{\eta}}_i^{(j+1)}(t) \end{bmatrix} = \begin{bmatrix} A_{11}(t) & A_{12}(t) \\ A_{21}(t) & A_{22}(t) \end{bmatrix} \begin{bmatrix} \underline{x}_i^{(j+1)}(t) \\ \underline{\eta}_i^{(j+1)}(t) \end{bmatrix} + \begin{bmatrix} \underline{e}_1{}^j(t) \\ \underline{e}_2{}^j(t) \end{bmatrix} \tag{138}$$

where the matrices

$$A_{11}(t) \triangleq \frac{\partial \underline{a}_i}{\partial \underline{x}_i}, \quad A_{12}(t) \triangleq \frac{\partial \underline{a}_i}{\partial \underline{\eta}_i},$$

$$A_{21}(t) \triangleq \frac{\partial \underline{b}_i}{\partial \underline{x}_i}, \quad A_{22}(t) \triangleq \frac{\partial \underline{b}_i}{\partial \underline{\eta}_i},$$

and

$$\begin{aligned} \underline{e}_1{}^j &\triangleq -A_{11}(t)\underline{x}_i{}^j(t) - A_{12}(t)\underline{\eta}_i{}^j(t) + \underline{a}_i \\ \underline{e}_2{}^j &\triangleq -A_{21}(t)\underline{x}_i{}^j(t) - A_{22}(t)\underline{\eta}_i{}^j(t) + \underline{b}_i \end{aligned} \tag{139}$$

are evaluated at $\underline{x}_i{}^j(t)$, $\underline{\eta}_i{}^j(t)$ and hence are known functions of time.

The method of complementary functions [24] can be incorporated with this linearization of the differential equations in the implementation of iterative search.

An initial guess, $\underline{x}_i{}^o$, $\underline{\eta}_i{}^o$, $t \in [t_o, t_f]$, is used to evaluate matrices in equations (139) at the beginning of the first iteration. In the next step, n sets of solutions to the 2n homogeneous differential equations

$$\dot{\underline{x}}_i{}^{(j+1)} = A_{11}(t)\underline{x}_i{}^{(j+1)}(t) + A_{12}(t)\underline{\eta}_i{}^{(j+1)}(t) \tag{140}$$

$$\dot{\underline{\eta}}_i{}^{(j+1)} = A_{21}(t)\underline{x}_i{}^{(j+1)}(t) + A_{22}(t)\underline{\eta}_i{}^{(j+1)}(t) \tag{141}$$

are generated by numerical integration. For $(j+1)$ st iteration, these solutions are denoted by $\underline{x}_i{}^{H1}$, $\underline{\eta}_i{}^{H1}$; $\underline{x}_i{}^{H2}$, $\underline{\eta}_i{}^{H2}$; ; $\underline{x}_i{}^{Hn}$, $\underline{\eta}_i{}^{Hn}$. The boundary conditions used in generating these solutions are

$$\underline{x}_i{}^{H1}(t_o) = \underline{0}, \quad \underline{\eta}_i{}^{H1}(t_o) = \begin{bmatrix} 1\,0\,0 \ldots 0 \end{bmatrix}^T,$$

$$\underline{x}_i{}^{H2}(t_o) = \underline{0}, \quad \underline{\eta}_i{}^{H2}(t_o) = \begin{bmatrix} 0\,1\,0 \ldots 0 \end{bmatrix}^T,$$

$$\vdots \qquad\qquad \vdots \tag{142}$$

$$\underline{x}_i^{Hn}(t_o) = \underline{0}, \qquad \underline{\eta}_i^{Hn}(t_o) = \begin{bmatrix} 0\,0\,0 \ \ldots 1 \end{bmatrix}^T .$$

Next, one particular solution at $(j+1)$ denoted by $\underline{x}_i^p$, $\underline{\eta}_i^p$, is generated by numerically integrating equation (138) from t_o, to t_f, using the boundary conditions $\underline{x}_i^p(t_o) = \underline{x}_o$, $\underline{\eta}_i^p(t_o) = \underline{0}$. Then, the complete solution of equation (138) can be obtained by using the principle of superposition and is of the form

$$\underline{x}_i^{(j+1)}(t) = c_1\underline{x}_i^{H1}(t) + c_2\underline{x}_i^{H2}(t) + \ldots. + c_n\underline{x}_i^{Hn}(t) + \underline{x}_i^p(t) \tag{143}$$

$$\underline{\eta}_i^{(j+1)}(t) = c_1\underline{\eta}_i^{H1}(t) + c_2\underline{\eta}_i^{H2}(t) + \ldots. + c_n\underline{\eta}_i^{Hn}(t) + \underline{\eta}_i^p(t) \tag{144}$$

where the values of c_1 , c_2 , ... , c_n which make $\underline{\eta}_i^{(i+1}(t_f) = \underline{\eta}_f$ are to be determined. To find these values of c_1 , c_2 , ... , c_n, we let $t = t_f$ in equation (144) and write it as

$$\underline{\eta}_f = \left[\underline{\eta}_i^{H1}(t_f) \ \ \underline{\eta}_i^{H2}(t_f) \ldots \underline{\eta}_i^{Hn}(t_f) \right]^{-1} \underline{c} + \underline{\eta}_i^p(t_f). \tag{145}$$

Here, $\underline{c} \ \underline{\Delta} \left[c_1\, c_2 \ldots . c_n \right]^T$ is unknown. Solving for $\underline{c}$ yields

$$\underline{c} = \left[\underline{\eta}_i^{H1}(t_f)\, \underline{\eta}_i^{H2}(t_f) \ldots . \underline{\eta}_i^{Hn}(t_f) \right]^{-1} \left[\underline{\eta}_f - \underline{\eta}_i^p \right]. \tag{146}$$

It is important to note that the indicated matrix inversion in equation (146) has to exist in order to solve for $\underline{c}$. Substituting this solution of $\underline{c}$ into equations (143) and (144) gives the $(j+1)$ st trajectory. This completes one iteration of the quasilinearization algorithm and this trajectory can be further utilized to begin another iteration, if required. Generally, the iterative scheme is terminated by comparing the j th and $j+1$ st trajectories by calculating the norm shown in the following equation and comparing it with a preselected termination constatnt, ρ.

$$\left|\left|\begin{bmatrix}\underline{x}_i^{(j+1)}\\ \underline{\eta}_i^{(j+1)}\end{bmatrix} - \begin{bmatrix}\underline{x}_i^{j}\\ \underline{\eta}_i^{j}\end{bmatrix}\right|\right| \leq \rho \tag{147}$$

Closed Loop Control

In order to obtain the closed loop control, the solution of the linearized equation (133) can be written as

$$\underline{y}(t_f) = \phi(t_f,t)\underline{y}(t) + \int_t^{t_f} \phi(t_f,\tau)\left[\underline{F}(\tau) - J\,\underline{y}(\tau)\right]d\tau \tag{148}$$

where ϕ is the state transition matrix of the system in equation (133). Rewriting equation (148) in terms of solutions of states and costates and replacing the integral terms by $\underline{p}_i(t)$

$$\begin{bmatrix}\underline{x}_i(t_f)\\ \underline{\eta}_i(t_f)\end{bmatrix} = \begin{bmatrix}\phi_{11}(t_f,t) & \phi_{12}(t_f,t)\\ \phi_{21}(t_f,t) & \phi_{22}(t_f,t)\end{bmatrix}\begin{bmatrix}\underline{x}_i(t)\\ \underline{\eta}_i(t)\end{bmatrix} + \begin{bmatrix}p_{i1}(t)\\ \underline{p}_{i2}(t)\end{bmatrix} . \tag{149}$$

From equations (128) and (149)

$$\underline{\eta}_i(t_f) = \frac{\partial P_i}{\partial \underline{x}_i} = \phi_{21}(t_f,t)\underline{x}_i(t_f,t) + \phi_{22}(t_f,t)\underline{\eta}_i(t) + \underline{p}_{i2}(t) . \tag{150}$$

Thus,

$$\underline{\eta}_i(t) = \phi_{22}^{-1}\left[\frac{\partial P_i}{\partial \underline{x}_i} - \phi_{21}\underline{x}_i(t) - p_{i2}(t)\right]$$

$$= \phi_{22}^{-1}\left[\frac{\partial P_i}{\partial \underline{x}_i} - \underline{p}_{i2}(t)\right] - \phi_{22}^{-1}\left[\phi_{21}(t)\right] . \tag{151}$$

It is important to note here that ϕ_{22}^{-1} always exists since it is a principal minor of the state transition matrix.

Substituting equation (151) into equation (124)

$$\underline{u}_i = \underline{c}_i\,(\underline{x}_i,\, t)\ . \tag{152}$$

4. NUMERICAL DATA

The analytics developed in the previous section are utilized together with the basic SCOLE data [1] and the three dimensional linear vibration analysis [4] to generate the following numerical data.

$m_1 = 6366.46 slugs.;\quad m_2 = 12.42 slugs.;\quad \rho = 0.0955 slugs/ft.;\quad L = 130 ft.$

$G_\psi = 7.2E+8 lb/ft^2;\ (EI)_x = (EI)_y = (EI) = 4E+7 lb-ft^2;$

$$\underline{r} = \begin{bmatrix} 0.036 \\ -0.036 \\ -0.379 \end{bmatrix}$$

$$\underline{c} = \begin{bmatrix} 0 \\ 0 \\ -65.0 \end{bmatrix}$$

$$I_1 = \begin{bmatrix} 905443.0 & 0.0 & 145393.0 \\ 0.0 & 6789100.0 & 0.0 \\ 145393.0 & 0.0 & 7086601.0 \end{bmatrix}$$

$$I_2 = \begin{bmatrix} 18000.0 & -7570.0 & 0.0 \\ -7570.0 & 9336.0 & 0.0 \\ 0 & 0.0 & 27407.0 \end{bmatrix}$$

The three dimensional vibration analysis is given in terms of the first ten modal frequencies and mode shapes in table 1. Here,

$$\phi_{xi}(s) = A_{xi}\sin\frac{\alpha_i s}{L} + B_{xi}\cos\frac{\alpha_i s}{L} + C_{xi}\sinh\frac{\alpha_i s}{L} + D_{xi}\cosh\frac{\alpha_i s}{L}$$

$$\phi_{yi}(s) = A_{yi}\sin\frac{\alpha_i s}{L} + B_{yi}\cos\frac{\alpha_i s}{L} + C_{yi}\sinh\frac{\alpha_i s}{L} + D_{yi}\cosh\frac{\alpha_i s}{L}$$

$$\phi_{\psi i}(s) = A_{\psi i}\sin\alpha_{\psi i}\frac{s}{L} + B_{\psi i}\cos\alpha_{\psi i}\frac{s}{L}$$

$$\alpha_i = \left[\frac{\omega_i^2 \rho L^4}{EI} \right]^{\frac{1}{4}}$$

$$\alpha_{\psi i} = \left[\frac{DL^2 \omega_i^2}{G} \right]^{\frac{1}{2}}$$

Using these data the following matrices are obtained.

$$I_o = \begin{bmatrix} 1216640 & -1.530307 & 175667.1 \\ -31.66433 & 7082976 & -52474.84 \\ 175690 & -52503.9 & 7131493 \end{bmatrix}$$

Table 1

First Ten Flexible Modes of SCOLE Model

THREE DIMENSIONAL MODE SHAPE CHARACTERISTICS		
MODE No.	1	2
FREQ. (HZ.)	0.27804240E+00	0.31357296E+00
α	0.12012084E+01	0.12756518E+01
A_x	0.16282665E+00	0.38855291E-02
B_x	-0.19670286E+00	-0.14998387E-01
C_x	-0.16983450E+00	-0.43321018E-02
D_x	0.19616259E+00	0.14985820E-01
A_y	-0.10274618E-01	0.14219781E+00
B_y	0.57579133E-02	-0.22695797E+00
C_y	0.11810057E-01	-0.19283105E+00
D_y	-0.57220462E-02	0.22644561E+00
α_ψ	0.19360955E-01	0.21835058E-01
A_ψ	-0.50748354E-01	0.31115282E-01
B_ψ	0.13978018E-04	-0.75992337E-05
MODE No.	3	4
FREQ. (HZ.)	0.81300189E+00	0.11856099E+01
α	0.20540387E+01	0.24804687E+01
A_x	0.40868188E-01	0.80641794E-01
B_x	-0.61958845E-01	-0.67233377E-01
C_x	-0.41309992E-01	-0.80913938E-01
D_x	0.61880796E-01	0.67106316E-01
A_y	-0.22438404E-01	0.13728679E+00
B_y	0.36509234E-01	-0.11746932E+00
C_y	0.24390447E-01	-0.14085209E+00
D_y	-0.36464758E-01	0.11725057E+00
α_ψ	0.56611842E-01	0.82557693E-01
A_ψ	0.92698901E-01	-0.16158934E-03
B_ψ	-0.87320799E-05	0.10437718E-07
MODE No.	5	6
FREQ. (HZ.)	0.20536300E+01	0.49716090E+01
α	0.32645546E+01	0.49716090E+01
A_x	0.99278129E-01	0.45739784E-01
B_x	-0.92344553E-01	-0.46365581E-01
C_x	-0.99442145E-01	-0.45763106E-01
D_x	0.92225801E-01	0.46329676E-01
A_y	-0.57396019E-01	0.78612940E-01
B_y	0.53976008E-01	-0.79952853E-01
C_y	0.58114853E-01	-0.78914485E-01
D_y	-0.53906980E-01	0.79891039E-01
α_ψ	0.14300062E+00	0.33165303E+00
A_ψ	-0.16588614E-02	-0.93394833E-05
B_ψ	0.61861804E-07	0.15017211E-09

THREE DIMENSIONAL MODE SHAPE CHARACTERISTICS		
MODE No.	7	8
FREQ. (HZ.)	0.55157833E+01	0.12281249E+02
α	0.53501560E+01	0.79833305E+01
A_x	0.81311804E-01	0.44835061E-01
B_x	-0.82056569E-01	-0.44834914E-01
C_x	-0.81344923E-01	-0.44840508E-01
D_x	0.81997259E-01	0.44813000E-01
A_y	-0.47145439E-01	0.77404756E-01
B_y	0.47703590E-01	-0.77465629E-01
C_y	0.47289807E-01	-0.77475327E-01
D_y	-0.47669155E-01	0.77427782E-01
α_ψ	0.38408110E+00	0.85518143E+00
A_ψ	-0.23855560E-02	0.15830371E-05
B_ψ	0.33122041E-07	-0.98715017E-11
MODE No.	9	10
FREQ. (HZ.)	0.12890442E+02	0.23679520E+02
α	0.81789349E+01	0.11085347E+02
A_x	0.78743585E-01	0.44348498E-01
B_x	-0.78755259E-01	-0.44367373E-01
C_x	-0.78752483E-01	-0.44350511E-01
D_x	0.78717693E-01	0.44351763E-01
A_y	-0.45569244E-01	0.76707490E-01
B_y	0.45609474E-01	-0.76762782E-01
C_y	0.45607884E-01	-0.76733612E-01
D_y	-0.45587726E-01	0.76735779E-01
α_ψ	0.89760145E+00	0.16488784E+01
A_ψ	0.94995483E-03	-0.51105957E-06
B_ψ	-0.56437766E-08	0.16528495E-11

$$A_3 = \begin{bmatrix} 0.12927E+2 & -0.46332E-1 & -0.56706E-1 & -0.23671E-1 & -0.24099E0 \\ -0.46332E-1 & 0.12931E+2 & 0.50635E-1 & -0.48234E-1 & 0.13228E0 \\ -0.56706E-1 & 0.50634E-1 & 0.13644E+2 & -0.29552E-2 & -0.30599E0 \\ -0.23671E-1 & -0.48234E-1 & -0.29553E-2 & 0.12541E+2 & 0.44849E-2 \\ -0.24099E0 & 0.13228E0 & -0.30599E0 & 0.448486E-2 & 0.1324E+2 \\ 0.32322E-2 & 0.65114E-2 & -0.41218E-3 & -0.11644E-1 & -0.22449E-3 \\ 0.12271E0 & -0.71133E-1 & -0.19374E-1 & -0.14618E-2 & -0.32102E0 \\ -0.11158E-2 & -0.23852E-2 & 0.22451E-3 & 0.42121E-2 & -0.10488E-3 \\ -0.57067E-1 & 0.34303E-1 & 0.65492E-1 & 0.40936E-3 & 0.11851E0 \\ 0.12044E-2 & 0.10106E-2 & 0.54187E-3 & -0.23616E-2 & -0.18768E-2 \end{bmatrix}$$

$$\begin{bmatrix} 0.32323E-2 & 0.12271E0 & -0.11158E-2 & -0.57067E-1 & 0.12045E-2 \\ 0.65114E-2 & -0.71133E-1 & -0.23852E-2 & 0.34302E-1 & 0.10106E-2 \\ -0.41218E-3 & -0.19374E-1 & 0.2245E-3 & 0.65491E-1 & 0.54187E-3 \\ -0.11644E-1 & -0.14618E-2 & 0.42121E-2 & 0.40936E-3 & -0.23616E-2 \\ -0.22449E-3 & -0.32102E0 & -0.10488E-3 & 0.11851E0 & -0.18768E-2 \\ 0.12432E+2 & 0.17594E-3 & -0.57146E-3 & -0.10095E-3 & 0.31955E-3 \\ 0.17594E-3 & 0.12606E+2 & 0.82787E-5 & -0.67559E-1 & 0.76582E-3 \\ -0.57146E-3 & 0.82787E-5 & 0.12425E+2 & 0.10429E-4 & -0.11519E-3 \\ -0.10095E-3 & -0.67559E-1 & 0.10423E-4 & 0.12477E+2 & -0.2948E-3 \\ 0.31955E-3 & 0.76582E-3 & -0.11519E-3 & -0.2948E-3 & 0.12423E+2 \end{bmatrix}$$

$$A_2^T = \begin{bmatrix} 0.7142542E2 & -0.3890922E+3 & 0.9536207E+1 \\ 0.2384121E+3 & -0.3622244E+2 & 0.2742315E+1 \\ -0.5915277E+2 & -0.1761796E+3 & 0.2077235E2 \\ 0.2843785E+3 & -0.4696011E+1 & 0.1623039E+1 \\ -0.3872402E+3 & 0.6004922E+2 & -0.1236509E+1 \\ -0.2010108E2 & 0.3311526E2 & -0.1009266E+1 \\ 0.1731334E+3 & 0.7672109E+2 & -0.4794385E+1 \\ 0.1495208E+2 & -0.2067402E+2 & 0.6422631E0 \\ -0.81759E+2 & -0.6396428E+2 & 0.3995166E1 \\ -0.3200308E+1 & 0.1692286E+2 & -0.4793963E0 \end{bmatrix}$$

The stiffness matrix K is calculated using equation (57) and the mode shape coefficients given in Table 1. This matrix is a diagonal matrix and is represented in terms of the diagonal elements as

$$K = \begin{bmatrix} k_{1,1} = 0.3666744E2 \\ k_{2,2} = 0.4647383E2 \\ k_{3,3} = 0.3148351E3 \\ k_{4,4} = 0.6870651E3 \\ k_{5,5} = 0.2065265E4 \\ k_{6,6} = 0.1114602E5 \\ k_{7,7} = 0.1490114E5 \\ k_{8,8} = 0.7391932E5 \\ k_{9,9} = 0.8131641E5 \\ k_{10,10} = 0.2748996E6 \end{bmatrix}$$

The damping matrix B used for this analysis is a diagonal matrix and for damping ratio $\zeta = 0.003$, it is calculated to be

$$B = \begin{bmatrix} b_{1,1} = 0.9685964E-3 \\ b_{2,2} = 0.1088608E-2 \\ b_{3,3} = 0.2834016E-2 \\ b_{4,4} = 0.4256808E-2 \\ b_{5,5} = 0.7387177E-2 \\ b_{6,6} = 0.1719014E-1 \\ b_{7,7} = 0.1984237E-1 \\ b_{8,8} = 0.4421234E-1 \\ b_{9,9} = 0.4633434E-1 \\ b_{10,10} = 0.8527647E-1 \end{bmatrix}$$

5. REFERENCES

[1] L. W. Taylor, Jr. and A. V. Balakrishnan, "A Mathematical Problem and a Spacecraft Control Experiment (SCOLE) Used to Evaluate Control Laws for Flexible Spacecraft... NASA/IEEE Design Challenge," Proceedings of the Fourth VPI/AIAA Symposium on Dynamics and Control of Large Structures, pp 311-318, June 1983.

[2] A. S. Debs and M. Athans, "On the Optimal Angular Velocity Control of Asymmetrical Space Vehicles," IEEE Trans. Automat. Contr., pp 80-83, Feb. 1969.

[3] T. A. W. Dwyer, III, "The Control of Angular Momentum for Asymmetric Rigid Bodies," IEEE Trans. Automat. Contr., pp 686-688, June 1982.

[4] D. K. Robertson, "Three-dimensional Vibration Analysis of a Uniform Beam with Offset Inertial Masses at the Ends," NASA TM-86393, September 1985.

[5] T. R. Kane, P. W. Likins, and D. A. Levinson, Spacecraft Dynamics, New York: McGraw-Hill, 1983.

[6] J. Storch, S. Gates and D. O'Connor, "Three Dimensional Motion of a Flexible Beam with Rigid Tip Bodies," Charles Stark Draper Laboratory Report, Interlab Memorandum, October 1985.

[7] Y. P. Kakad, "Slew Maneuver Control of the Spacecraft Control Laboratory Experiment (SCOLE)," Proceedings of ACC Conference, pp 1039-1044 June 1986.

[8] Y. P. Kakad, "Dynamics and Control of Slew Maneuver of Large Flexible Spacecraft," Proceedings of AIAA Guidance, Navigation and Control Conference, pp 629-634, August 1986.

[9] B. Friedland, Control System Design - An Introduction to State-space Methods, New York: McGraw-Hill, 1986.

[10] H. Goldstein, Classical Mechanics, Reading: Addison-Wesley, Second Edition, 1981.

[11] M. Balas, "Feedback Control of Flexible Systems," IEEE Trans. Automat. Contr., pp 673-679, August 1978.

[12] A. E. Bryson, Jr. and Y. C. Ho, Applied Optimal Control - Optimization, Estimation, and Control, New York: John Wiley, revised printing, 1975.

[13] L. Meirovitch, Analytical Methods in Vibrations, New York: The Macmillan Company, 1967.

[14] E. S. Armstrong, "ORACLS - A System for Linear-Quadratic-Gaussian Control Law Design," NASA TP-1106, 1978.

[15] S. Joshi, "SCOLE Equations of Motion-A New Formulation," Proceedings of the 2nd Annual SCOLE Workshop, NASA TM-89048, pp. 14-25, December 1985.

[16] Y. P. Kakad, "Dynamics of Spacecraft Control Laboratory Experiment (SCOLE) Slew Maneuvers," NASA CR-4098 October 1987.

[17] M. G. Singh, Dynamical Hierarchical Control, New York: North-Holland Publishing Company, 1980.

[18] J. L. Junkins, and J. D. Turner, Optimal Spacecraft Rotational Maneuvers, New York: Elsevier Science Publishers B.V., 1986.

[19] P. L. Falb, and J. L. de Jong, Some Successive Approximation Methods in Control and Oscillation Theory, New York: Academic Press, 1969.

[20] H. B. Keller, Numerical Methods for Two-point Boundary-Value Problems, Waltham, Massachusetts: Blaisdell Publishing Company, 1968.

[21] R. E. Bellman, and R. E. Kalaba, Quasilinearization and Nonlinear Boundary-Value Problems, New York: American Elsevier Publishing Company, 1965.

[22] M. G. Singh, and A. Titli, "Closed Loop Hierarchical Control for Non-linear Systems Using Quasilinearization," Automatica, Vol. 11, pp 541-546, 1975.

[23] S. M. Roberts, and J. S. Shipman, Two-point Boundary Value Problems: Shooting Methods, New York: American Elsevier Publishing Company, 1972.

[24] M. S. Mahmoud, M. F. Hassan, and M. G. Darwish, Large-Scale Control Systems, New York: Marcel Dekker Inc., 1985.

[25] D. Luenberger, Optimization by Vector Space Methods, New York: John Wiley, 1969.

[26] D. E. Kirk, Optimal Control Theory - An Introduction, Englewood Cliffs, New Jersey, Prentice-Hall Inc., 1970.

[27] P. W. Likins, "Geometric Stiffness Characteristics of a Rotating Elastic Appandage," International Journal of Solids and Structures, Vol. 10, No. 2, 1974, pp. 161-167.

[28] A. K. Banerjee, and J. M. Dickens, "Dynamics of an Arbitrary Flexible Body in Large Rotation and Translation," Journal of Guidace, Control, and Dynamics, Vol. 13, March-April, 1990, pp. 221-227.

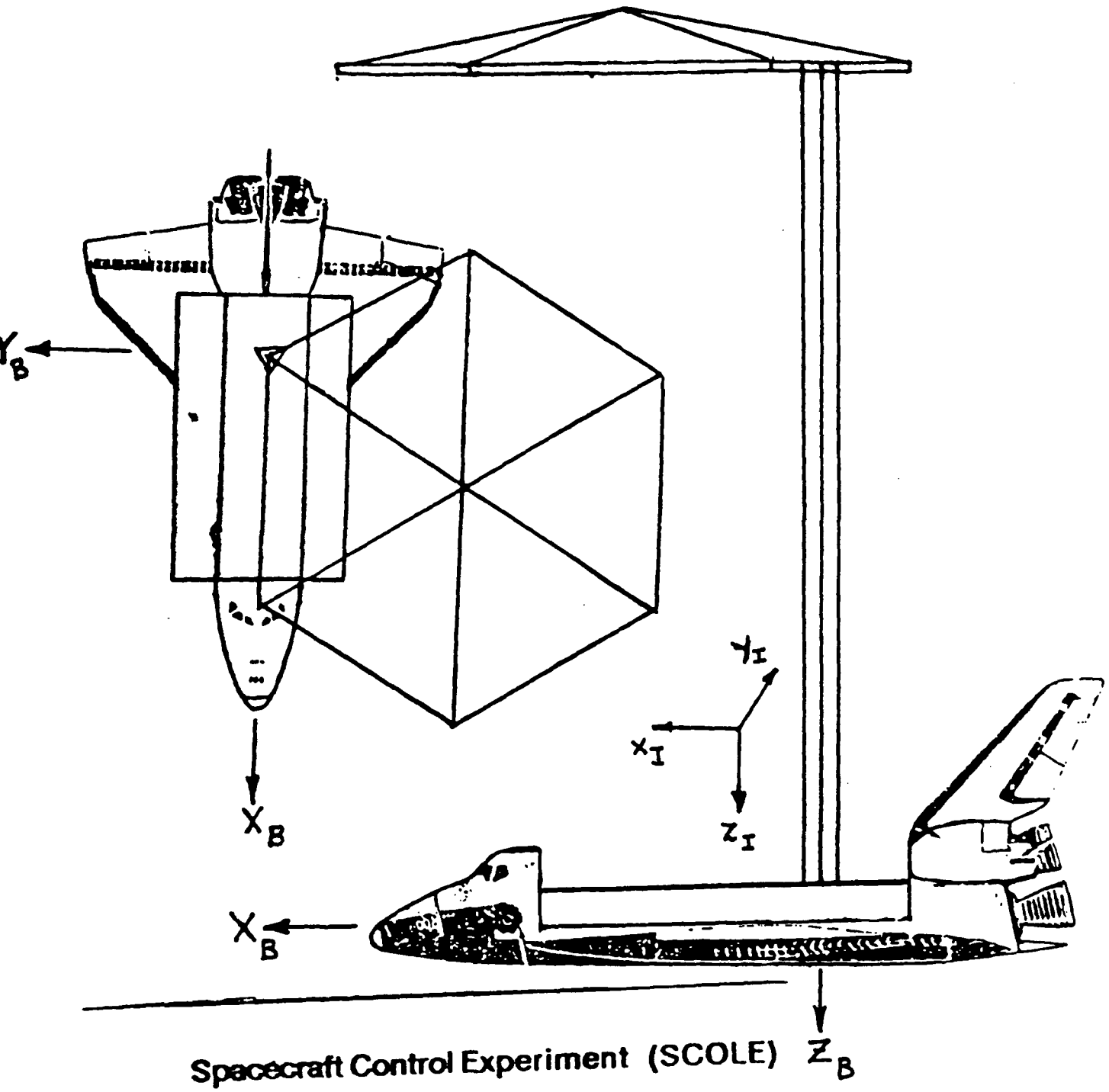
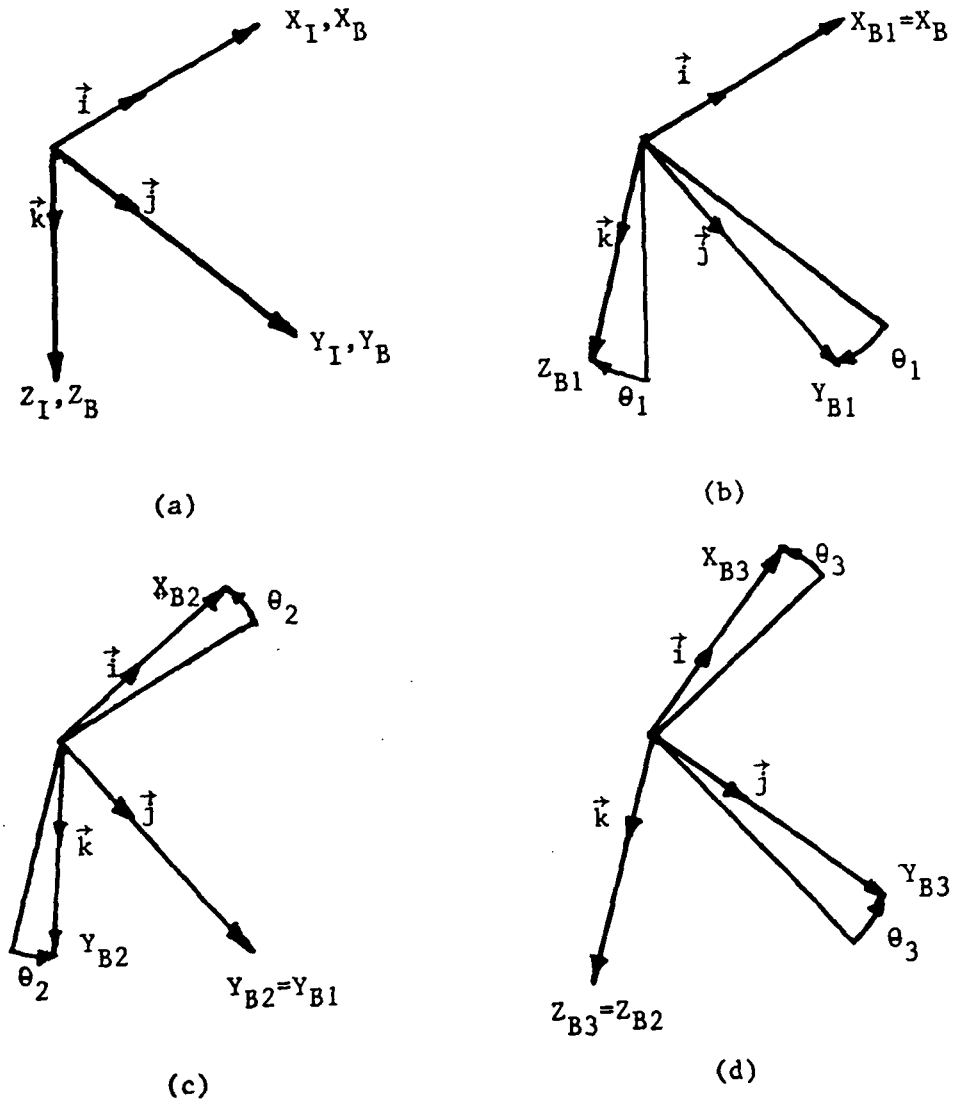


FIGURE 1



(a) Axes in reference position (b) First rotation-about x axis
(c) Second rotation-about y axis (d) Final rotation-about z axis

FIGURE 2

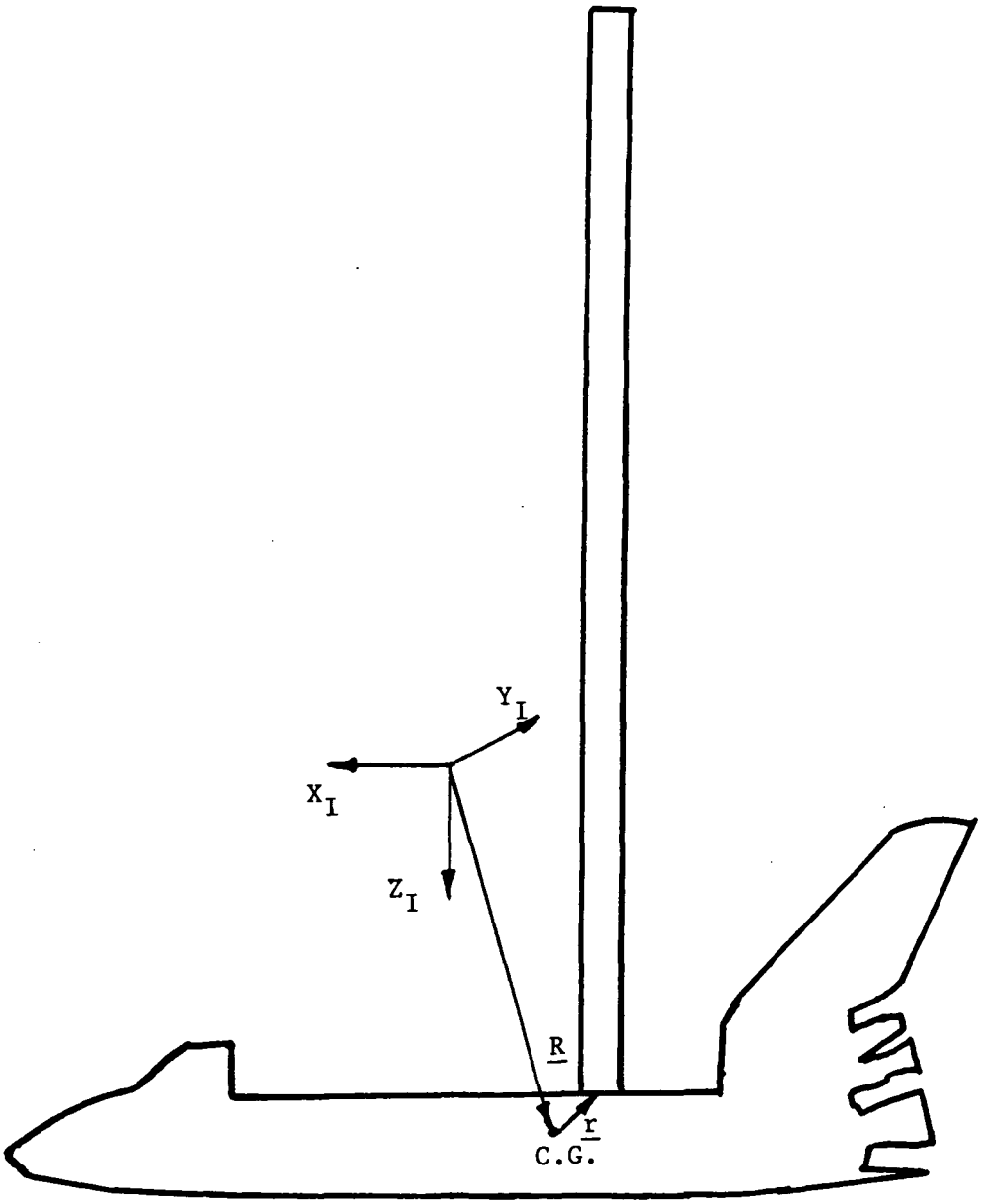


Figure 3- Position Vectors in Inertial Frame

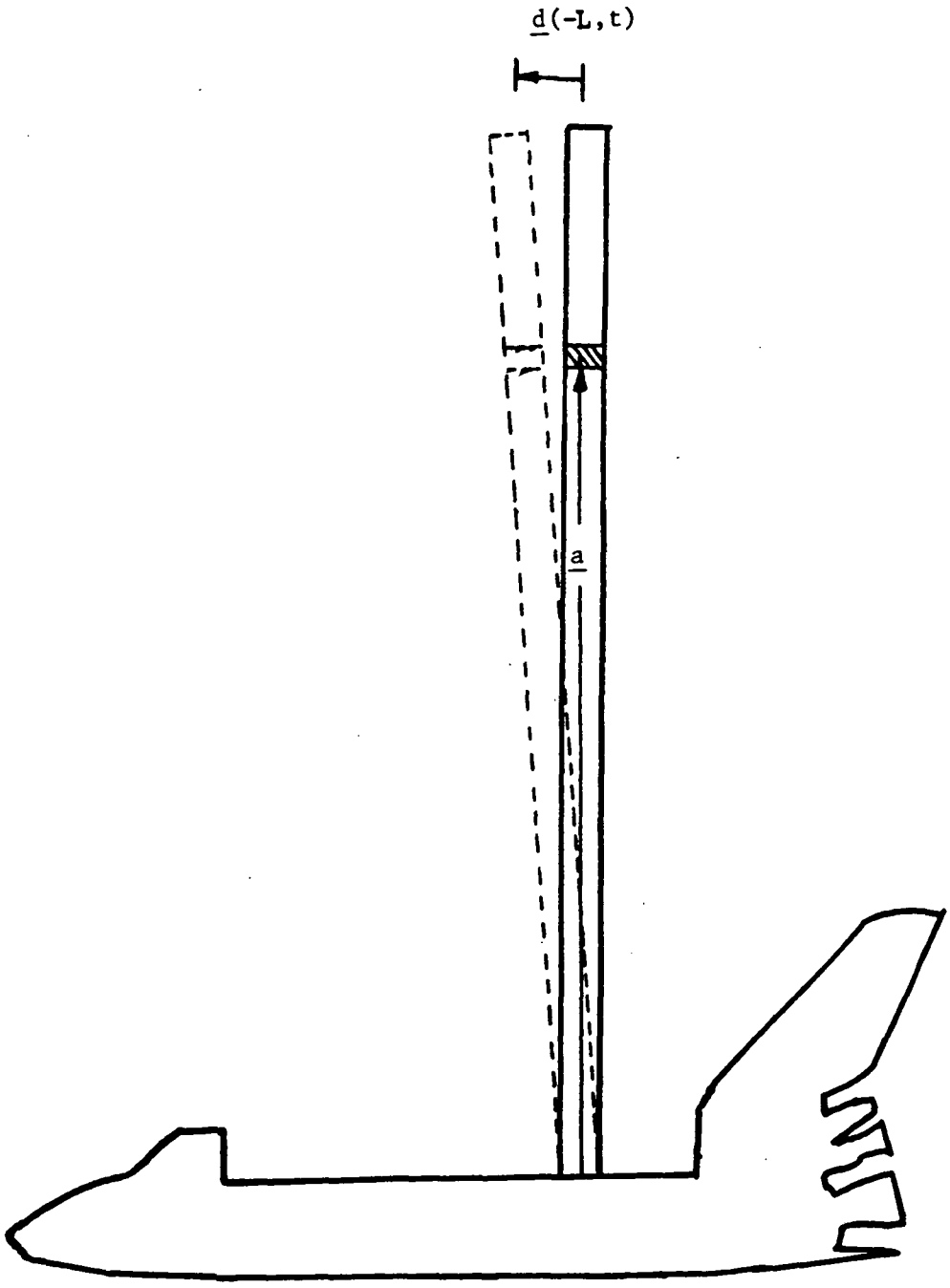


Figure 4- Vectors in Body-fixed Frame

APPENDIX I

The following is a summary of transformations between inertial frame and body-fixed frame. Here, s_i and c_i $(i=1,2,3)$ denote $\sin\theta_i$ and $\cos\theta_i$ $(i=1,2,3)$ respectively.

(a) Space-three Angles

$$C = \begin{bmatrix} c_2c_3 & c_2s_3 & -s_2 \\ s_1s_2c_3-s_3c_1 & s_1s_2s_3+c_3c_1 & s_1c_2 \\ c_1s_2c_3+s_3s_1 & c_1s_2s_3-c_3s_1 & c_1c_2 \end{bmatrix}$$

$$M^T = \begin{bmatrix} 1 & 0 & -s_2 \\ 0 & c_1 & s_1c_2 \\ 0 & -s_1 & c_1c_2 \end{bmatrix}$$

(b) Space-two Angles

$$C = \begin{bmatrix} c_2 & s_2s_3 & -s_2c_3 \\ s_1s_2 & -s_1c_2s_3+c_3c_1 & s_1c_2c_3+s_3c_1 \\ c_1s_2 & -c_1c_2s_3-c_3s_1 & c_1c_2c_3-s_3s_1 \end{bmatrix}$$

$$M^T = \begin{bmatrix} 1 & 0 & c_2 \\ 0 & c_1 & s_1s_2 \\ 0 & -s_1 & c_1s_2 \end{bmatrix}$$

(c) Body-two Angles

$$C = \begin{bmatrix} c_2 & s_1s_2 & -c_1s_2 \\ s_2s_3 & -s_1c_2s_3+c_3c_1 & c_1c_2s_3+c_3s_1 \\ s_2c_3 & -s_1c_2c_3-s_3c_1 & c_1c_2c_3-s_3s_1 \end{bmatrix}$$

$$M^T = \begin{bmatrix} c_2 & 0 & 1 \\ s_2s_3 & c_3 & 0 \\ s_2c_3 & -s_3 & 0 \end{bmatrix}$$

APPENDIX II

The transformation that relates the orientation angles $\underline{\theta}$ to Euler parameters $\underline{\varepsilon}$ is a nonlinear transformation. This transformation is developed for body-three angles representation in this appendix and similar transformations can be derived for other three representations, namely space-three angles, space-two angles, and body-two angles.

(a) For $\sin\theta_2 \neq 1$:

If $-\frac{\pi}{2} < \theta_2 < \frac{\pi}{2}$, then

$$\theta_2 = \sin^{-1}\left[\, 2(\varepsilon_3\varepsilon_1 + \varepsilon_2\varepsilon_4)\right] \,. \tag{A.1}$$

If $(\cos\theta_1\cos\theta_2) \geq 0$, then

$$\theta_1 = \sin^{-1}\left[\frac{-2\,(\varepsilon_2\varepsilon_3 - \varepsilon_1\varepsilon_4\,)}{\cos\left\{\sin^{-1}\left[\,2(\,\varepsilon_3\varepsilon_1 + \varepsilon_2\varepsilon_4\,)\right]\right\}}\right] . \tag{A.2}$$

If $(\cos\theta_1\cos\theta_2) < 0$, then

$$\theta_1 = \pi - \sin^{-1}\left[\frac{-2\,(\varepsilon_2\varepsilon_3 - \varepsilon_1\varepsilon_4\,)}{\cos\left\{\sin^{-1}\left[\,2(\,\varepsilon_3\varepsilon_1 + \varepsilon_2\varepsilon_4\,)\right]\right\}}\right] . \tag{A.3}$$

If $(\cos\theta_2\cos\theta_3) \geq 0$, then

$$\theta_3 = \sin^{-1}\left[\frac{-2\,(\varepsilon_1\varepsilon_2 - \varepsilon_3\varepsilon_4\,)}{\cos\left\{\sin^{-1}\left[\,2(\,\varepsilon_3\varepsilon_1 + \varepsilon_3\varepsilon_2\,)\right]\right\}}\right] . \tag{A.4}$$

If $(\cos\theta_2 \cos\theta_3) < 0$, then

$$\theta_3 = \pi - \sin^{-1}\left[\frac{-2\,(\varepsilon_1\varepsilon_2 - \varepsilon_3\varepsilon_4\,)}{\cos\left\{\sin^{-1}\left[\,2(\,\varepsilon_3\varepsilon_1 + \varepsilon_3\varepsilon_2\,)\right]\right.} \right] . \qquad \text{(A.5)}$$

(b) For $\sin\theta_2 = \pm 1$, θ_2 is a constant. For $\sin\theta_2 = 1$, $\theta_2 = \frac{\pi}{2}$. However, if $\sin\theta_2 = -1$, then $\theta_2 = -\frac{\pi}{2}$. For this case, if $(\sin\theta_1 \sin\theta_2 \sin\theta_3 + \cos\theta_3 \cos\theta_1\,) \geq 0$, then

$$\theta_1 = \sin^{-1}\left[\,2\,(\,\varepsilon_2\varepsilon_3 + \varepsilon_1\varepsilon_4\,)\right] . \qquad \text{(A.6)}$$

If $(\sin\theta_1 \sin\theta_2 \sin\theta_3 + \cos\theta_3 \cos\theta_1\,) < 0$, then

$$\theta_1 = \pi - \sin^{-1}\left[\,2\,(\,\varepsilon_2\varepsilon_3 + \varepsilon_1\varepsilon_4\,)\right] . \qquad \text{(A.7)}$$

For this entire case, $\theta_3 = 0$.

APPENDIX III

Feedback Linearization and Control of NASA SCOLE System by Output Feedback

Misbahul Azam, Sahjendra N. Singh, Ashok Iyer

Department of Electrical and Competer Engineering
University of Nevada Las Vegas
Las Vegas, NEVADA 89154

and

Y. P. Kakad

Department of Electrical Engineering
University of North Carolina Charlotte
Charlotte, NORTH CAROLINA

Abstract

We treat the question of large rotational maneuver and vibration stabilization of NASA Spacecraft Control Laboratory Experiment system (SCOLE). The mathematical model of SCOLE system includes the dynamical equations for rigid body slew maneuver and three-dimensional vibration of the rigid shuttle, the flexible beam and the reflector with an offset mass. The design approach taken here is to decompose the rigid mode control from vibration stabilization. Feedback input (Shuttle torque)-output (attitude angles) map linearization technique is used for designing attitude control system for large-angle slewing. Linearization of input-output (i-o) map is accomplished by nonlinear *inversion* theory. It is shown that attitude control system assymptotically decouples the flexible dynamics and linear feedback law is easily designed for vibration suppression. For the synthesis of the control law an *observer* is designed. Simulation results are presented to show in the closed-loop system large angle maneuver can be accomplished using only the measured state variables .

1. Introduction

An important class of shuttle deployed payloads consists of cantilevered beam-like structures with massive tip bodies. A design challange was posed by *Taylor and Balakrishnan* [1] for the control of such a system. In the design challange, the Spacecraft Control Laboratory Experiment (SCOLE) was set up by NASA Langley Research Center to provide a standerd configuration to test control laws for investigators.

The laboratory apparatus includes the Space Shuttle (orbiter) connected by a long (130ft) flexible beam to hexagonal antenna or reflector, as shown in Fig. 1. The reflector and Shuttle are treated as rigid bodies. When the Shuttle maneuvered, the flexible modes of the beam are excited. Two force actuators and a torquer have been provided to exert sufficient force to suppress the unwanted vibration of the beam.

The design challange attracted the attention of many researchers. Research related to both dynamics and control system design has been performed and reported in litrature and SCOLE workshops at NASA Langley Research Center [2-10]. Nonlinear invertibility theory has been used in [11-12] for designing controller for a simplified spacecraft system. For such a system adaptive control system and sliding mode controllers have been also designed to compensate for parameter uncertainty and disturbance torques acting on the spacecraft [13-14].

We treat the question of large-angle rotational maneuver and elastic mode stabilization of SCOLE system based on input (Shuttle torque)-output (attitude angles) feedback linearization for attitude control and linear feedback for vibration suppression. An i-o feedback linearizing control law is derived by using the *inversion* theory for nonlinear dynamical systems. The *inverse* technique gives rise to decouple linear attitude dynamics and allows independent control of attitude angles. The use of *inversion* theory has an additional advantage since the elastic dynamics of the SCOLE configuration representing transverse vibration in two orthogonal plans and the torsional deformation of the elastic beam are assyptotically decoupled from the rigid mode dynamics. Since as usual only small elastic deformations are assumed here, the decoupled elastic dynamics are linear. Using linear control theory stabilizer is then designed for elastic mode stabilization. For the synthesis

of the controller only attitude angles, angular rates, tip elastic deflection components and torsion deflection at the tip of the beam are assumed to be measured by sensors. An *observer* is designed to estimate the elastic modes and their derivatives, and these are used for synthesizing the control law. Although the design approach has similarity to that of [11], this study differs in several ways. The mathematical model considerably differs from that of [11] since the end body combined here has mass and inertia also torsional modes are included. Furthermore, representation of elastic deformation differs from [11]. The design of observer has led to realistic implimentation of control law in this paper using measured variables. The control of [11] requires knowledge of the complete state vector.

The organization of the paper is as follows. Section 2 presents the mathematical model. Inverse attitude control law is derived in section 3. Section 4 presents elastic mode stabilizer. Observer design is presented in section 5 and finally section 6 presents simulation results.

2. Mathematical Model of SCOLE System

We shall be interested in the rotational and elastic dynamics of SCOLE system in this study. To describe the orientation of the orbiter a body fixed orthogonal coordinate system with axes x,y,z is utilized. The attitude of the orbiter is defined by a sequence of rotation $\theta_1, \theta_2, \theta_3$ (roll,pitch,yaw), with respect to an *inertial* coordinate system. The body-fixed coordinate frame has its origin at the point of attachment of the flexible appendage with the rigid Shuttle for this study.

The orientation of the orbiter is completely described by the differential equations relating the rotation angles and the angular velocity components $(\omega_1, \omega_2, \omega_3)$ of the orbiter which are

$$\dot{\theta} = M^{-T}\omega \tag{1}$$

where

$$M^{-T} \triangleq (M^T)^{-1}$$

and

$$M^T = \begin{bmatrix} cos\theta_2 cos\theta_3 & sin\theta_3 & 0 \\ -cos\theta_2 sin\theta_3 & cos\theta_3 & 0 \\ sin\theta_2 & 0 & 1 \end{bmatrix}$$

The elastic beam is allowed to undergo transverse elastic deformations along axes x and y, and torsional deformation about axis z. Elastic deformations are assumed to be linear combinations of admissible functions $\phi_{xi}(s), \phi_{yi}(s)$ and $\phi_{\psi i}(s)$, i=1,2,3,...,n, where s denotes the distance on the beam from the attachment point of the beam and the orbiter. The chosen admissible functions are

$$\phi_{xi}(s) = A_{xi}sin\frac{\alpha_i s}{L} + B_{xi}cos\frac{\alpha_i s}{L} + C_{xi}sinh\frac{\alpha_i s}{L} + D_{xi}cosh\frac{\alpha_i s}{L} \tag{2}$$

$$\phi_{yi}(s) = A_{yi}sin\frac{\alpha_i s}{L} + B_{yi}cos\frac{\alpha_i s}{L} + C_{yi}sinh\frac{\alpha_i s}{L} + D_{yi}cosh\frac{\alpha_i s}{L} \tag{3}$$

$$\phi_{\psi i}(s) = A_{\psi i}sin\alpha_{\psi i}\frac{s}{L} + B_{\psi i}cos\alpha_{\psi i}\frac{s}{L} \tag{4}$$

The parameters A_{xi}, A_{yi}, α_i etc, are explained in [5].

The elastic deformations are explained as linear combinations of admissible functions as

$$u_x(s) = \sum_{i=1}^{n} \phi_{xi}(s)q_i(t) \tag{5}$$

$$u_y(s) = \sum_{i=1}^{n} \phi_{yi}(s)q_i(t) \tag{6}$$

$$u_\psi(s) = \sum_{i=1}^{n} \phi_{\psi i}(s)q_i(t) \tag{7}$$

where u_x, u_y are the elastic deformations along x, y axes and u_ψ is the torsional deformation about z-axis respectively. Here q_i(t), i=1,2,3,...,n, are the modal deformation co-ordinates for the beam. Define $\omega = (\omega_1, \omega_2, \omega_3)^T, q = (q_1, q_2, ..., q_n)^T$ (T denotes transposition). Let $G_0 = (G_{01}, G_{02}, G_{03})^T$ be the external torquue vector applied on the orbiter, $F = (F_x, F_y)^T$ be the external control forces applied at the reflector center of the mass and $M_{\psi r}$ be the moment applied about z-axis at the reflector center of mass.

The equations of motion are obtained by using *Lagrangian* approach. For this, the expressions for the kinetic and potential energies are first obtained. The potential energy includes the *strain* energy due to transverse bending as well as due to torsional deformation of the elastic beam. The complete equations of motion describing rotational and elastic behavior of the SCOLE system have been derived in [5] (Readers may refer for the details). In this

study we shall be interested only in the rotational and elastic dynamics. These are

$$\begin{bmatrix} I_0 & A_2 \\ A_2^T & A_3 \end{bmatrix} \begin{bmatrix} \dot{\omega} \\ \ddot{q} \end{bmatrix} = \begin{bmatrix} N_2(\theta, \dot{\theta}, \omega, \dot{q}) \\ -Kq \end{bmatrix} + \begin{bmatrix} B_1 \\ B_2 \end{bmatrix} u \tag{8}$$

where $\theta = (\theta_1, \theta_2, \theta_3)^T$, $\mathbf{K}$ is the stiffness matrix, $\mathbf{N_2}$ is a nonlinear vector function, $\mathbf{B_i}$ (i=1,2,3,...,n) are the constant input matrices, $u = (G_0^T, F^T, M_{\psi r})^T \in R^6$ is the control input vector and

$$B_1 = [I_{3\times 3} \quad B_{12}]$$
$$B_2 = [O_{n\times 3} \quad B_{22}]$$

Here $\mathbf{I}$ and $\mathbf{O}$ denote identity and null matrices of indicated dimensions. The matrix $\mathbf{D}$

$$D = \begin{bmatrix} I_0 & A_2 \\ A_2^T & A_3 \end{bmatrix}$$

is possitive definite symmetric matrix.

Defining the state vector x=$(\theta^T, \omega^T, q^T, \dot{q}^T)^T \in R^{n_0}, n_0 = (2n + 6)$, one can obtain a state variable representation from (8) of the form

$$\dot{x} = \bar{f}(x) + Bu \tag{9}$$

where

$$\bar{f}(x) = ((M^{-T}\omega)^T, f_\omega^T(x), \dot{q}^T, f_q^T(x))^T \tag{10}$$

$f_\omega(x), f_q(x)$ and $\mathbf{B}$ are easily determined by comparing (8) and (9).

Let the controlled output vector be

$$y = \theta = c(x) \tag{11}$$

and $y_c(t) \in R^3$ be any given reference trajectory. We are interested in deriving a control law such that in the closed-loop system the output *y(t)* tracks the reference trajectory $y_c(t)$, and elastic modes are stabilized. This design objective will be accomplished by designing an *inverse* attitude controller for the orbiter for attitude angle tracking using orbiter moments; and an elastic mode stabilizer for vibration suppression using tip body external forces and moments.

3. Inverse Attitude Control

In this section the design of control system for attitude trajectory tracking is considered. To derive the control law the inversion of the input (G_0)-output (θ) map is considered. In the following, an inversion algorithm [15-16] will be used to obtain an invertible system which will give the structure of the controller. This algorithm essentially gives a systematic procedure for obtaining a sequence of systems by the differentiation of the output and applying nonlinear transformations. Although, the algorithm is applicible for more general systems, the actuator dynamics have been neglected here for simplicity.

Let $\mathbf{B}_g$ be the first three columns of matrix $\mathbf{B}$ and $\mathbf{B} = [B_g \quad B_r]$. Then the system (9) can be written as

$$\dot{x}(t) = f(x, u_r) + B_g u_g \tag{12}$$

where

$$u = (u_g^T, u_r^T)$$

$$u_g = G_0$$

$$u_r = (F^T, M_{\psi r})^T$$

and

$$f(x, u_r) = \bar{f}(x) + B_r u_r$$

In the following we define certain operators which will be useful in the sequel. For the vector function $c(x)$, we define

$$\begin{aligned} L_f(c)(x) &= [\partial c(x)/\partial x] f(x) \\ L_f^2(c)(x) &= L_f(L_f(c))(x) \\ L_{B_g} L_f(c)(x) &= [\partial L_f(c)(x)/\partial x] B_g \end{aligned} \tag{13}$$

Differentiating y and using (12) gives System 1 and System 2 of the form

System 1:

$$\dot{x}(t) = f(x, u_r) + B_g u_g$$

$$z_1 = L_f(c)(x) \tag{14}$$

System 2:

$$\dot{x}(t) = f(x, u_r) + B_g u_g$$

$$z_2 = L_f^2(c)(x, u_r) + D^*(x) u_g \tag{15}$$

where $L_f^2(c)(x)$ is easily obtained using definition (13), $z_1 = \dot{y}$, $z_2 = \ddot{y}$, and $D^*(x) = L_{B_g} L_f(c)(x)$. Let $\mathbf{R}$ be the 3×3 submatrix formed by the first three rows and first three columns of D^{-1}. Then it can be easily seen that

$$D^* = M^{-T} R \tag{16}$$

We shall be interested in a region Ω of the state space where $\Omega = \{x: \theta_2 \neq \pi \pm \pi/2\}$. We notice that $\mathbf{R}$ is nonsingular and M^{-T} exists in Ω. Thus D^* is invertible in Ω and each component of the output has relative degree 2. The *inversion* algorithm terminates here; and System 2 is invertible.

Following [11], in view of (15), one obtains an i-o feedback linearizing control of the form

$$u_g = D^{*-1}[-L_f^2(c)(x) - P_2\dot{\tilde{\theta}} - P_1\tilde{\theta} - P_0 x_s + \ddot{\theta}_c] \tag{17}$$

where $P_i = diag(p_{i,j})$, *i=0,1,2; j=1,2,3;* $\tilde{\theta}=(\theta - \theta_c)$ is the tracking error and x_s is the integral of the tracking error, *i.e*,

$$\dot{x}_s = \tilde{\theta} \tag{18}$$

The nonlinear control law includes *proportional, derivative* and *integral* (PID) type feedback. Integral feedback of trajectory error introduces robustness in the control system.

Substituting control law (17) in the output equation (15), gives

$$\dddot{\tilde{\theta}} + P_2\ddot{\tilde{\theta}} + P_1\dot{\tilde{\theta}} + P_0\tilde{\theta} + P_0 x_s = 0 \tag{19}$$

which can be differentiated to yield

$$\dddot{\tilde{\theta}} + P_2\ddot{\tilde{\theta}} + P_1\dot{\tilde{\theta}} + P_0\tilde{\theta} = 0 \tag{20}$$

It is obvious from (20) that each component $\tilde{\theta}_i(t)=(\theta_i(t) - \theta_{ci}(t))$ can be independently controlled where $\theta_c = (\theta_{c1}, \theta_{c2}, \theta_{c3})^T$. Let the characteristic polynomial associated with $\tilde{\theta}_i$ in (20) is of the form

$$(s + \lambda_{ci})(s^2 + 2\zeta_{ci}\omega_{nci}s + \omega_{nci}^2) = 0 \tag{21}$$

The matrices P_i are easily determined from (21). The parameters λ_{ci}, ζ_{ci}, and ω_{nci} are chosen such that (20) is assymptotically stable.

The *inverse* attitude control law causes tracking of the command trajectory θ_c. Indeed if matching conditions

$$\begin{aligned} \tilde{\theta}(0) &= 0 \\ \dot{\tilde{\theta}}(0) &= 0 \\ \ddot{\tilde{\theta}}(0) &= 0 \end{aligned} \tag{22}$$

are satisfied; one has $\theta(t) \equiv \theta_c(t)$, $t \geq 0$, and $\theta_c(t)$ is exactly reproduced. However, slewing of the spacecraft excites the flexible modes and it becomes essential to damp the elastic oscillations so that the target in the space is tracked.

4. Elastic Mode Stabilizer

We assume in this section that the reference trajectory is such that $\theta_c(t) \rightarrow \theta^*$, where θ^* corresponds to a desired terminal orientation of the orbiter and $\dot{\theta}_c \rightarrow 0$, $\ddot{\theta}_c \rightarrow 0$, as $t \rightarrow \infty$. For such a trajectory, in the closed-loop system, one has $\theta(t) \rightarrow \theta_c \rightarrow \theta^*$, and $\dot{\theta}(t) \rightarrow 0$, $\dot{\omega}(t) \rightarrow 0$, $\ddot{\theta}(t) \rightarrow 0$, as $t \rightarrow \infty$. Interestingly, in the closed-loop system, in view of (8), the elastic dynamics are assymptotically decoupled, and reduces to

$$A_3\ddot{q} = -Kq + B_{22}u_r \tag{23}$$

Defining $z=(q^T, \dot{q}^T)$, one obtains a state variable for (23) as

$$\dot{z} = \begin{bmatrix} 0_{n\times n} & I_{n\times n} \\ -A_3^{-1}K & 0_{n\times n} \end{bmatrix} z + \begin{bmatrix} 0 \\ A_3^{-1}B_{22} \end{bmatrix} u_r \tag{24}$$

$$\dot{z} \triangleq A_e z + B_e u_r$$

For the stabilization of (24), one can use *linear quadratic optimization* or *pole assignment* technique. We have chosen pole assignment technique in this study. The closed-loop poles are chosen to be located at -.2±.1j, -.2±.3j, -.2±.5j, and -.2±.7j
The linear feedback control law is

$$u_r = -F_e z \tag{25}$$

The closed-loop system matrix $A_{ec} = (A_e - B_e F_e)$ is a *Hurwitz* matrix.

It is interesting to note that use of *inverse* attitude controller simplifies the stabilization problem to a linear design problem of a lower order system and this design is carried out independently.

5. Observer Design

The control laws (17) and (25) require knowledge of complete ststе variables. We assume that only measured variables are θ, ω, and the elastic deformation $u_x(L)$, $u_y(L)$, and $u_\psi(L)$ at the tip of the beam. For the synthesis of the controller, it is essential to construct the variables q and $\dot{q}$. With these measurements, the system (8) can be considered as an online linear time-varying system since the nonlinear function is of the form $N_2 = N_{2c}(\theta, \dot{\theta}, \omega) + N_{2f}(\theta, \dot{\theta}, \omega)\dot{q}$ which is linear in $\dot{q}$ and N_{2f} depends on measured variables. However, design of observer for a time varying system is not easy. Since N_2 contains terms of second order in derivatives of θ_i, and q_i; N_{2f} is small and , therefore, it can be neglected for simplicity in design of the observer.

Setting $N_{2f}\dot{q}$=0 in N_2 in (8); one obtains the following equation for elastic modes

$$\ddot{q} = R_2 \begin{bmatrix} N_{2c}(\theta, \dot{\theta}, \omega) + B_1 u \\ -Kq + B_2 u \end{bmatrix} \tag{26}$$

where R_2 consists of last n rows of D^{-1}. Since N_{2c}, and u are known, a state variable representation of (26) is

$$\dot{z} = \begin{bmatrix} 0 & I \\ -R_{22}K & 0 \end{bmatrix} z + g(\theta, \dot{\theta}, \omega, u) \tag{27}$$

where g is obtained from (26), $\mathbf{R}_2 = [R_{21} \quad R_{22}]$, and R_{22} is $n \times n$ matrix. The associated measurement equation is linear function of q of the form

$$y_m = C_m q \tag{28}$$

Define A_m as

$$A_m = \begin{bmatrix} 0 & I \\ -R_{22}K & 0 \end{bmatrix}$$

then the state observer takes the form

$$\dot{\hat{z}} = A_m \hat{z} + g(\theta, \dot{\theta}, \omega, u) + H(y_m - C_m \hat{z}) \tag{29}$$

where $\hat{z}$ is the estimate of state z, and the matrix H is determined such that the matrix $(A_m - HC_m)$ is *Hurwitz*. Again, the matrix H can be found using *LQR* or *pole assignment* technique. In this study, we use the pole assignment technique.

The observation error $\tilde{z} = (z - \hat{z})$ satisfies

$$\dot{\tilde{z}} = (A_m - HC_m)\tilde{z} \tag{30}$$

which is assymptotically stable and $z(t) \rightarrow \tilde{z}$, as $t \rightarrow \infty$. For simulation matrix H is chosen such that the observer poles (eigen values of $[A_m - HC_m]$) are at $-8 \pm 4j$, $-8 \pm 6j$, $-8 \pm 8j$, $-8 \pm 10j$.

For the synthesis of the controller, q, $\dot{q}$ in control law (17) and (25) are replaced by $\hat{q}$ and $\dot{\hat{q}}$. The complete closed-loop system is shown in Fig. 2.

6. Simulation Results

We present here the results of digital simulation for various initial conditions and parameters. The appendix lists the maximum limits of control inputs system. The mass of the antenna is $400 lbs$, and the mass of the Shuttle body is $2.050 \times 10^5 lbs$ [8].

For tracking a representative command *reference trajetory* is generated using a third order filter

$$\dddot{\theta}_{ci} + (2\zeta_{ci}\omega_{nci} + \lambda_{ci})\ddot{\theta} + 2(\zeta_{ci}\omega_{nci}\lambda_{ci} + \omega_{nci}^2)\dot{\theta}_{ci} + \omega_{nci}^2\lambda_{ci}\theta_{ci} = \omega_{nci}^2\lambda_{ci}\theta^* \tag{31}$$

such that its poles are at $-\lambda_{ci}$ and $\{-\zeta_{ci}\omega_{nci} \pm j\omega_{nci}(1 - \zeta_{ci}^2)^{1/2}\}$. The paramaters chosen are $\zeta_{ci} = .707$, and $\omega_{nci} = \lambda_{ci}/\zeta_{ci}$. By a prorer choice of λ_{ci},

one can obtain desireable fast reference attitude trajestories for trcking. The terminal angles θ_i^* are chosen 4°, 10°, and 25° (roll, pitch, and yaw respectively).

(a) **Trajectory Control: Stabilizer Open Loop**

In order to observe the behavior of the closed-loop system (8), (17), and (18), this simulation was done *without* the stabilizer. In this case the forces and moment $M_{\psi r}$ are zero. The initial conditions were set as $\theta(0)$=0, $\omega(0)$=0, $x_s(0)$=0, $q(0)$=0, $\hat{q}(0)$=(-.1,-.1,-.1,-.1), $\dot{q} = \dot{\hat{q}} = 0$. The elastic mode error $(q(0) - \hat{q}(0))$ was introduced to examine the state reconstruction ability of the observer. Only measured and estimated states are used for synthesis of the contrller. Selected response plots are shown in Fig. 3. The response time for the θ is nearly *20 seconds.* The simulation results show the periodic and bounded oscillations of elastic modes and control moments as expected.

(b) **Trajectory Control: Stabilizer Loop Closed**

The complete closed-loop system *including* the stabilizer (24), and (25) was simulated. The initial conditions and inverse controller parameters of case *(a)* were retained. The selected simulation results are shown in Fig. 4. The attitude angle response remained very similar to those of case *(a).* The stabilizer was switched at *20* seconds. The stabilizer exerts a force in both x and y axes which causes a sudden change in responses when it is switched on. The poles of the stabilizer are properly selected such that the elastic oscillations are rapidly suppressed. Although, one can design a stabilizer for even faster stabilization, this will require larger control forces and moments. We notice only a small elastic deformation. Of course, the actual deformation will be more since the contribution of residual modes need to be added. We observed smooth attitude trajectory following and elastic mode stabilization.

7. Conclusion

The control of slewing maneuvers of NASA SCOLE system was considered. The design was accomplished by decomposing the slew maneuver problem from the elastic mode stabilization problem. Orbiter orientation control system was designed using nonlinear i-o map *inversion* theory. Using the inverse attitude controller any smooth attitude trajectory can be followed. The inverse controller includes PID feedback of attitude errors. Stabilization of elastic modes was accomplished by a linear stabilizer using end body forces and moment. Interestingly, the design of stabilizer was carried out offline seperately. For the synthesis of the controller, a linear state estimater was designed using elastic deformations of the beam at the tip. Extensive simulation results showed that the large maneuvers of the spacecraft can be performed to follow precise attitude trajectories and elastic modes can be stabilized using only output feedback.

8. References

1. Taylor, L. W. and Balakrishnan, A. V., "A Laboratory Experiment Used to Evaluate Control Laws for Flexible Spacecraft...NASA/IEEE Design Challange," *Proceedings of the Fourth AIAA/VPI&SU Symposium on Dynamics and Control of Large structures,* AIAA, New York, 1983, pp. 311-318; revised June 1984.

2. Taylor, L. W. (ed), *SCOLE Workshop-1986. Proceedings,* NASA TM 80975, Nov. 1986;*SCOLE Workshop-1985. Proceedings,* NASA TM 89048, Dec. 1985; *SCOLE Workshop-1984, Proceedings,* Dec. 1984, NASA Lanley Research Center, Hampton, VA.

3. Meirovitch, L. and Quinn, R. D., "Equations of Motion for Maneuvaring Flexible Spacecraft," *Journal of Guidance, Controls, and Dynamics.*

4. Lin, J. G., "Rapid Torque Limited Line-of-Sight Pointing of SCOLE," *Proceedings of the AIAA Guidance, Nevigation and Control Conference,* AIAA, New York, 1986, pp. 106-114.

5. Kakad, Y. P., "Dynamics of Spacecraft Control Laboratory Experiment (SCOLE) Slew Maneuvar," NASA CR 4098, Oct. 1987.

6. Kakad, Y. P., "Dynamics and Control of Slew Maneuvar of Large, Flexible Spacecraft," *Proceedings of the AIAA Guidance, Navigation and Control Conference,* AIAA, New York, 1986, pp. 629-634.

7. Bainum, P. M., et al. "The Dynamics and Control of Large Flexible Space Structures-X," Final Report, Part II, NASA Grant NSG-1414, Suppl. 9, Howerd University, Washington D.C. 20059, Jan. 1988.

8. Fisher, S., "Application of Actuators to Control Beam Flexure in a Large Space Structure," *Journal of Guidance, Control, and Dynamics* Nov.- Dec. 1989. pp. 874-879.

9. Storch, J. and Gates, S., "Three Dimensional Motion of a Flexible Beam with Rigid Tip Bodies," *Charles Stark Draper Laboratory Report,* Inter-lab Memorandum, Oct. 1985.

10. Joshi, S., "SCOLE Equations of Motion-A New Formulation," *Proceedings of the Second Annual SCOLE Workshop,* NASA TM-89048, Dec. 1985, pp. 14-25.

11. Singh, S. N., "Flexible Spacecraft Maneuver: Inverse Attitude Control and Mode Stabilization," *Acta Astronautica 13,* Sep. 1986, pp. 507-514.

12. Singh, S. N., "Robust Nonlinear Attitude Control of Flexible Spacecraft," *IEEE Transactions on Aerospace and Electronic Systems,* Vol. AES-23, No. 3, May, 1987, pp. 380-387.

13. Singh, S. N., "Nonlinear Adaptive Attitude Control of Spacecraft," *IEEE Transactions on Aerospace and Electronic System,* Vol. AES-23, No. 3, May 1987, pp. 371-379.

14. Iyer, A. and Singh, S. N., "Sliding Mode Control of Flexible Spacecraft under Disturbance Torque," 1990.

15. Hirschorn, R. M., "Invertibility of Nonlinear Control Systems," *IEEE Transactions Automat. Control 24,* 1979, pp. 855-865.

16. Singh, S. N., " A Modified Algotiehm for Invertibility in Nonlinear Systems," *IEEE Transactions Automat. Control AC-26,* 1981, pp. 595-598.

9. APPENDIX

- **CONTROL LIMITS**

$G_0(t) = 100{,}000$ *ft-lbs* (moment applied at the orbitr mass center)
$F_0(t) = 800$*lbs* (force applied at the orbiter mass center)
$M_{\psi r} = 100{,}000$ *ft-lbs* (moment applied at the reflector *c.g.*)

- **FIRST *FOUR* FLEXIBLE MODES OF SCOLE MODEL**

THREE DIMENSIONAL MODE SHAPE CHARACTERISTICS		
MODE No.	1	2
FREQ. (Hz.)	0.27804240E+00	0.31357296E+00
α	0.12012084E+01	0.12756518E+01
A_x	0.16282665E+00	0.38855291E-02
B_x	-0.19670286E+00	-0.14998387E-01
C_x	-0.16983450E+00	-0.43321018E-02
D_x	0.19616259E+00	0.14985820E-01
A_y	-0.10274618E-01	0.14219781E+00
B_y	0.57579133E-02	-0.22695797E+00
C_y	0.11810057E-01	-0.19283105E+00
D_y	-0.57220462E-02	0.22644561E+00
α_ψ	0.19360955E-01	0.21835058E-01
A_ψ	-0.50748354E-01	0.31115282E-01
B_ψ	0.13978018E-04	-0.75992337E-05
MODE No.	3	4
FREQ. (Hz.)	0.81300189E+00	0.11856099E+01
α	0.20540387E+01	0.24804687E+01
A_x	0.40868188E-01	0.80641794E-01
B_x	-0.61958845E-01	-0.67233377E-01
C_x	-0.41309992E-01	-0.80913938E-01
D_x	0.61880796E-01	0.67106316E-01
A_y	-0.22438404E-01	0.13728679E+00
B_y	0.36509234E-01	-0.11746932E+00
C_y	0.24390447E-01	-0.14085209E+00
D_y	-0.36464758E-01	0.11725057E+00
α_ψ	0.56611842E-01	0.82557693E-01
A_ψ	0.92698901E-01	-0.16158934E-03
B_ψ	-0.87320799E-05	0.10437718E-07

- MATRICES A_3 AND A_2^T

$$A_3 = \begin{bmatrix} 0.45879E+2 & 0.36305E-1 & -0.89042E-1 & -0.14067E0 \\ 0.36305E-1 & 0.6211E+2 & 0.11263E0 & -0.1471E0 \\ -0.89042E-1 & 0.11263E0 & 0.32737E+2 & -0.6392E-1 \\ -0.14067E0 & -0.1471E0 & -0.6392E-1 & 0.2547E+3 \end{bmatrix}$$

$$A_2^T = \begin{bmatrix} -0.2133821E0 & -0.3687057E+3 & -0.7253901E-1 \\ 0.3808921E+3 & -0.3030935E+2 & -0.8427658E-1 \\ -0.1808478E+3 & -0.1318596E+3 & -0.125799E0 \\ 0.1423380E+3 & -0.1135851E+1 & -0.2367351E-1 \end{bmatrix}$$

$$K = \begin{bmatrix} k_{1,1} = 0.2820217E0 \\ k_{2,2} = 0.3574692E0 \\ k_{3,3} = 0.2412807E1 \\ k_{4,4} = 0.5285116E1 \end{bmatrix}$$

• CAPTIONS FOR FIGURES

Fig. 1:
SCOLE configuration showing the three-body model, coordinate system, and actuator control points.

Fig. 2:
Block diagram of the system.

Fig. 3:
Trajectory control: Stabilizer open loop

(a) Attitude angles.
(b) Control moments G_0.
(c) Torsional deformations, u_ψ.
(d) State errors, $(q_1 - \hat{q}_1)$, $(q_2 - \hat{q}_2)$.
(e) Resultant tip defflection, $\sqrt{u_x^2 + u_y^2}$.

Fig. 4:
Trajectory control: Stabilizer closed loop

(a) Control moments G_0.
(b) Control forces F.
(c) Control moment $M_{\psi\tau}$.
(d) Torsional deformations, u_ψ.
(e) Resultant tip defflection, $\sqrt{u_x^2 + u_y^2}$.

• FIGURES .

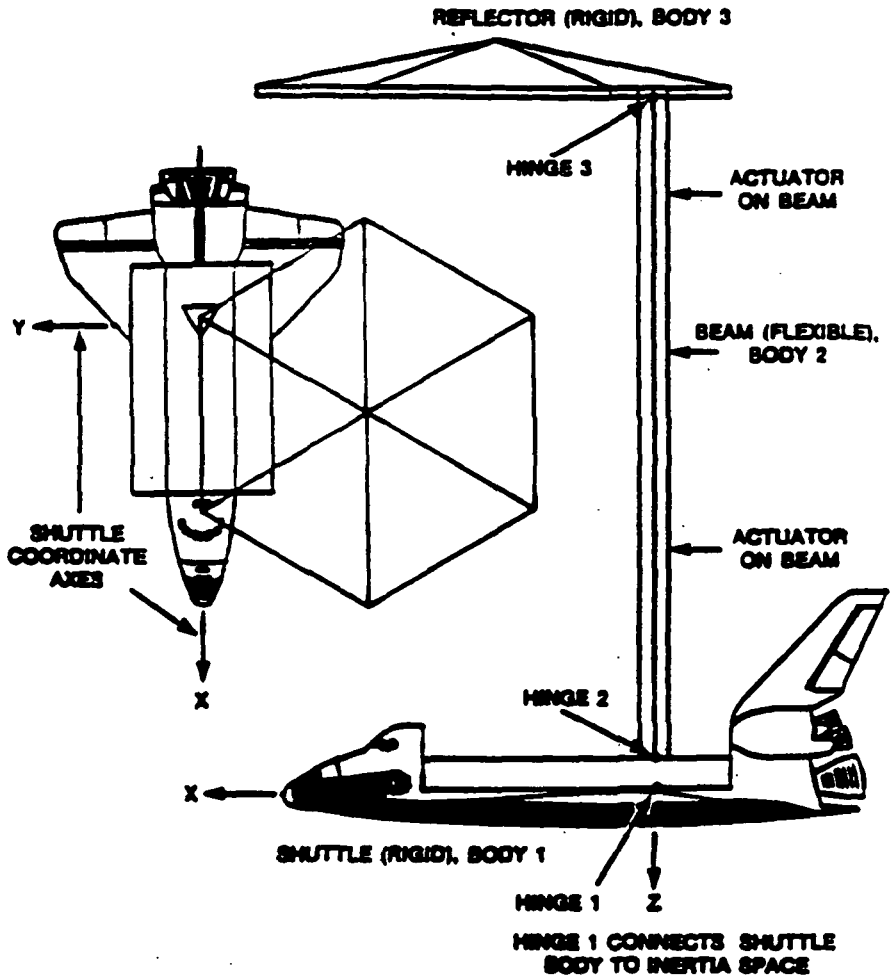


Fig. 1

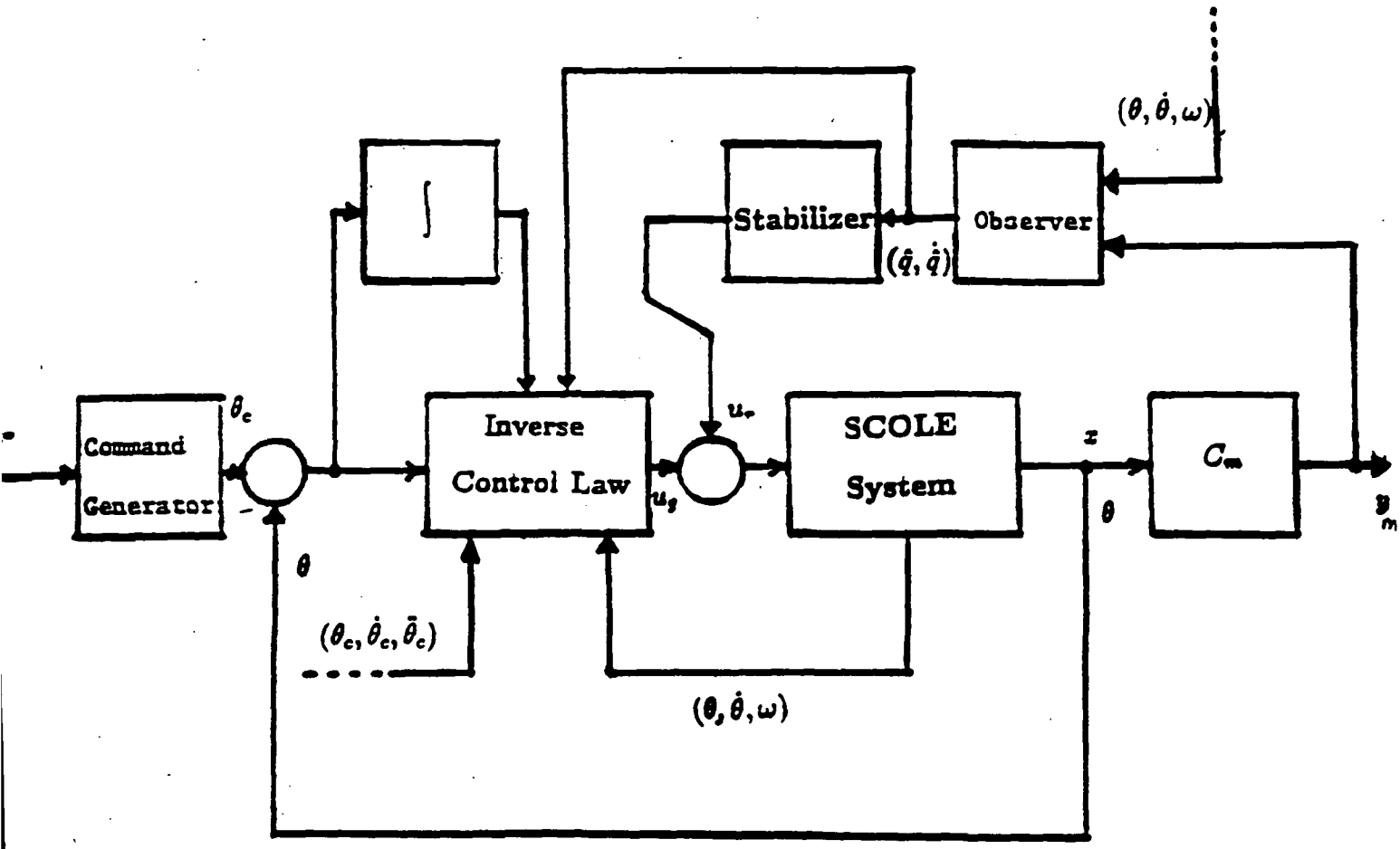

$(\theta, \dot{\theta}, \omega)$
$\int$
Stabilizer
Observer
$(\hat{q}, \dot{\hat{q}})$
Command Generator
θ_c
Inverse Control Law
u_p
u_g
SCOLE System
x
C_m
y_m
θ
$(\theta_c, \dot{\theta}_c, \ddot{\theta}_c)$
$(\theta, \dot{\theta}, \omega)$

Fig. 2

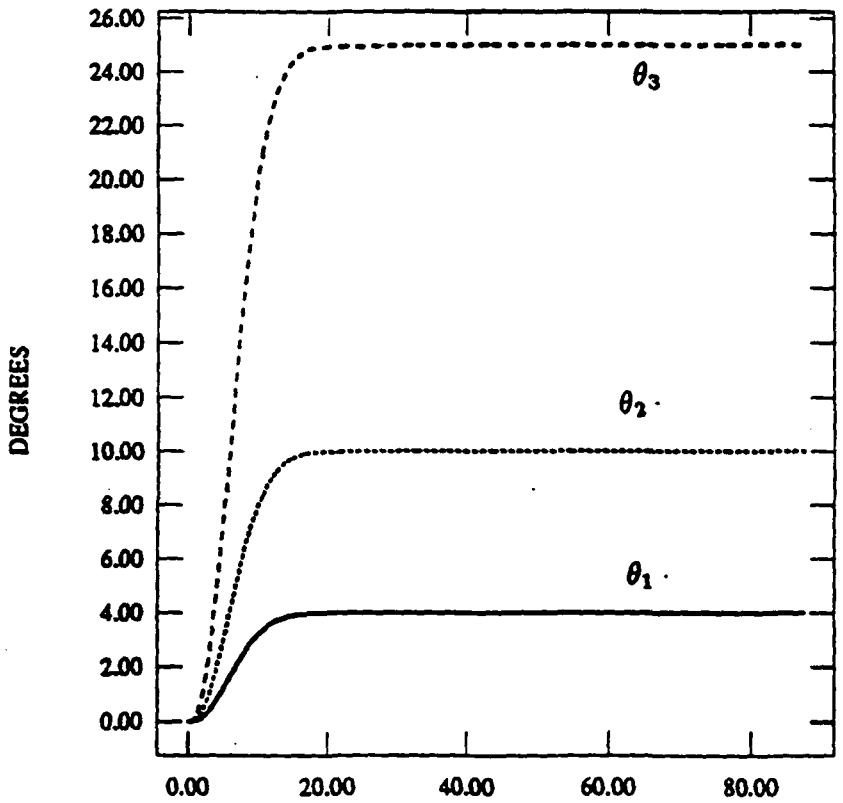

26.00
24.00
22.00
20.00
18.00
16.00
14.00
12.00
10.00
8.00
6.00
4.00
2.00
0.00
DEGREES
θ_3
θ_2
θ_1
0.00
20.00
40.00
60.00
80.00

Fig. 3(a)

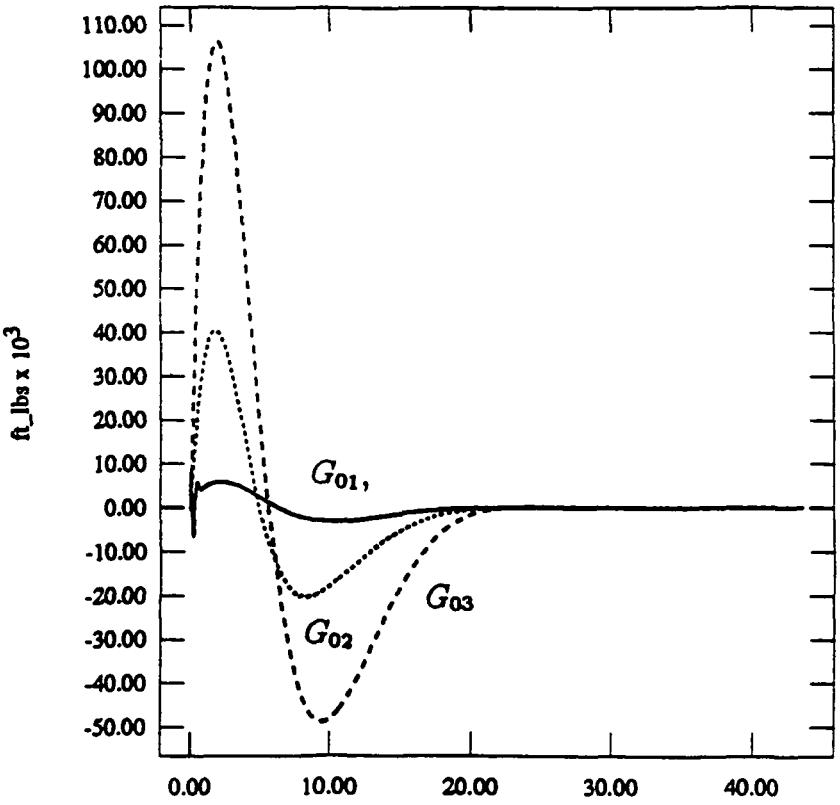

110.00
100.00
90.00
80.00
70.00
60.00
50.00
40.00
30.00
20.00
10.00
0.00
-10.00
-20.00
-30.00
-40.00
-50.00
ft_lbs x 10^3
0.00
10.00
20.00
30.00
40.00
G01,
G02
G03

Fig. 3(b)

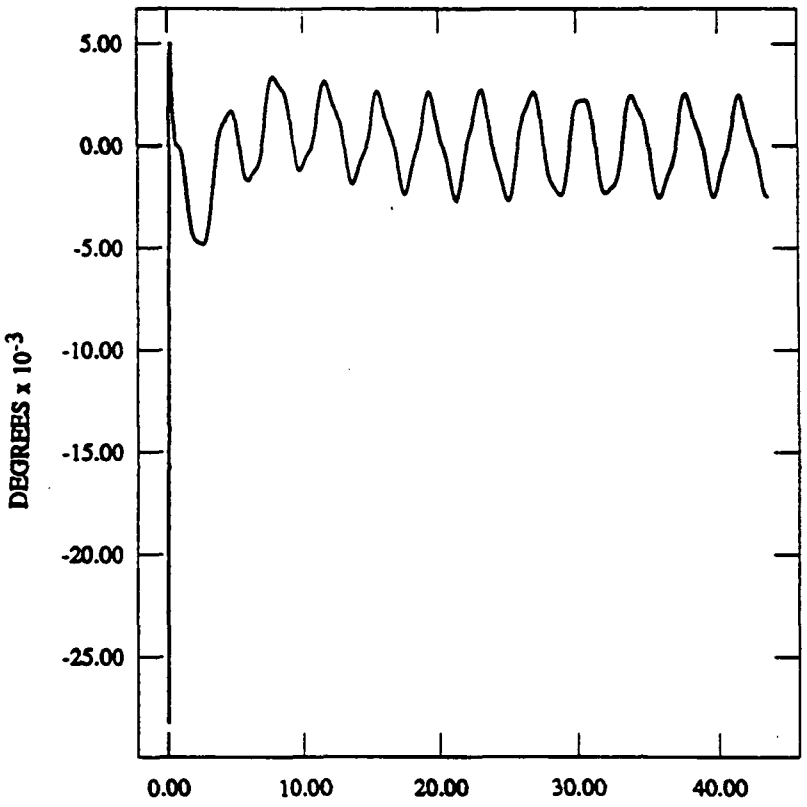

5.00
0.00
-5.00
-10.00
-15.00
-20.00
-25.00
DEGREES x 10^-3
0.00
10.00
20.00
30.00
40.00

Fig. 3(c)

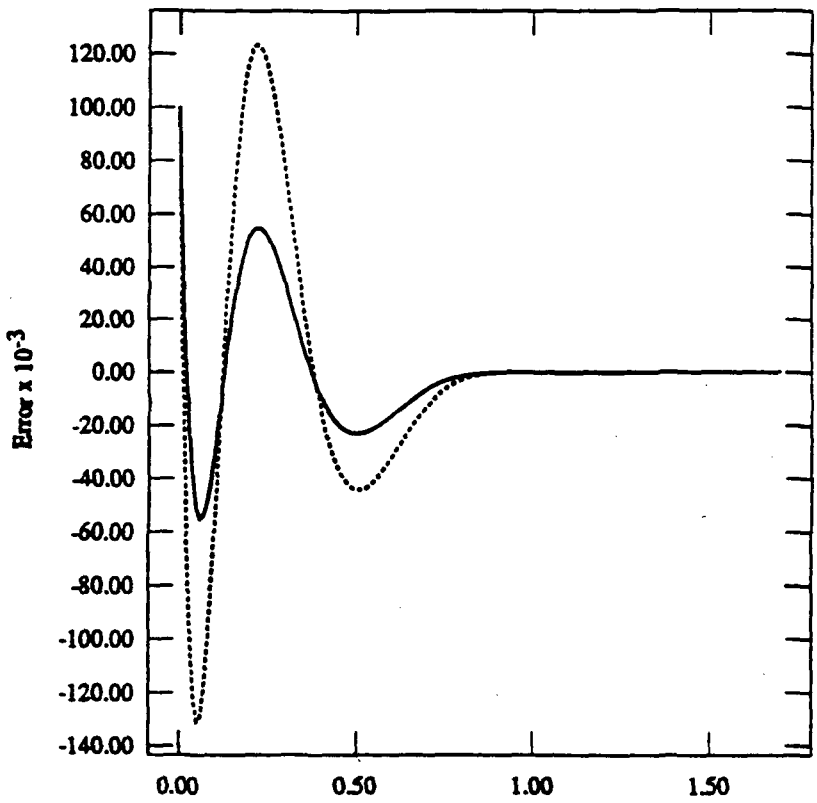

120.00
100.00
80.00
60.00
40.00
20.00
0.00
-20.00
-40.00
-60.00
-80.00
-100.00
-120.00
-140.00
Error x 10^-3
0.00
0.50
1.00
1.50

Fig. 3(d)

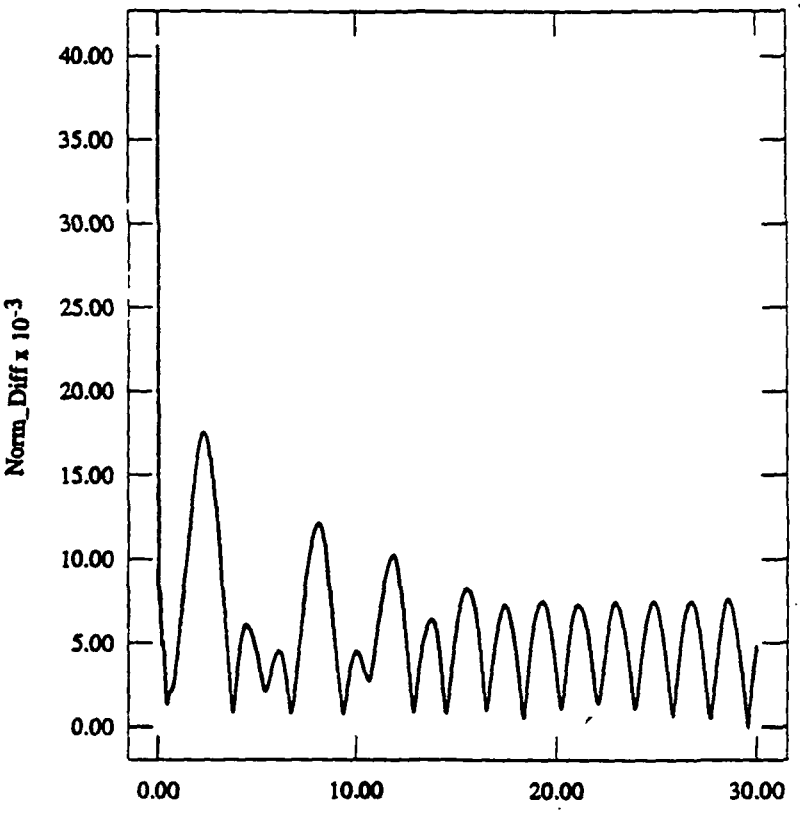

Norm_Diff x 10^-3
40.00
35.00
30.00
25.00
20.00
15.00
10.00
5.00
0.00
0.00
10.00
20.00
30.00

Fig. 3(e)

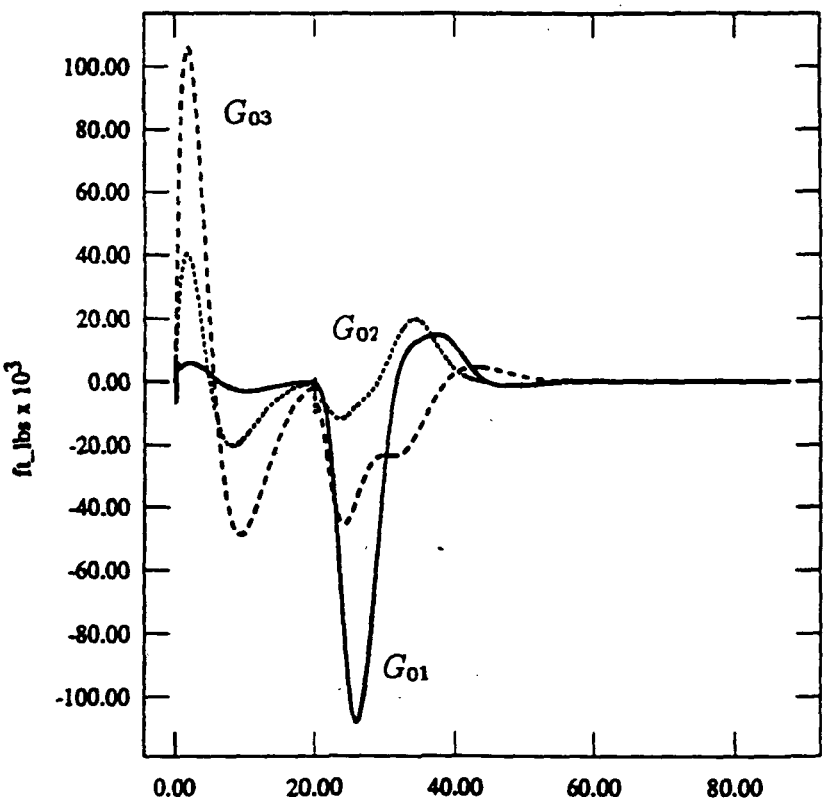

100.00
80.00
60.00
40.00
20.00
0.00
-20.00
-40.00
-60.00
-80.00
-100.00
ft_lbs x 10^3
G03
G02
G01
0.00
20.00
40.00
60.00
80.00

Fig. 4(a)

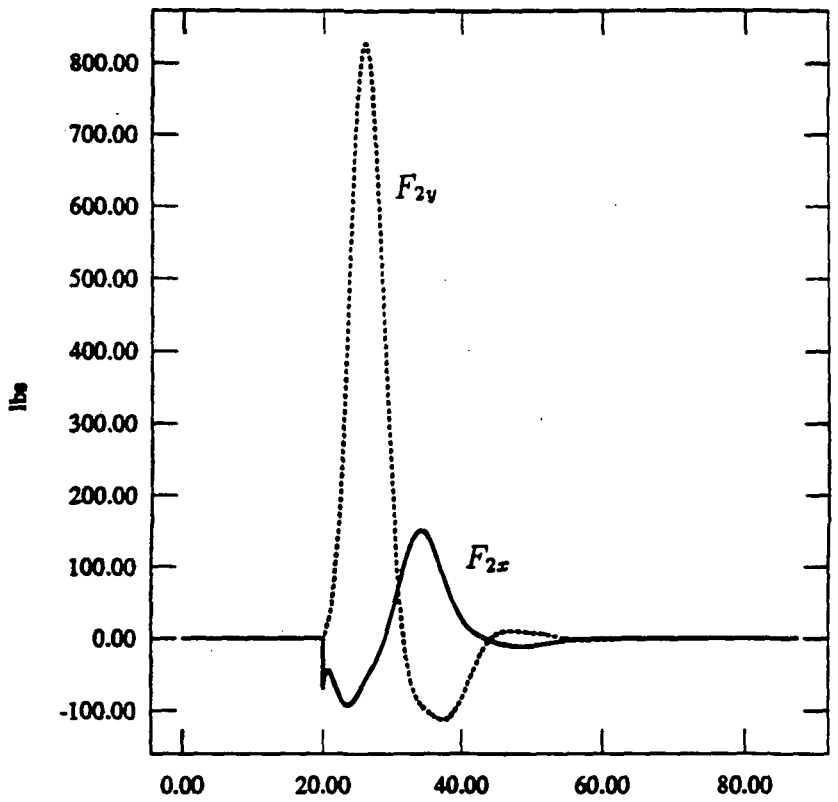

800.00
700.00
600.00
500.00
400.00
300.00
200.00
100.00
0.00
-100.00
lbs
F_{2y}
F_{2x}
0.00
20.00
40.00
60.00
80.00

Fig. 4(b)

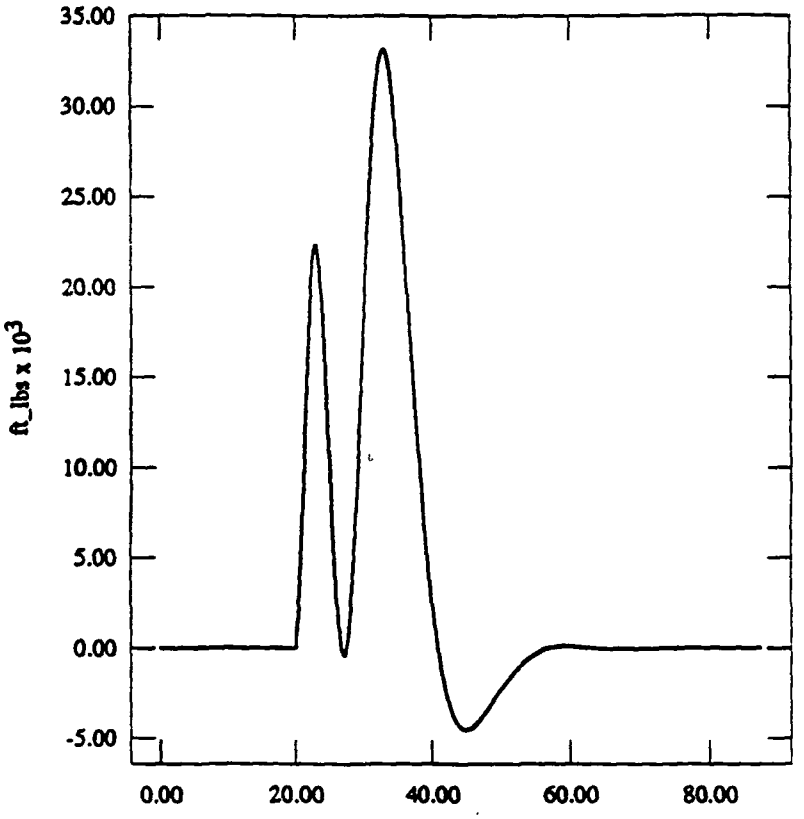

35.00
30.00
25.00
20.00
15.00
10.00
5.00
0.00
-5.00
ft_lbs x 10^3
0.00
20.00
40.00
60.00
80.00

Fig. 4(c)

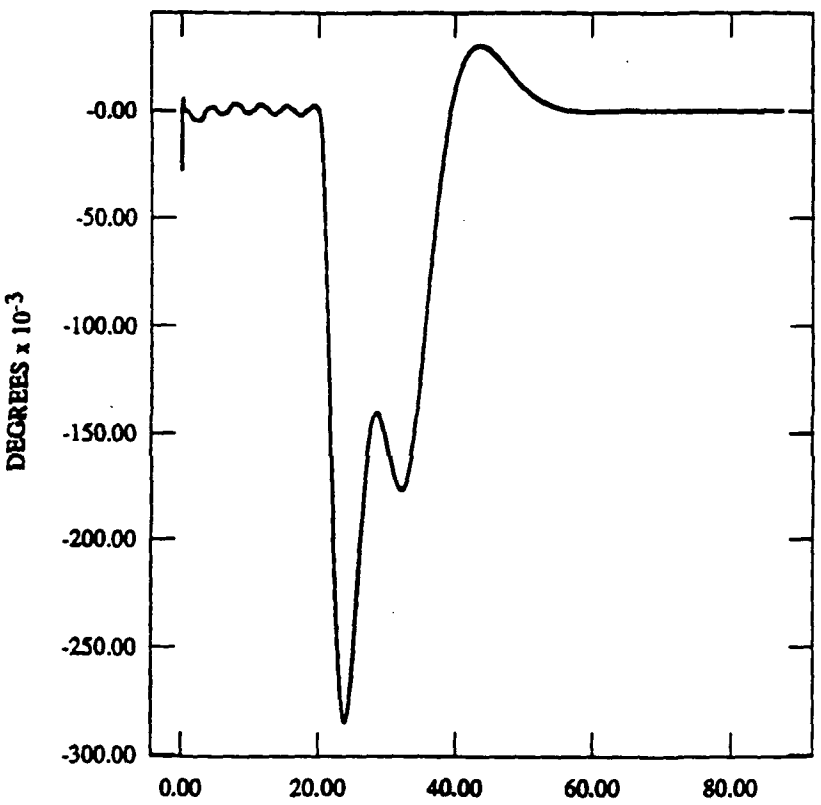

DEGREES x 10^-3
-0.00
-50.00
-100.00
-150.00
-200.00
-250.00
-300.00
0.00
20.00
40.00
60.00
80.00

Fig. 4(d)

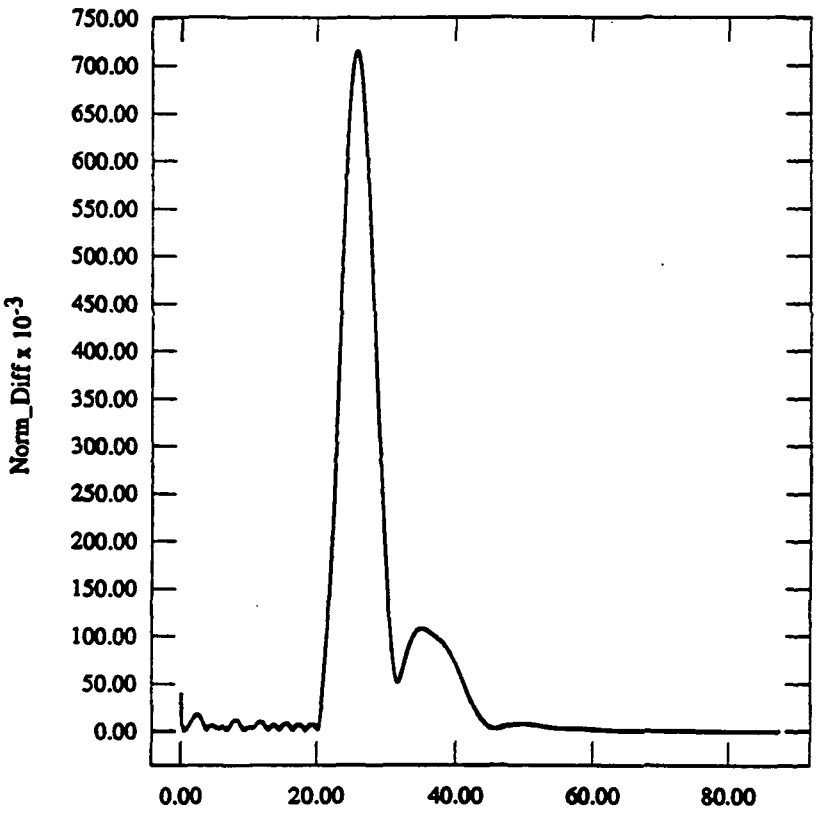

750.00
700.00
650.00
600.00
550.00
500.00
450.00
400.00
350.00
300.00
250.00
200.00
150.00
100.00
50.00
0.00
Norm_Diff x 10-3
0.00
20.00
40.00
60.00
80.00

Fig. 4(e)

Output Feedback Detumbling and Reorientation Maneuvers and Vibration Damping of NASA SCOLE System

Misbahul Azam, Sahjendra N. Singh, Ashok Iyer

Department of Electrical and Computer Engineering
University of Nevada Las Vegas
Las Vegas, NEVADA 89154

and

Y. P. Kakad

Department of Electrical Engineering
University of North Carolina Charlotte
Charlotte, NORTH CAROLINA 28223

Abstract

The question of rotational maneuver and vibration stabilization of NASA Spacecraft Control Laboratory Experiment (SCOLE) System is considered. The mathematical model of SCOLE system includes the rigid body dynamics as well as the elastic dynamics representing transverse and torsional deformations of the elastic beam connecting the orbiter and end body (reflector). For the rotational maneuver, a new control law (orbiter control law) is derived using orbiter input torque vector. Using this control law *detumbling* and reorientation maneuvers of SCOLE system are accomplished, however, this excites the elastic modes of the beam. Interestingly the orbiter control law asymptotically linearizes flexible dynamics. Using the linearized model, a linear feedback control law is designed for vibration suppression. An observer is designed for estimating the state variables using sensor outputs which are used for the synthesis of the control law. Simulation results are presented to show that in the closed-loop system detumbling and reorientation maneuvers can be accomplished and the effect of control and *observation spillover* is insignificant .

1. Introduction

An important class of shuttle deployed payloads consists of cantilevered beam-like structures with massive tip bodies. A design challenge was posed by Taylor and Balakrishnan [1] for the control of such a system. In the design challenge, the Spacecraft Control Laboratory Experiment (SCOLE) was set up by NASA Langley Research Center to provide a standard configuration to test control laws for investigators.

The laboratory apparatus includes the Space Shuttle (orbiter) connected by a long (130ft) flexible beam to a hexagonal antenna or reflector, as shown in Fig. 1. The reflector and Shuttle are treated as rigid bodies. When the Shuttle is maneuvered, the flexible modes of the beam are excited. Two force actuators and a torquer have been provided to exert sufficient force and moment to suppress the unwanted vibration of the beam.

Research related to both dynamics and control system design has been performed and reported in literature, NASA reports, and SCOLE workshops [2-10] at NASA Langley Research Center. Nonlinear invertibility theory has been used in [11-12] for designing controller for a simplified spacecraft system. Recently, this approach has been extended for the control of SCOLE system [12].

In this paper, Control System design for reorientation and detumbling maneuvers and elastic mode stabilization of SCOLE system is considered. A new Orbiter Control Law is derived such that detumbling maneuver and attitude control of orbiter can be accomplished using shuttle input torque. Using this control law, any given reference angular velocity trajectory, ω_r, can be reproduced by the control system during detumbling maneuver. Furthermore, by a judicious choice of the

reference trajectory $\omega_r(t)$, desired orientation of orbiter can be attained inspite of the elastic oscillations of the beam caused due to maneuver of the space vehicle. In the closed-loop system including the orbiter control law, the elastic dynamics of the SCOLE configuration representing transverse vibration in two orthogonal planes and the torsional deformation of the elastic beam, are asymptotically decoupled from the rigid mode dynamics. Using linear control theory, a stabilizer is designed for elastic mode stabilization. For the synthesis of the controller only attitude angles, angular rates, tip elastic deflection components and torsion deflection at the tip of the beam are assumed to be measured by sensors. An *observer* is designed to estimate the elastic modes and their derivatives, and these are used for synthesizing the control law.

The organization of the paper is as follows. Section 2 presents the mathematical model. The orbiter control law is derived in section 3. Section 4 and section 5 present elastic mode stabilizer and observer design, respectively, and finally section 6 presents simulation results.

2. Mathematical Model of SCOLE System

A body fixed orthogonal coordinate system with axes x, y, z is utilized to describe the orientation of the orbiter. The body-fixed coordinate frame has its origin at the point of attachment of the flexible appendage with the rigid Shuttle for this study. The attitude of the orbiter is defined by a sequence of rotation $\theta_1, \theta_2, \theta_3$ (roll,pitch,yaw), with respect to an *inertial* coordinate system.

The orientation is completely described by the differential equation

$$\dot{\theta} = M^{-T}(\theta)\omega \tag{1}$$

where T denotes transposition and

$$\omega = (\omega_1, \omega_2, \omega_3)^T,\ \theta = (\theta_1, \theta_2, \theta_3)^T,\ M^{-T} \triangleq (M^T)^{-1}$$

and

$$M^T = \begin{bmatrix} cos\theta_2 cos\theta_3 & sin\theta_3 & 0 \\ -cos\theta_2 sin\theta_3 & cos\theta_3 & 0 \\ sin\theta_2 & 0 & 1 \end{bmatrix}$$

Often the arguments of functions will be suppressed for simplicity. Equation (1) relates the rotation angles and the angular velocity components $(\omega_1, \omega_2, \omega_3)$ of the orbiter. It is seen that M^T becomes singular at $\theta_2 = \pm(\pi/2)$ for the chosen choice of rotations of the coordinate systems. However, this singularity can be avoided by a choice of different sequence of rotations of coordinate frames if it is required. In the following we shall be interested in the region of state space Ω in which $\theta_2 \neq \pm\pi/2$.

The elastic beam undergoes transverse elastic deformations along axes x and y, and torsional deformation about axis z. Elastic deformations are assumed to be linear combinations of admissible functions $\phi_{xi}(s), \phi_{yi}(s)$ and $\phi_{\psi i}(s)$, $i=1,2,3,...,n$, where 's' denotes the distance on the beam from the attachment point of the beam and the orbiter. Here it is assumed that elastic deformations are adequately represented by n modes. The admissible functions $\phi_{xi}(s), \phi_{yi}(s)$ and $\phi_{\psi i}(s)$ are

$$\phi_{xi}(s) = A_{xi} sin\frac{\alpha_i s}{L} + B_{xi} cos\frac{\alpha_i s}{L} + C_{xi} sinh\frac{\alpha_i s}{L} + D_{xi} cosh\frac{\alpha_i s}{L} \tag{2}$$

$$\phi_{yi}(s) = A_{yi} sin\frac{\alpha_i s}{L} + B_{yi} cos\frac{\alpha_i s}{L} + C_{yi} sinh\frac{\alpha_i s}{L} + D_{yi} cosh\frac{\alpha_i s}{L} \tag{3}$$

$$\phi_{\psi i}(s) = A_{\psi i} sin\alpha_{\psi i}\frac{s}{L} + B_{\psi i} cos\alpha_{\psi i}\frac{s}{L} \tag{4}$$

The parameters A_{xi}, A_{yi}, α_i etc, are explained in [6].

The elastic deformations are expressed as linear combinations of admissible functions as

$$u_x(s) = \sum_{i=1}^{n} \phi_{xi}(s) q_i(t) \tag{5}$$

$$u_y(s) = \sum_{i=1}^{n} \phi_{yi}(s) q_i(t) \tag{6}$$

$$u_\psi(s) = \sum_{i=1}^{n} \phi_{\psi i}(s) q_i(t) \tag{7}$$

where u_x, u_y are the elastic deformations along x, y axes and u_ψ is the torsional deformation about z-axis, respectively. Here q_i(t), *i=1,2,3,...,n*, are the modal deformation co-ordinates for the beam. Define $q=(q_1, q_2, ..., q_n)^T$, the elastic modes vector, and $G_0 = (G_{01}, G_{02}, G_{03})^T$ the external torque vector applied on the orbiter. $F = (F_x, F_y)^T$ is the external control force vector applied at the reflector center of the mass and $M_{\psi r}$ is the moment applied about z-axis at the reflector center of mass.

The complete equations of motion describing rotational and elastic behavior of the SCOLE system have been derived in [6] using *Lagrangian* approach (Readers may refer for the details). In this study we shall be interested only in the rotational and elastic dynamics. These are

$$\begin{bmatrix} I_0 & A_2 \\ A_2^T & A_3 \end{bmatrix} \begin{bmatrix} \dot{\omega} \\ \ddot{q} \end{bmatrix} = \begin{bmatrix} N_2(\theta, \dot{\theta}, \omega, \dot{q}) \\ -Kq \end{bmatrix} + \begin{bmatrix} B_1 \\ B_2 \end{bmatrix} u \tag{8}$$

where K is the stiffness matrix, N_2 is a nonlinear vector function, B_i (*i=1,2*) are the constant input matrices, $u = (G_0^T, F^T, M_{\psi r})^T \in R^6$ is the control input vector and

$$B_1 = [I_{3\times 3} \quad B_{12}]$$
$$B_2 = [O_{n\times 3} \quad B_{22}]$$

The matrices I_0, A_i, and B_i have been derived in [6], and I and O denote identity and null matrices of indicated dimensions. The matrix D

$$D = \begin{bmatrix} I_0 & A_2 \\ A_2^T & A_3 \end{bmatrix}$$

is positive definite symmetric matrix.

We are interested in deriving control laws such that in the closed-loop system detumbling and reorientation maneuvers can be performed.

Detumbling Maneuver:

Let a reference angular velocity trajectory ω_r, be given such that $\omega_r(t) \rightarrow 0$, as $t \rightarrow \infty$. We are interested in deriving a control law such that in the closed-loop system $\tilde{\omega}(t) = \omega(t) - \omega_r(t) \rightarrow 0$, as $t \rightarrow \infty$, and the elastic modes are stabilized. The derivation of orbiter control torque vector for ω_r trajectory tracking will be based on nonlinear inversion of an input-output map.

Reorientation Maneuver:

Let $\theta_r(t)$ be a given reference attitude trajectory, such that $\theta_r(t) \rightarrow \theta^*$, a desired attitude angle, as $t \rightarrow \infty$. We are interested in deriving a control law such that in the closed-loop system $\theta(t) \rightarrow \theta_r(t)$, as $t \rightarrow \infty$, and elastic modes are stabilized. The rotational maneuver to attain desired orientation will be accomplished by a judicious choice of $\omega_r(t)$ in the *detumbling* control law.

3. Control Laws for Rotational Maneuver

In this section, control laws for rotational maneuvers will be derived.

3.1 *Detumbling Maneuver:*

Here first the design of control system for ω_r trajectory tracking is considered. To derive the control law the inversion of the input (G_0)- output (ω) map is considered. For the inversion of input-output (I-O) map, we consider the derivative of ω from (8) which is

$$\dot{\omega} = R_{11}[N_2(\theta, \dot{\theta}, \omega, \dot{q}) + B_1 u] + R_{12}[-Kq + B_2 u] \tag{9}$$

where $D^{-1}=(R_{ij})$, $i,j = 1,2$ and R_{ij} are submatrices of D^{-1} of appropriate dimensions. Define $u_r=(F^T, M_{\psi r})^T$, and $u_g = G_0$. Then in view of the special form of

matrices B_i, it follows that

$$\dot{\omega} = [R_{11}\{N_2(\theta,\dot{\theta},\omega,\dot{q}) + B_{12}u_r\} + R_{12}\{-Kq + B_{22}u_r\}] + R_{11}u_g \qquad (10)$$

$$\triangleq a^*(\theta,\dot{\theta},\omega,q,\dot{q},u_r) + R_{11}u_g$$

where

$$a^* = R_{11}\{N_2 + B_{12}u_r\} + R_{12}\{-Kq + B_{22}u_r\}$$

Since it is desired to track the reference trajectory ω_r, we choose a control law u_g of the form

$$u_g = R_{11}^{-1}[-a^* - \lambda\tilde{\omega}(t) + \dot{\omega}_r(t)] \qquad (11)$$

where $\lambda > 0$. Substituting control law (11) in (10) gives

$$\dot{\tilde{\omega}}(t) = -\lambda\tilde{\omega}(t) \qquad (12)$$

Solving (12) gives,

$$\tilde{\omega}(t) = exp(-\lambda t)\tilde{\omega}(0).$$

Thus $\omega(t) \rightarrow \omega_r(t)$, as $t \rightarrow \infty$; and if $\tilde{\omega}(0)$=0, it follows that $\omega(t) = \omega_r(t)$, for all $t \geq 0$. By choosing suitable smooth trajectory $\omega_r(t)$ converging to zero, one can accomplish desirable detumbling maneuver. If $\omega_r(t) \rightarrow 0$ as $t \rightarrow \infty$; then $\dot{\theta}(t) \rightarrow 0$ and $\theta(t) \rightarrow \theta_d$, a constant vector. In such a case when detumbling maneuver is completed, the orbiter attains a fixed orientation.

3.2 *Reorientation Maneuver:*

Now we shall derive a control law u_g such that $\theta(t) \rightarrow \theta_r(t)$, a given reference attitude trajectory, as $t \rightarrow \infty$, giving a desired orientation of the orbiter. This will be accomplished by a suitable choice of reference trajectory $\omega_r(t)$ in the detumbling control law (11), such that the desired orientation is asymptotically attained.

Since in the closed-loop system (8) and (11), $\omega(t) \rightarrow \omega_r(t)$, we have that $M^{-1}(\theta)\omega(t) \rightarrow M^{-1}(\theta)\omega_r(t)$, as $t \rightarrow \infty$. Thus the asymptotic relationship between $\dot{\theta}$ and ω obtained from (1) is

$$\dot{\theta} = M^{-T}(\theta)\omega_r \tag{13}$$

as $t \rightarrow \infty$. Since it is desired to track $\theta_r(t)$, in view of (13), it follows that a suitable choice of ω_r is

$$\omega_r = M^T(\theta)[-\mu\tilde{\theta} + \dot{\theta}_r] \tag{14}$$

where $\mu > 0$, and $\tilde{\theta} = (\theta - \theta_r)$.

From equation (1), we have

$$\begin{aligned} \dot{\theta} &= M^{-T}(\theta)(\tilde{\omega} + \omega_r) \\ &= M^{-T}(\theta)[\tilde{\omega} + M^T(\theta)(-\mu\tilde{\theta} + \dot{\theta}_r)] \end{aligned} \tag{15}$$

which yields

$$\dot{\tilde{\theta}} = -\mu\tilde{\theta} + M^{-T}(\theta)\tilde{\omega} \tag{16}$$

Since for any choice of $\omega_r(t)$, in the closed-loop system including the control law (11), $\tilde{\omega} \rightarrow 0$ as $t \rightarrow \infty$, asymptotically (16) reduces to

$$\dot{\tilde{\theta}} = -\mu\tilde{\theta} \tag{17}$$

It is interesting to note that by a proper choice of reference trajectory ω_r as given in (14), one obtains a first order linear differential equation asymptotically for the attitude angle tracking error. It is obvious from (17) that for any $\omega(0)$, $\omega_r(0)$, $\theta(0)$, and $\theta_r(0)$; $\tilde{\theta}(t) \rightarrow 0$, as $t \rightarrow \infty$. Let $\theta = \theta^*$ corresponds to a desired orientation of the orbiter. Thus if $\theta_r(t) \rightarrow \theta^*$, then $\theta(t) \rightarrow \theta^*$, as $t \rightarrow \infty$, and the desired orientation of the orbiter is attained.

Furthermore, with the choice of $\tilde{\omega}(0) = 0$ and $\tilde{\theta}(0) = 0$, it follows from (12) that $\tilde{\omega}(t) \equiv 0$ for all $t \geq 0$. Then substituting $\tilde{\omega}(t)$=0 in (16), and using $\tilde{\theta}(0)$=0, it

follows that $\tilde{\theta}(t) \equiv 0$ for all $t \geq 0$, and in the closed-loop system trajectories $\omega_r(t)$ and $\theta_r(t)$ are exactly reproduced for all $t \geq 0$. This way, the SCOLE system can be maneuvered to attain specified time-varying orientation at each instant $t \geq 0$, which is useful for tracking a rotating target in space.

The control law for reorientation maneuver is obtained by combining (11) and (14) which is

$$u_g = R_{11}^{-1}[-a^* - \lambda\{\omega - M^T(\theta)(-\mu\tilde{\theta} + \dot{\theta}_r)\} + \dot{M}^T(\theta,\dot{\theta})(-\mu\tilde{\theta} + \dot{\theta}_r) + M^T(\theta)(-\mu\dot{\tilde{\theta}} + \dot{\tilde{\theta}}_r)] \tag{18}$$

where $\dot{M}(\theta,\dot{\theta}) \triangleq [(\partial M_{ij}/\partial\theta)\dot{\theta}]$, *i,j=1,2,3* and M_{ij} are the elements of the matrix M.

We notice from (18) that the second order derivative of θ_r is required in the control law. For this purpose one can choose a third order attitude angle command generator of the form *(i=1,2,3)*

$$\dddot{\theta}_{ri} + (2\zeta_{ri}\omega_{nri} + \lambda_{ri})\ddot{\theta}_{ri} + 2(\zeta_{ri}\omega_{nri}\lambda_{ri} + \omega_{nri}^2)\dot{\theta}_{ri} + \omega_{nri}^2\lambda_{ri}\theta_{ri} = \omega_{nri}^2\lambda_{ri}\theta^* \tag{19}$$

where $\theta_r = (\theta_{r1}, \theta_{r2}, \theta_{r3})^T$. The parameters ζ_{ri}, λ_{ri}, and ω_{nri} are appropriately chosen to obtain desired reference trajectory $\theta_r(t)$ terminating at θ^*. It can be easily varified that the poles associated with (19) are at $-\lambda_{ri}$ and $\{-\zeta_{ri}\omega_{nri} \pm j\omega_{nri}(1-\zeta_{ri}^2)^{1/2}\}$.

4. Elastic Mode Stabilizer

We note that when the detumbling controller (11) is used, $\omega(t) \rightarrow 0$, and $\dot{\omega}(t) \rightarrow 0$, as $t \rightarrow \infty$ for an approriate choice of $\omega_r(t)$. Also in the closed-loop system including the reorientation controller (18), one can choose $\theta_r(t)$ such that $\theta(t) \rightarrow \theta^*$, $\dot{\theta}(t) \rightarrow 0$, $\omega(t) \rightarrow 0$, and $\dot{\omega}(t) \rightarrow 0$, as $t \rightarrow \infty$. However, rotational maneuvers cause transverse and torsional vibrations of the beam. Thus it becomes necessary to design a stabilizer so that the elastic modes can be stabilized.

In this section the design of an elastic mode stabilizer is considered. Since in the closed-loop system (8) and (11) or (8) and (18), $\omega(t) \rightarrow 0$ and $\dot{\omega}(t) \rightarrow 0$, irrespective of the elastic oscillation of the beam; it follows from (8) that the elastic dynamics get asymptotically decoupled from the rigid dynamics as $t \rightarrow \infty$. Setting $\dot{\omega}(t) = 0$ in (8), gives the decoupled elastic dynamics of the form

$$A_3\ddot{q} = -Kq + B_{22}u_r \tag{20}$$

For the damping of the vibration, it is necessary to stabilize system (20).

Define $z=(q^T, \dot{q}^T)$, to obtain a state variable form from (20) as

$$\dot{z} = \begin{bmatrix} 0_{n\times n} & I_{n\times n} \\ -A_3^{-1}K & 0_{n\times n} \end{bmatrix} z + \begin{bmatrix} 0 \\ A_3^{-1}B_{22} \end{bmatrix} u_r \tag{21}$$

$$\triangleq A_e z + B_e u_r$$

where matrices A_e, and B_e are defined by (21). For the stabilization of (21), *linear quadratic optimization* or *pole assignment* technique can be used. We have chosen pole assignment technique in this study. The linear feedback control law is

$$u_r = -F_e z \tag{22}$$

The matrix F_e is chosen such that the closed-loop matrix $A_{ec} = (A_e - B_e F_e)$ is a *Hurwitz* matrix and has specified eigenvalues. It is interesting to note that the use of *orbiter* attitude controller simplifies the stabilization problem to a linear design problem of a lower order system and this design is carried out independently.

Although, the control laws u_g and u_r have been derived independently and the derivation of u_r is based on a reduced order linear model, boundedness of elastic modes can be established in the complete full order closed-loop system for any bounded trajectory $\omega_r(t)$ and $\dot{\omega}_r(t)$. In the following we shall obtain a bound on the elastic modes.

In the closed-loop system with control law u_g of (11), we note that $\tilde{\omega} \rightarrow 0$ as $t \rightarrow \infty$. The elastic dynamics obtained from the systems (8), (11), and (22) are given by

$$\dot{z} = A_{ec}z + B_s\dot{\omega} \tag{23}$$

where B_s=[O $(-A_3^{-1}A_2^T)^T]^T$. Using $\dot{\omega} = \dot{\omega}_r - \lambda\tilde{\omega}$ obtained from (12), (23) gives

$$\dot{z} = A_{ec}z + B_s(\dot{\omega}_r - \lambda\tilde{\omega}) \tag{24}$$

The solution of (24) is

$$z(t) = \phi(t - t_0)z_0 + \int_{t_0}^{t} \phi(t - \tau)B_s(\dot{\omega}_r - \lambda\tilde{\omega})d\tau \tag{25}$$

where $z_0 = z(t_0)$ and the transition matrix $\phi(t)$ associated with the matrix A_{ec} is given by

$$\phi(t) = exp(A_{ec}t)$$

We assume in the following that ω_r and $\dot{\omega}_r$ are bounded. Furthermore, the solution of (12) gives, $\|\tilde{\omega}\| = e^{-\lambda t}\|\omega(0)\| < \infty$, where $\|.\|$ denotes the *Euclidean norm* of a vector. Thus it follows that there exists a function $\gamma(t) < \infty$ such that for all $t \geq 0$.

$$\|B_s(\dot{\omega}_r - \lambda\tilde{\omega})\| \leq \gamma(t) \leq \gamma_0 < \infty$$

where γ_0 is a constant. Since A_{ec} is a *Hurwitz* matrix $\|\phi(t - t_0)\|_i \leq me^{-\alpha(t-t_0)}$ for some $m > 0$ and $\alpha > 0$, where $\|.\|_i$ is the *induced matrix norm* [13]. Let $\omega_d \triangleq \dot{\omega}_r - \lambda\tilde{\omega}$ and $z(t_0) \triangleq z_0$. Taking the norm and using triangle inequality, (25) gives ($t_0 \geq 0$)

$$\|z(t)\| \leq \|\phi(t - t_0)\|.\|z_0\| + \int_{t_0}^{t} \|\phi(t - \tau)\|_i.\|B_s\omega_d(\tau)\|d\tau$$

$$\leq me^{-\alpha(t-t_0)}\|z_0\| + m\int_{t_0}^{t} e^{-\alpha(t-\tau)}\gamma(\tau)d\tau$$

$$\leq me^{-\alpha(t-t_0)}\|z_0\| + (m/\alpha)(1 - e^{-\alpha(t-t_0)})\gamma_0$$

$$\leq m(\|z_0\| + \alpha^{-1}\gamma_0) < \infty \tag{26}$$

This proves that in the closed-loop system $q(t)$ and $\dot{q}(t)$ are bounded provided that the reference trajectory is such that $\omega_r(t)$ and $\dot{\omega}_r(t)$ are bounded functions and (26) gives a *bound* on $\|z(t)\|$.

For a choice of a reference trajectory $\omega_r(t)$ in the closed-loop system with the detumbling control law, for which $\omega_r(t) \to 0$ and $\dot{\omega}_r(t) \to 0$, as $t \to \infty$, $\omega(t)$ and $\dot{\omega}(t) \to 0$ as well, as $t \to \infty$. In such a case, in the closed-loop system, it is obvious from (23) that $z(t) \to 0$ as $t \to \infty$, since A_{ec} is *Hurwitz* matrix.

The stabilizer has been designed by setting $\dot{\omega}(t) = 0$ in (8). Since $\omega(t)$ and $\dot{\omega}(t)$ asymptotically tend to zero for a proper choice of $\omega_r(t)$, a question arises: at what instant should the elastic mode stabilizer-loop be closed? According to (26), if the stabilizer is switched at the instant t_0, following a rotational maneuver command beginning at $t = 0$, the elastic modes remain bounded for all $t \geq t_0$, provided $z(t_0)$ is bounded. However, since the stabilizer is not in the loop during the period $[0,t_0]$, *divergent* elastic oscillations will result during this period in the system (23) in which A_{ec}=A_e (since $F_e = 0$, *i.e*; zero stabilization signal) if the reference trajectories $\omega_r(t)$ happen to contain sinusoidal signals of frequencies coinciding with the natural frequencies of vibration of the beam. These natural frequencies of oscillation are given by the purely imaginary eigenvalues of the open-loop matrix A_e. Thus it is preferable to keep the stabilizer loop closed from the instant $t = 0$ to avoid structural resonance.

5. Observer Design

In this section, the design of an observer to estimate the states is considered. The estimation of state is necessary so that the controller can be synthesized using

measured signals. In this study it is assumed that the only measured variables are θ, ω, and the elastic deformations $u_x(L)$, $u_y(L)$, and $u_\psi(L)$ at the tip of the beam. The variable $\dot{\theta}$ is computed using (1). For the synthesis of the controller, it is essential to estimate the variables q and $\dot{q}$. With these measurements, the system (8) can be considered as an on-line linear time-varying system since the nonlinear function is of the form $N_2 = N_{2c}(\theta, \dot{\theta}, \omega) + N_{2f}(\theta, \dot{\theta}, \omega)\dot{q}$ which is linear in $\dot{q}$ and N_{2f} depends on measured variables. It is interesting to note that N_2 contains terms of second order in derivatives of $\dot{\theta}_i$, and $\dot{q}_i$; therefore, N_{2f} can be neglected for simplicity in design of the observer. We shall make this simplification, since designing observer for the nonlinear model is extremely difficult.

Setting $N_{2f}\dot{q}$=0 in N_2; one obtains from (8) the following equation for the elastic modes

$$\ddot{q} = R_2 \begin{bmatrix} N_{2c}(\theta, \dot{\theta}, \omega) + B_1 u \\ -Kq + B_2 u \end{bmatrix} \tag{27}$$

where R_2 consists of last n rows of D^{-1}. Since N_{2c}, and u are known, a state variable representation of (27) is

$$\dot{z} = \begin{bmatrix} 0 & I \\ -R_{22}K & 0 \end{bmatrix} z + g(\theta, \dot{\theta}, \omega, u) \tag{28}$$

where g is easily obtained from (27), $R_2 = [R_{21} \quad R_{22}]$, and R_{22} is an $n \times n$ matrix. The associated measurement equation is linear function of q of the form

$$y_m = C_m q \tag{29}$$

where y_m=$(u_x(L),\ u_y(L),\ u_\psi(L))^T$. C_m is computed using (2)-(7). Since the system (28) is linear and the function g can be measured *on-line*, one can design an observer using linear control theory.

Define A_m as

$$A_m = \begin{bmatrix} 0 & I \\ -R_{22}K & 0 \end{bmatrix}$$

then the state observer takes the form

$$\dot{\hat{z}} = A_m\hat{z} + g(\theta, \dot{\theta}, \omega, u) + H(y_m - C_m\hat{z}) \tag{30}$$

where $\hat{z} = (\hat{q}^T, \dot{\hat{q}}^T)^T$ is the estimate of state z, and the matrix H is determined such that the matrix $(A_m - HC_m)$ is *Hurwitz*. In this study, we use the pole assignment technique to obtain feedback matrix H.

The observation error $\tilde{z} = (z - \hat{z})$ satisfies

$$\dot{\tilde{z}} = (A_m - HC_m)\tilde{z} \tag{31}$$

which is asymptotically stable and $\tilde{z}(t) \to 0$, as $t \to \infty$.

For the synthesis of the controller, q, $\dot{q}$ in control law (11), (18), and (22) are replaced by the estimated variables $\hat{q}$ and $\dot{\hat{q}}$. The complete closed-loop system is shown in Fig. 2.

6. Simulation Results

We present here the results of digital simulation. The numerical values of various matrices I_0, A_2^T, K, B_1, B_2 and C_m, and the complete expression of nonlinear function N_2 have been taken from [6]. Here we set $n = 8$. The appendix lists the maximum limits of control inputs. The mass of the antenna is $400 lbs$, and the mass of the Shuttle body is $2.050 \times 10^5 lbs$ [8].

We chose $\lambda = \mu = 0.55$ for reorientation control law and detumbling control law. For tracking, a representative command *reference attitude trajectory* is generated using filter (19) with parameters $\lambda_{ri} = 0.55$ $\zeta_{ri} = .707$, and $\omega_{nri} = \lambda_{ri}/\zeta_{ri}$. The terminal angles θ_i^* (i=1,2,3), are chosen as 15°, 14°, and 13° (roll, pitch, and yaw, respectively). Since in the practical situation, the control magnitudes are limited, we have introduced control saturation functions in digital simulation. In this study, the initial conditions are $\theta(0) = 0$, and $q(0) = \dot{q}(0) = 0$. The observer poles are

placed at $-18 \pm j1.2424$, $-18 \pm j2.1571$, $-18 \pm j4.7615$, $-18 \pm j7.4541$, $-18 \pm j12.5634$, $-18 \pm j29.9435$, $-18 \pm j34.3916$, and $-18 \pm j77.1321$. The stabilizer poles are located at $-1.2 \pm j1.6841$, $-1.2 \pm j1.8951$, $-1.2 \pm j4.8035$, $-1.2 \pm j7.4018$, $-1.2 \pm j12.4961$, $-1.2 \pm j29.9426$, $-1.2 \pm j34.3913$, and $-1.2 \pm j77.1313$, by using pole placement technique. These pole locations have been selected by trial and error and by observing the simulated response.

(a) **A Detumbling Maneuver:**

For detumbling maneuver, an exponentially decaying reference trajectory of the form $\omega_r(t) = \omega_r(0)exp(-0.5t)$ for tracking was considered. The initial conditions were $\omega(0) = (3, 2, 1)^T$ degrees/sec, and $\omega_r(0) = (5, 4.5, 4)^T$ degrees/sec. The initial conditions of the observer were $\hat{q}_i(0) = (-0.01)$ and $\dot{\hat{q}}_i(0) = 0$, *i=1,2,....,8.* Thus $\tilde{q}(0) = (0.01)$ and initial tracking error $\tilde{\omega}(0) = (-2, -4.5, -3)^T$ degrees/sec. Selected responses are shown in Fig. 3. It is interesting to observe that inspite of the control saturation and the use of only estimated states in the control law, the tracking error tends to zero in about 10 seconds. We observe that θ converges to a constant value as predicted, and elastic modes oscillations are suppressed.

(b) **A Reorientation Maneuver:**

Simulation was done to examine the reorientation maneuver capability of the controller. For this purpose, the tracking of the reference attitude trajectory, $\theta_r(t)$, terminating at $\theta^*(t) = (15°, 14°, 13°)^T$ was considered. The initial conditions were the same as described in case (a). The selected responses are shown in Fig. 4. The response of an estimated state was somewhat similar to those of case (a). Here the attitude angle response $\theta(t)$ closely followed the reference attitude trajectory $\theta_r(t)$, but

state was somewhat similar to those of case (a). Here the attitude angle response $\theta(t)$ closely followed the reference attitude trajectory $\theta_r(t)$, but due to the control limits and the state estimation error, there was a small error in θ tracking. The attitude angle θ converged to θ^* and elastic oscillation was suppressed in less than 10 seconds.

(c) **Effect of the Modal Error: The Spillover:**

Simulation was done to examine the effect of control and observation spillover by assuming that the actual dynamical model of SCOLE System has 10 elastic modes $q_i(t)$. However, the controller, designed for the lower order model having only 8 elastic modes, was retained. To include the effect of observation spillover, the measured signal $y_m(t)$ in the observer (30) was replaced by $y_m = C_{ma}q_a$, where $q_a = (q_1, q_2, ..., q_{10})^T$. Here C_{ma} is a 3×10 output matrix whereas C_m is a 3×8 matrix. The initial conditions of case (b) were retained except $\hat{q}_i(0) = (-1.1)$, *i=1,2,3,....,8*; $\omega(0) = 0$; and $q_i(0) = \dot{q} = 0$, *i=1,2,3,....,10*. Selected responses are shown in Fig. 5. We observe only a small effect of model truncation on on the controller. Stable responses were obtained. The desired orientation is attained in about 30 seconds. Bounded and convergent oscillation of the beam was observed in the simulation. These oscillatory responses are insignificant after 100 seconds. However it should be noted that the structural damping (which has been neglected in the study) will cause the dissipation of energy and eventually even these insignificantly small oscillations will vanish.

7. Conclusion

The control of slewing maneuvers of NASA SCOLE system was considered.

The design was accomplished by decomposing the slew maneuver problem from the elastic mode stabilization problem. Orbiter control system were for detumbling and reorientation maneuvers. The orbiter attitude controller was obtained by a judicious choice of reference angular velocity trajectory in the detumbling control law such that any smooth attitude trajectory can be followed. Stabilization of elastic modes was accomplished by a linear stabilizer using end body forces and moment. For the synthesis of the controller, a linear state estimater was designed using elastic deformations of the beam at the tip. Extensive simulation results showed that rotational maneuvers of the spacecraft can be performed to follow precise angular velocity or attitude trajectories and elastic modes can be stabilized using only output feedback.

8. References

1. Taylor, L. W. and Balakrishnan, A. V. (1984)
 A Laboratory Experiment Used to Evaluate Control Laws for Flexible Spacecraft...NASA/IEEE Design Challenge.
 Proceedings of the Fourth AIAA/VPI&SU Symposium on Dynamics and Control of Large structures, AIAA, New York, pp. 311-318, 1984.

2. Taylor, L. W. (ed)
 SCOLE Workshop-1986. Proceedings, NASA TM 80975, Nov. 1986;
 SCOLE Workshop-1985. Proceedings, NASA TM 89048, Dec. 1985;
 SCOLE Workshop-1984, Proceedings, Dec. 1984, NASA Langley Research Center, Hampton, VA.

3. Quinn, R. D. and Meirovitch, L. (1986)
 Maneuver and Vibration Control of SCOLE.

Proceedings of the AIAA Guidance, Navigation and Control Conference, AIAA, New York, pp. 115-129, 1986.

4. Lin, J. G. (1986)
 Rapid Torque Limited Line-of-Sight Pointing of SCOLE.
 Proceedings of the AIAA Guidance, Navigation and Control Conference, AIAA, New York, pp. 106-114, 1986.

5. Kakad, Y. P. (1986)
 Dynamics and Control of Slew Maneuver of Large, Flexible Spacecraft.
 Proceedings of the AIAA Guidance, Navigation and Control Conference, AIAA, New York, pp. 629-634, 1986.

6. Kakad, Y. P. (1987)
 Dynamics of Spacecraft Control Laboratory Experiment (SCOLE) Slew Maneuvers. NASA CR 4098, 1987.

7. Bainum, P. M. and Diarra, C. M., (1989)
 The Dynamics and Control of the orbiting Spacecraft Control Laboratory Experiment (SCOLE) During Station Keepingr.
 Journal of Astronautical Science, Vol. 37, No. 4, pp. 513-527, 1989.

8. Fisher, S. (1989)
 Application of Actuators to Control Beam Flexure in a Large Space Structure.
 Journal of Guidance, Control, and Dynamics pp. 874-879, 1989.

9. Storch, J. and Gates, S. (1985)
 Three Dimensional Motion of a Flexible Beam with Rigid Tip Bodies.
 Charles Stark Draper Laboratory Report, Inter-lab Memorandum, 1985.

10. Joshi, S. (1985)
SCOLE Equations of Motion-A New Formulation.
Proceedings of the Second Annual SCOLE Workshop, NASA TM-89048, pp. 14-25, 1985.

11. Singh, S. N. (1986)
Flexible Spacecraft Maneuver: Inverse Attitude Control and Mode Stabilization.
Acta Astronautica 13, pp. 507-514, 1986.

12. Azam, M., Singh, S. N., Iyer, A., Kakad, Y. P. (1990)
Feedback Linearization ond Control of NASA SCOLE System by Output Feedback.
Report No. *EER 90-031*, 1990.

13. Vidysagar, M. (1978)
Nonlinear System analysis.
New Jersy: Prentice-Hall, Inc; 1978

9. APPENDIX

- **CONTROL LIMITS**

 $G_0(t) = 100{,}000$ *ft-lbs* (moment applied at the orbiter mass center)

 $F_0(t) = 800$*lbs* (force applied at the orbiter mass center)

 $M_{\psi r} = 100{,}000$ *ft-lbs* (moment applied at the reflector *c.g.*)

- **CAPTIONS FOR FIGURES**

Fig. 1:
SCOLE configuration showing the three-body model, coordinate system, and actuator control points.

Fig. 2:
Block diagram of the system.

Fig. 3:
Detumbling Control Law:

(a) Attitude angles.

(b) Control moments G_0.

(c) Control forces F.

(d) Angular velocity ω.

(e) Tracking error $\tilde{\omega}$

(f) Control moment $M_{\psi r}$.

(g) Torsional deformations, u_ψ.

(h) Resultant tip deflection, $\sqrt{u_x^2 + u_y^2}$.

(i) Estimation error $\tilde{q}_1$ and $\tilde{q}_2$.

Fig. 4:
Reorientation Control Law:

(a) Attitude angles.

(b) Control moments G_0.

(c) Control forces F.

(d) Tracking error $\tilde{\theta}$.

(e) Control moment $M_{\psi r}$.

(f) Torsional deformations, u_ψ.

(g) Resultant tip deflection, $\sqrt{u_x^2 + u_y^2}$.

Fig 5.
Reorientation Control Law: Spillover:

(a) Attitude angles.

(b) Torsional deformations, u_ψ.

(c) Resultant tip deflection, $\sqrt{u_x^2 + u_y^2}$.

• FIGURES .

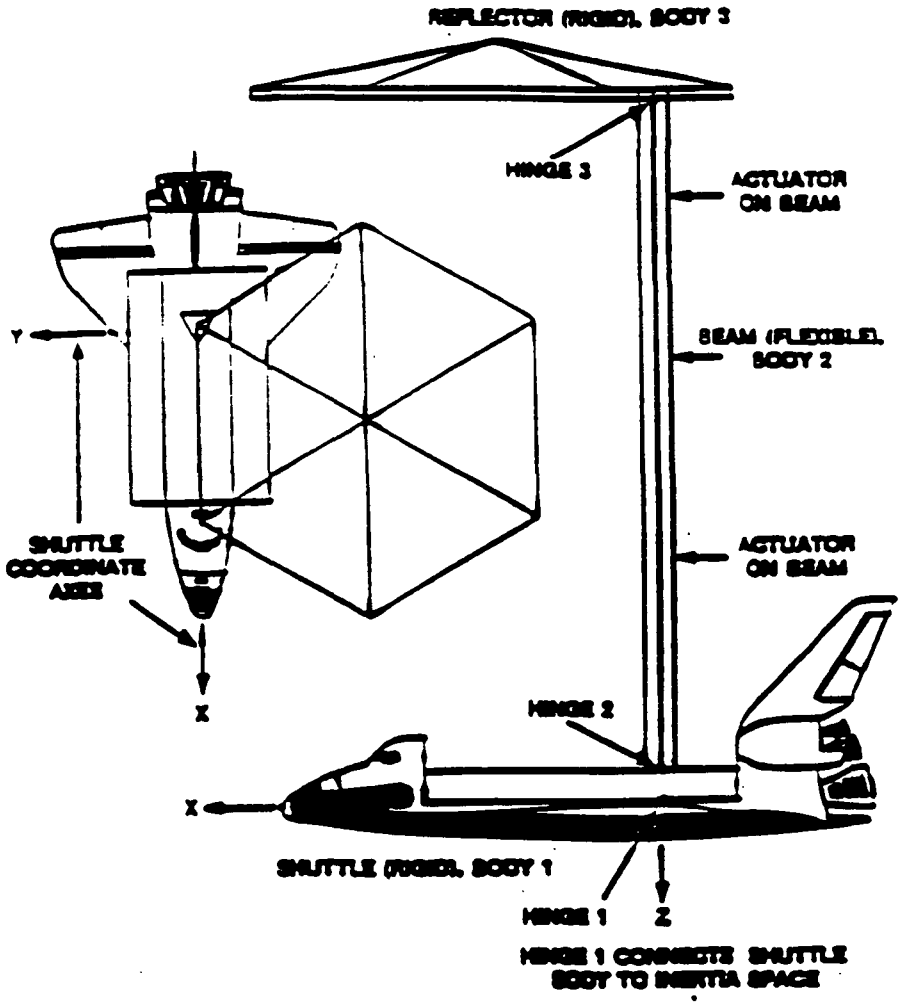


Fig. 1

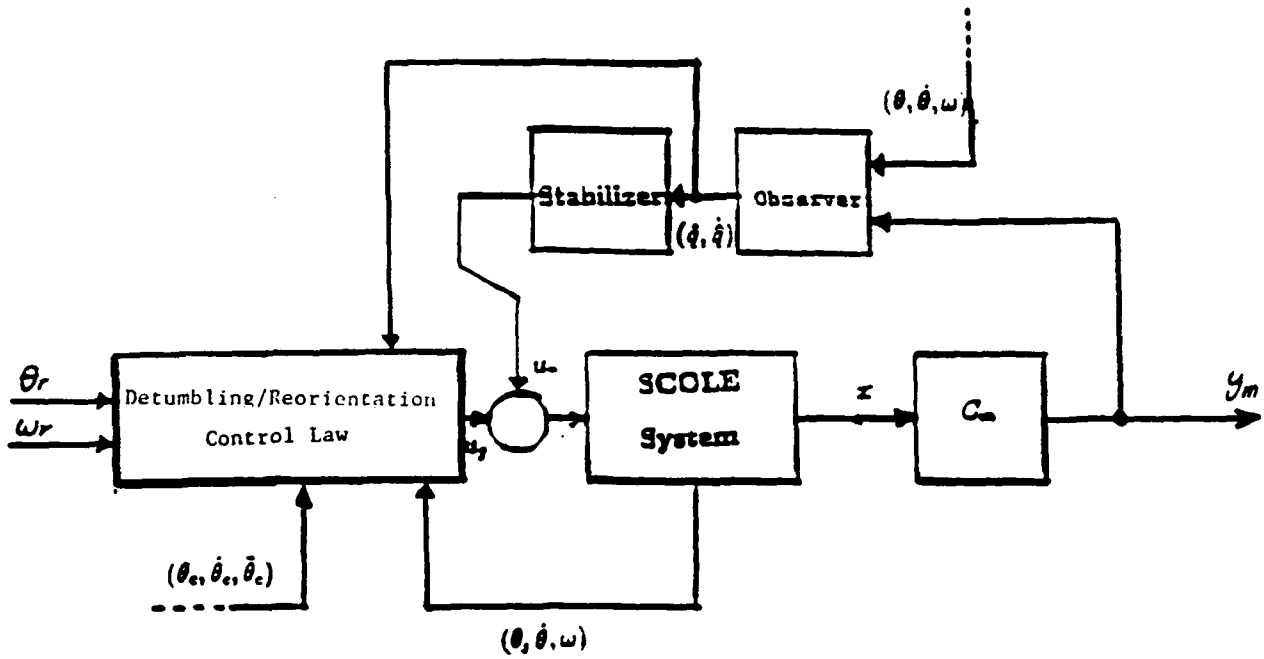

$(\theta, \dot{\theta}, \omega)$
Stabilizer
Observer
$(\hat{q}, \dot{\hat{q}})$
θ_r
ω_r
Detumbling/Reorientation
Control Law
u_c
u_g
SCOLE
System
x
C_m
y_m
$(\theta_c, \dot{\theta}_c, \ddot{\theta}_c)$
$(\theta, \dot{\theta}, \omega)$

Fig. 2

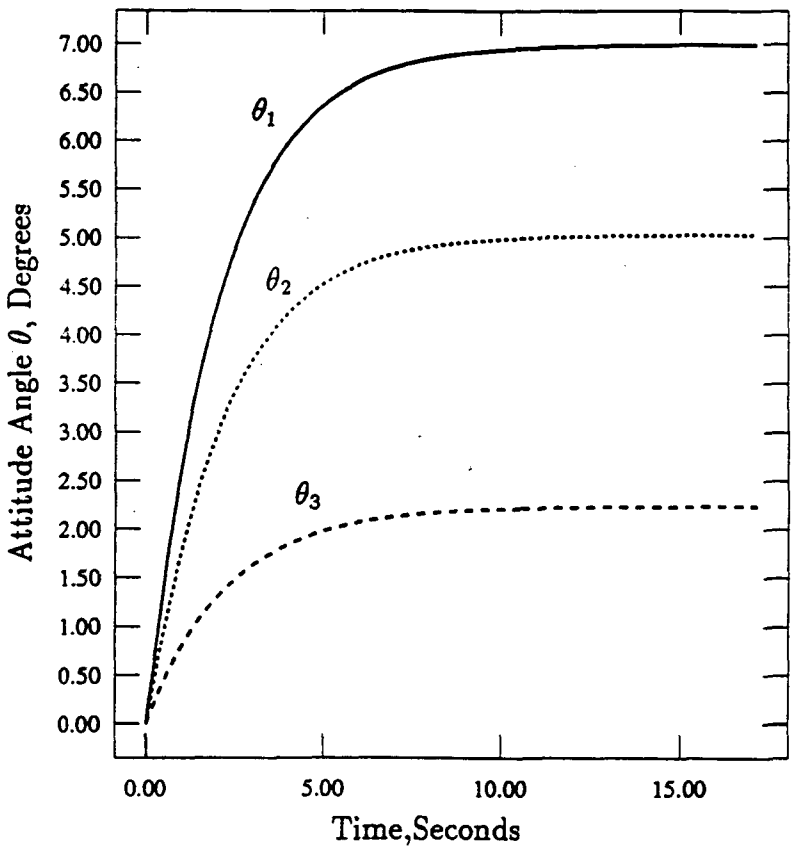

7.00
6.50
6.00
5.50
5.00
4.50
4.00
3.50
3.00
2.50
2.00
1.50
1.00
0.50
0.00
Attitude Angle θ, Degrees
θ1
θ2
θ3
0.00
5.00
10.00
15.00
Time,Seconds

Fig. 3(a)

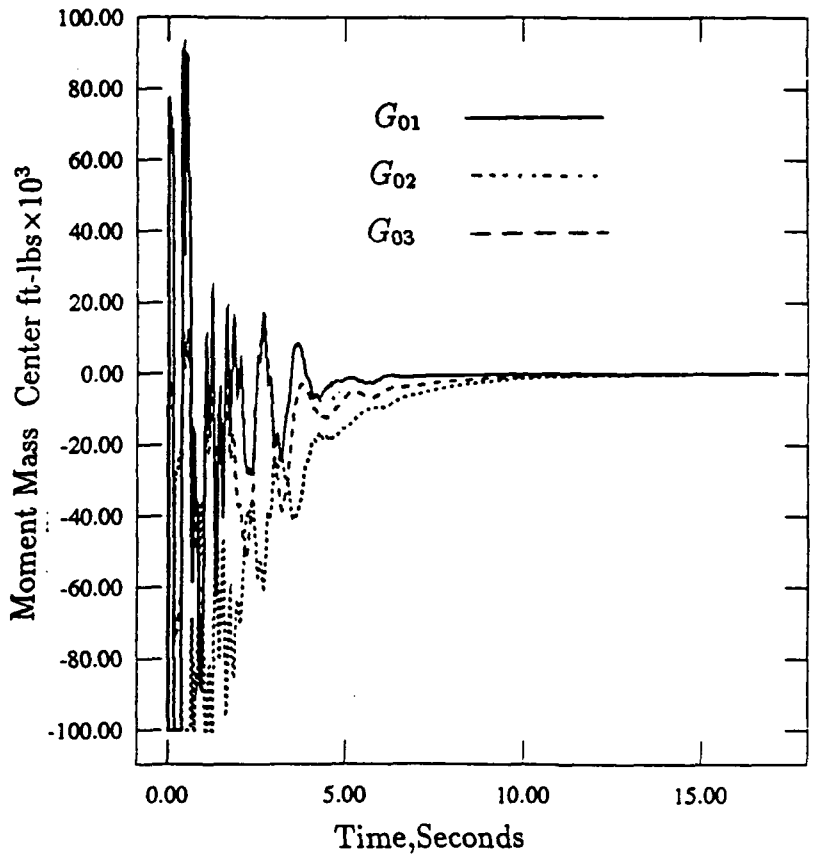

100.00
80.00
60.00
40.00
20.00
0.00
-20.00
-40.00
-60.00
-80.00
-100.00
Moment Mass Center ft-lbs×10³
G_{01}
G_{02}
G_{03}
0.00
5.00
10.00
15.00
Time,Seconds

Fig. 3(b)

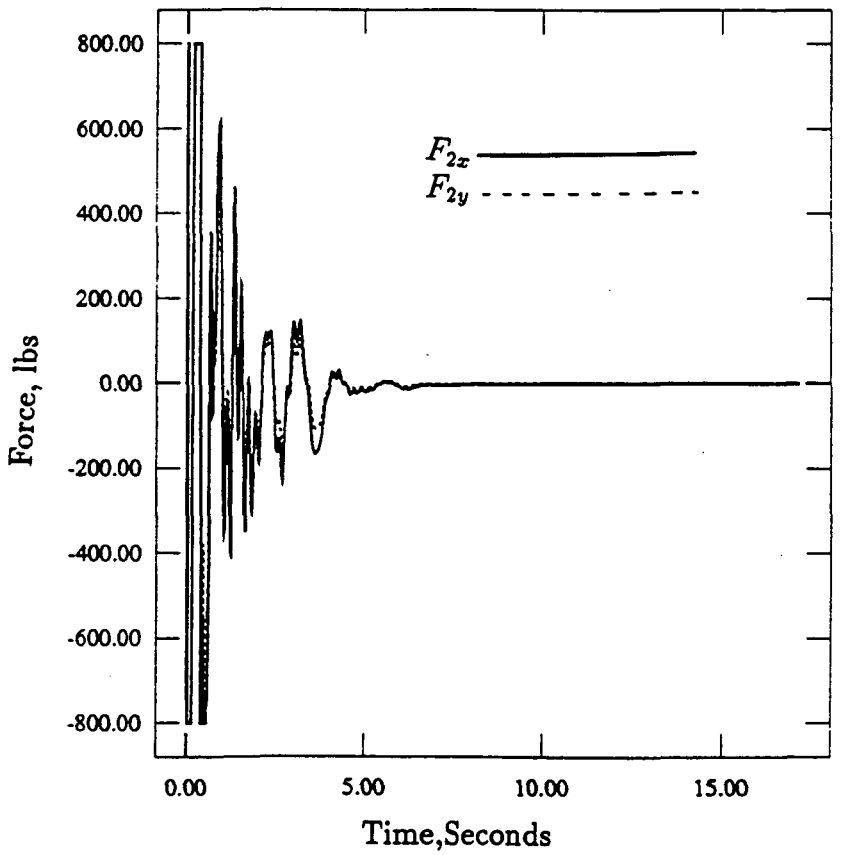

800.00
600.00
400.00
200.00
0.00
-200.00
-400.00
-600.00
-800.00
Force, lbs
F_{2x}
F_{2y}
0.00
5.00
10.00
15.00
Time,Seconds

Fig. 3(c)

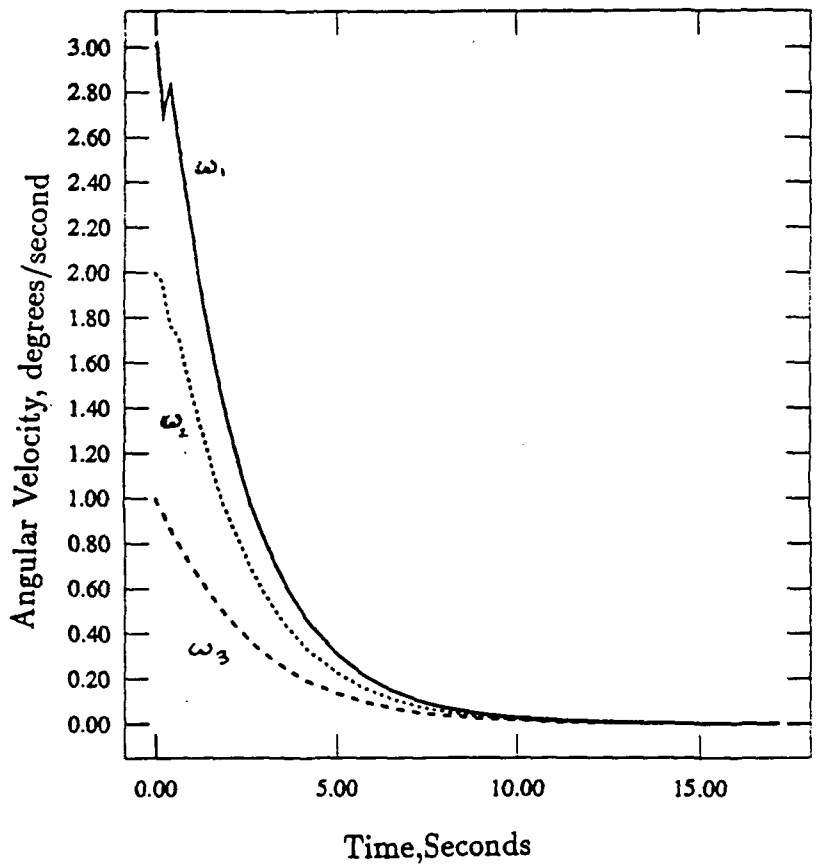

3.00
2.80
2.60
2.40
2.20
2.00
1.80
1.60
1.40
1.20
1.00
0.80
0.60
0.40
0.20
0.00
Angular Velocity, degrees/second
ω_1
ω_2
ω_3
0.00
5.00
10.00
15.00
Time,Seconds

Fig. 3(d)

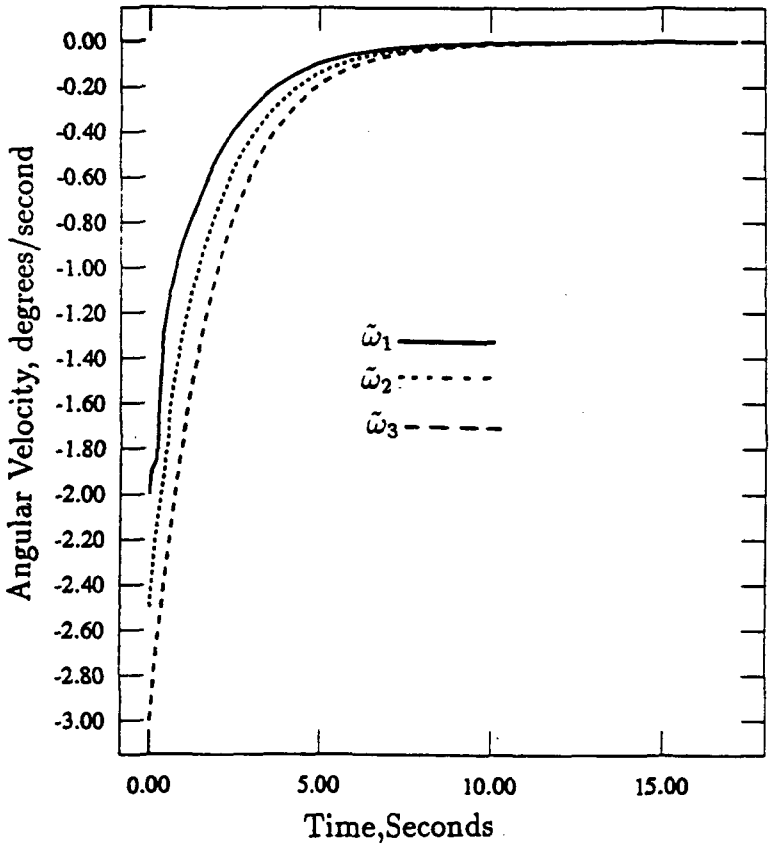

0.00
-0.20
-0.40
-0.60
-0.80
-1.00
-1.20
-1.40
-1.60
-1.80
-2.00
-2.20
-2.40
-2.60
-2.80
-3.00
Angular Velocity, degrees/second
$\tilde{\omega}_1$
$\tilde{\omega}_2$
$\tilde{\omega}_3$
0.00
5.00
10.00
15.00
Time,Seconds

Fig. 3(e)

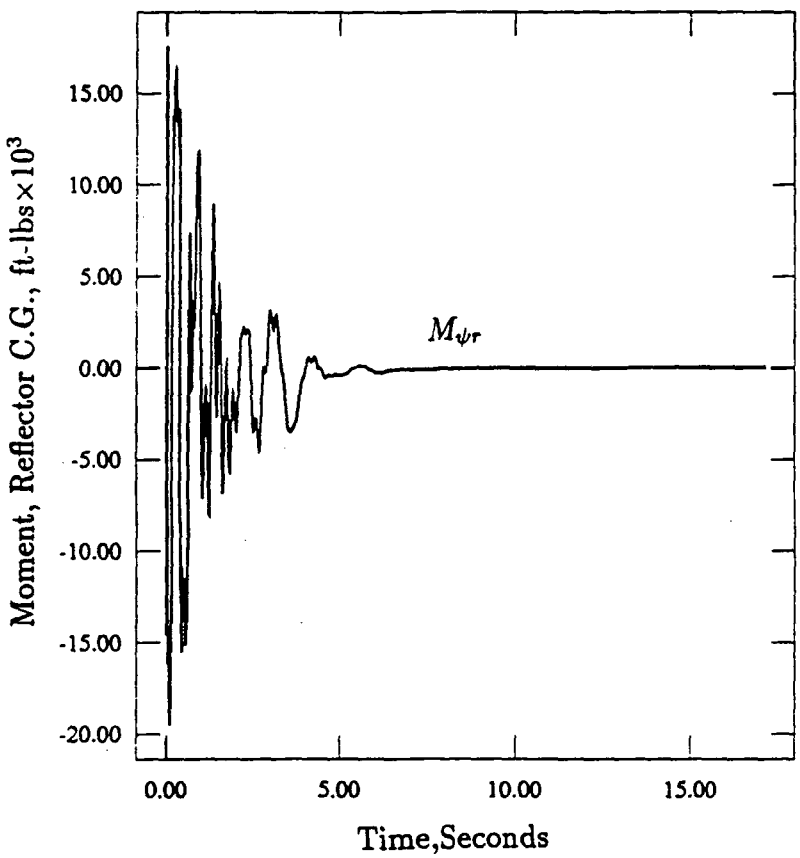

15.00
10.00
5.00
0.00
-5.00
-10.00
-15.00
-20.00
Moment, Reflector C.G., ft-lbs×10³
$M_{\psi r}$
0.00
5.00
10.00
15.00
Time,Seconds

Fig. 3(f)

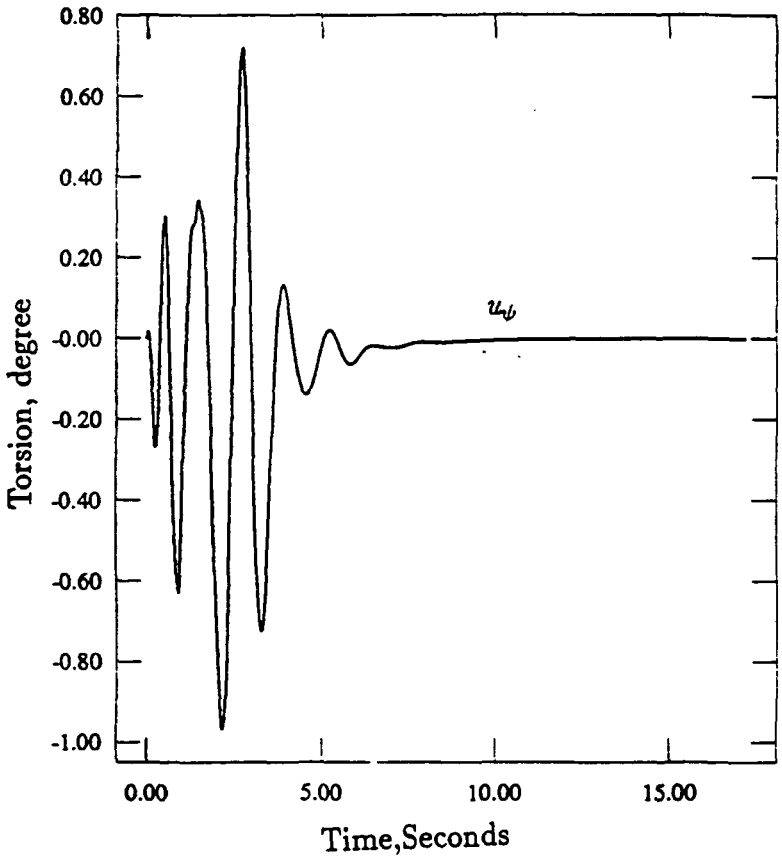

0.80
0.60
0.40
0.20
-0.00
-0.20
-0.40
-0.60
-0.80
-1.00
Torsion, degree
u_ψ
0.00
5.00
10.00
15.00
Time,Seconds

Fig. 3(g)

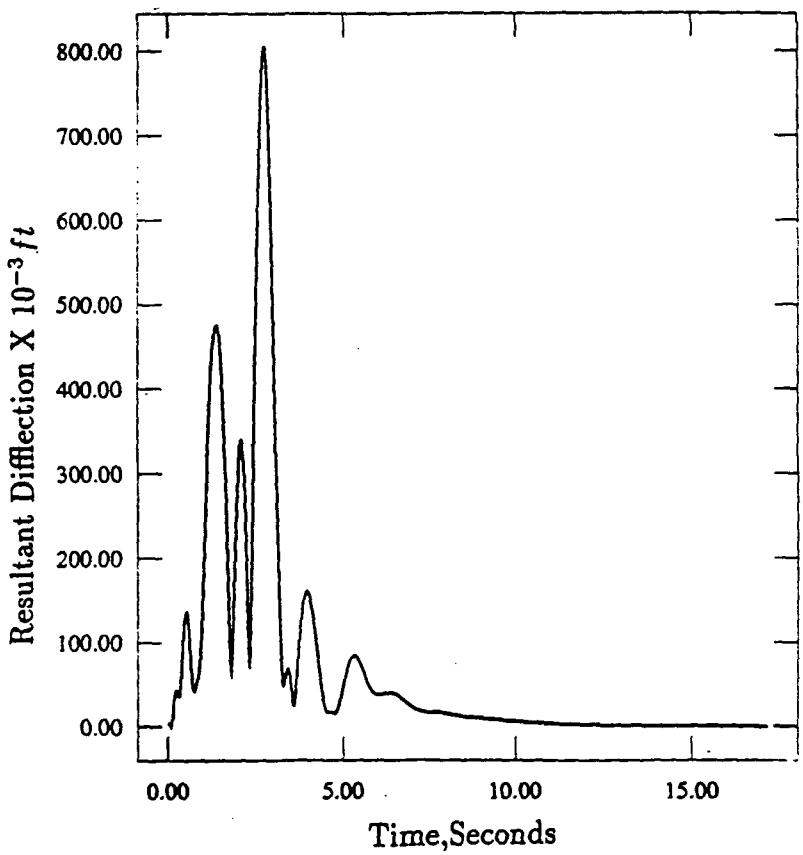

800.00
700.00
600.00
500.00
400.00
300.00
200.00
100.00
0.00
Resultant Diffection X 10^{-3} ft
0.00
5.00
10.00
15.00
Time,Seconds

Fig. 3(h)

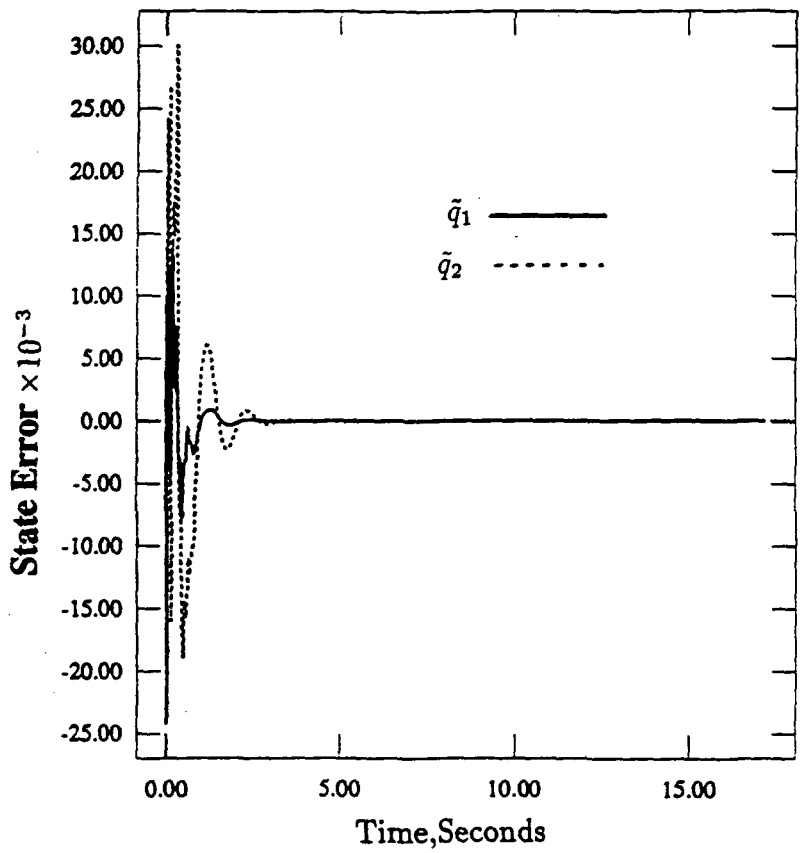

30.00
25.00
20.00
15.00
10.00
5.00
0.00
-5.00
-10.00
-15.00
-20.00
-25.00
State Error $\times 10^{-3}$
$\tilde{q}_1$
$\tilde{q}_2$
0.00
5.00
10.00
15.00
Time,Seconds

Fig. 3(i)

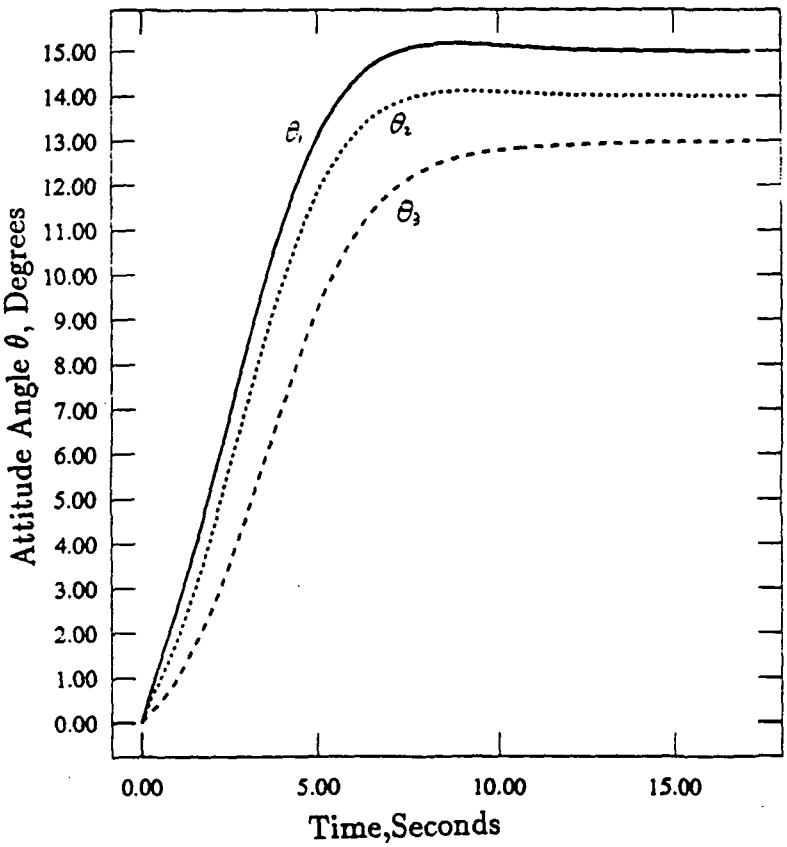

15.00
14.00
13.00
12.00
11.00
10.00
9.00
8.00
7.00
6.00
5.00
4.00
3.00
2.00
1.00
0.00
Attitude Angle θ, Degrees
θ1
θ2
θ3
0.00
5.00
10.00
15.00
Time,Seconds

Fig. 4(a)

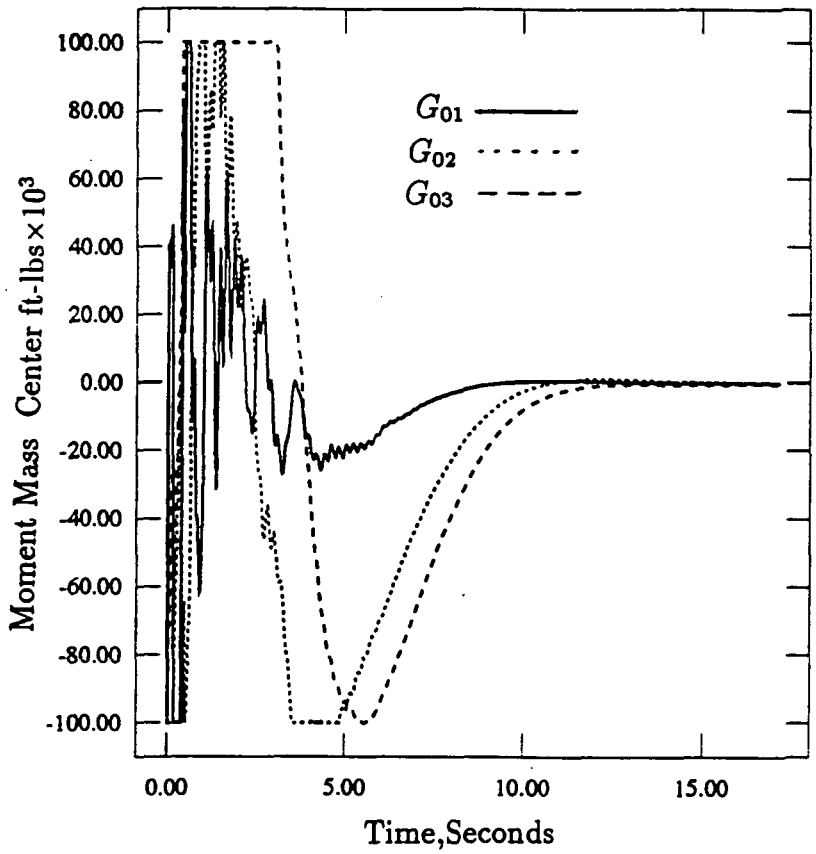

100.00
80.00
60.00
40.00
20.00
0.00
-20.00
-40.00
-60.00
-80.00
-100.00
Moment Mass Center ft-lbs×10³
G_{01}
G_{02}
G_{03}
0.00
5.00
10.00
15.00
Time,Seconds

Fig. 4(b)

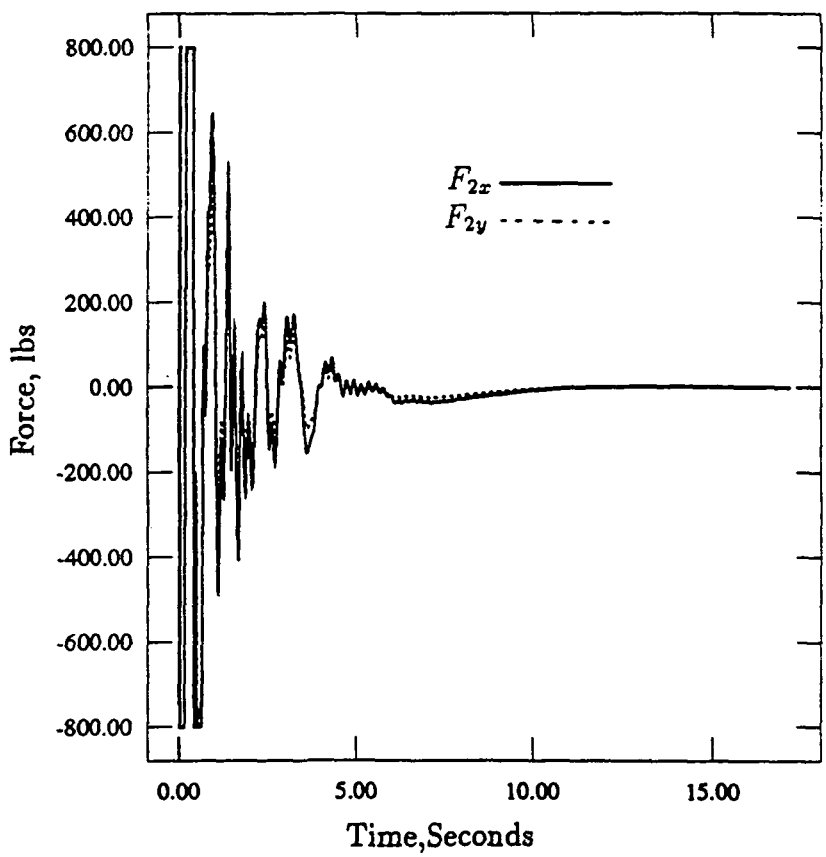

800.00
600.00
400.00
200.00
0.00
-200.00
-400.00
-600.00
-800.00
Force, lbs
F_{2x}
F_{2y}
0.00
5.00
10.00
15.00
Time,Seconds

Fig. 4(c)

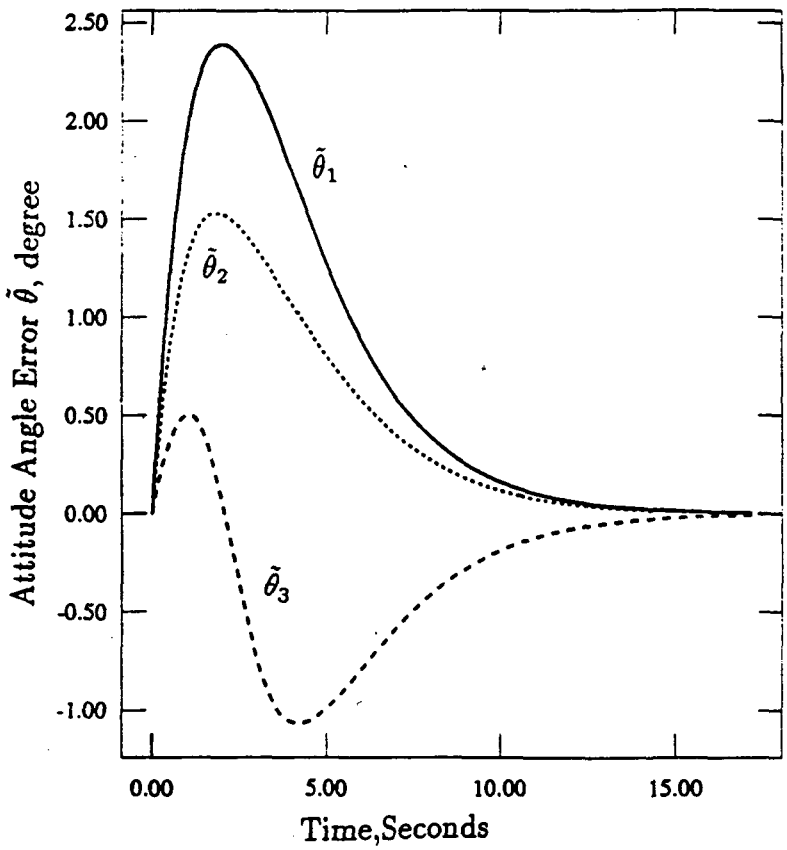

2.50
2.00
1.50
1.00
0.50
0.00
-0.50
-1.00
Attitude Angle Error $\tilde{\theta}$, degree
$\tilde{\theta}_1$
$\tilde{\theta}_2$
$\tilde{\theta}_3$
0.00
5.00
10.00
15.00
Time,Seconds

Fig. 4(d)

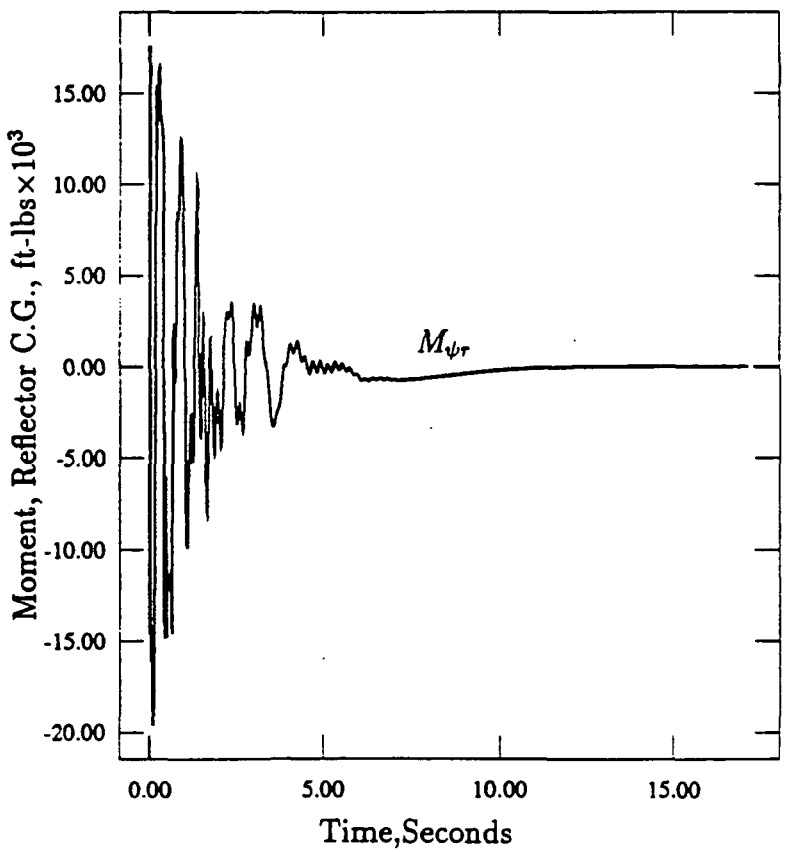

15.00
10.00
5.00
0.00
-5.00
-10.00
-15.00
-20.00
Moment, Reflector C.G., ft-lbs×10³
$M_{\psi r}$
0.00
5.00
10.00
15.00
Time,Seconds

Fig. 4(e)

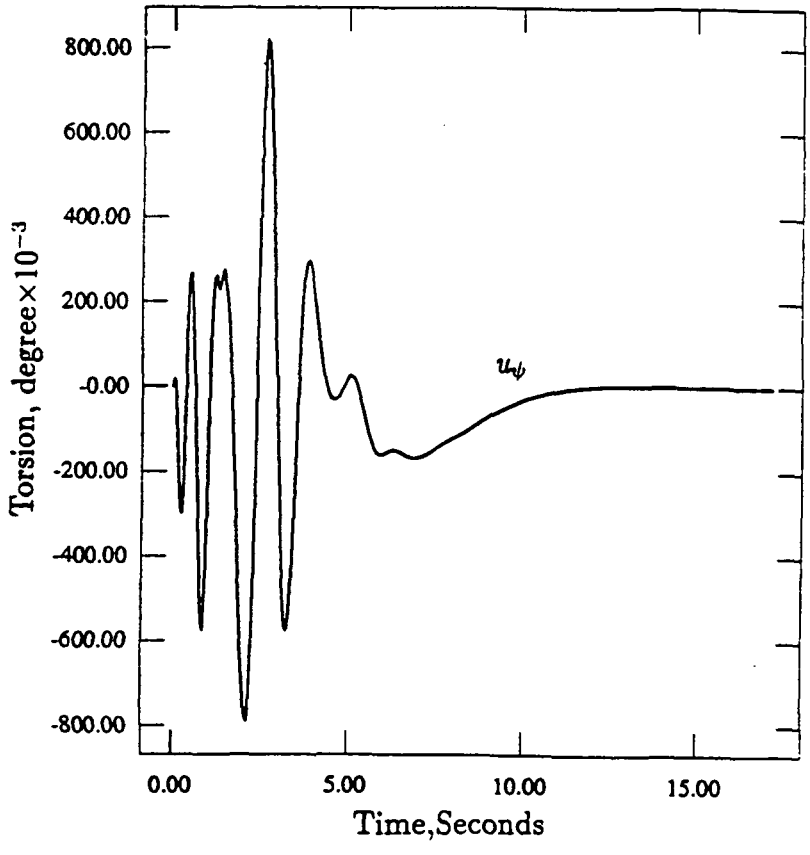

800.00
600.00
400.00
200.00
-0.00
-200.00
-400.00
-600.00
-800.00
Torsion, degree×10⁻³
0.00
5.00
10.00
15.00
Time,Seconds
u_ψ

Fig. 4(f)

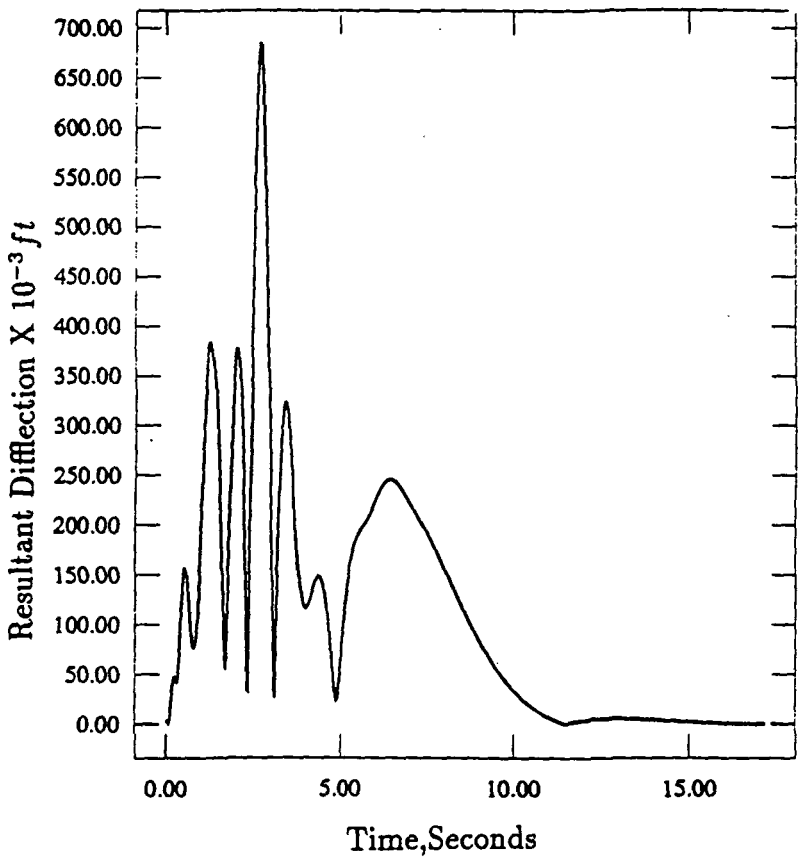

700.00
650.00
600.00
550.00
500.00
450.00
400.00
350.00
300.00
250.00
200.00
150.00
100.00
50.00
0.00
Resultant Diffection X 10^{-3} ft
0.00
5.00
10.00
15.00
Time,Seconds

Fig. 4(g)

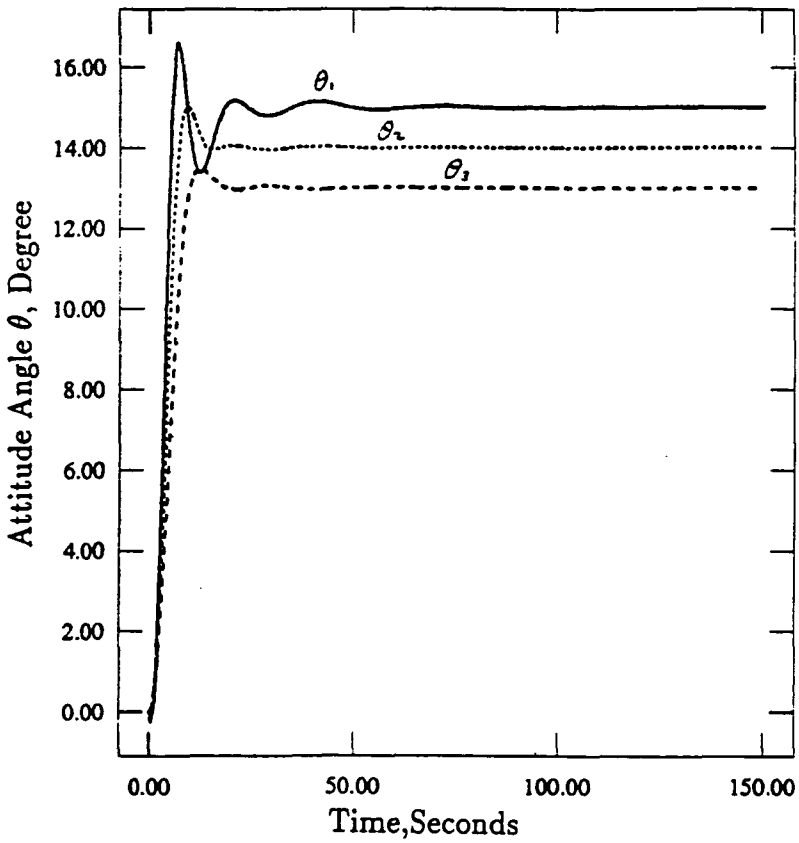

16.00
14.00
12.00
10.00
8.00
6.00
4.00
2.00
0.00
Attitude Angle θ, Degree
θ1
θ2
θ3
0.00
50.00
100.00
150.00
Time,Seconds

Fig. 5(a)

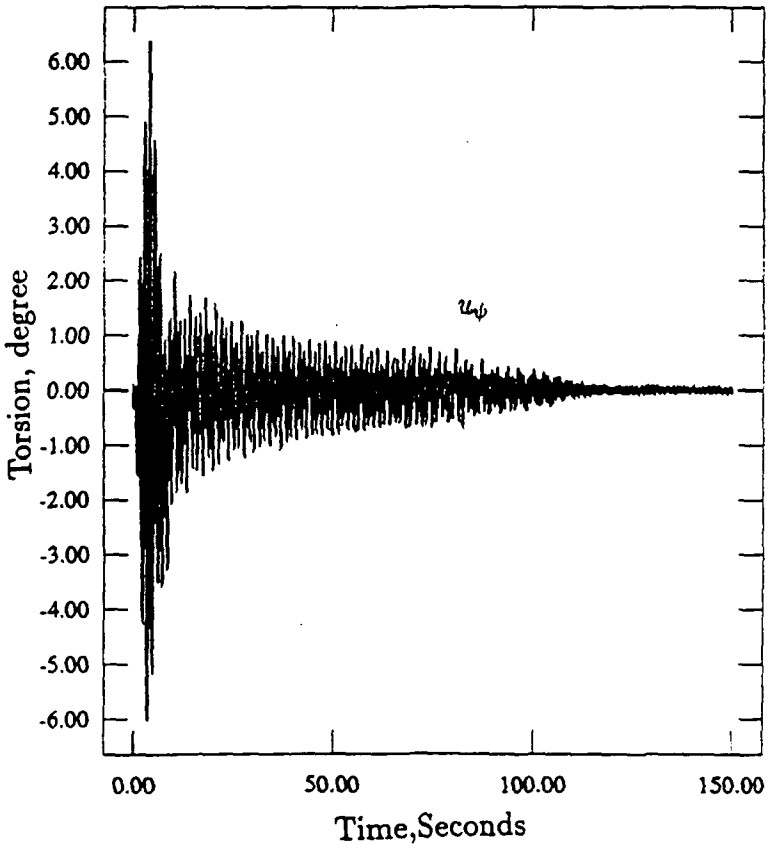

6.00
5.00
4.00
3.00
2.00
1.00
0.00
-1.00
-2.00
-3.00
-4.00
-5.00
-6.00
Torsion, degree
0.00
50.00
100.00
150.00
Time,Seconds

Fig. 5(b)

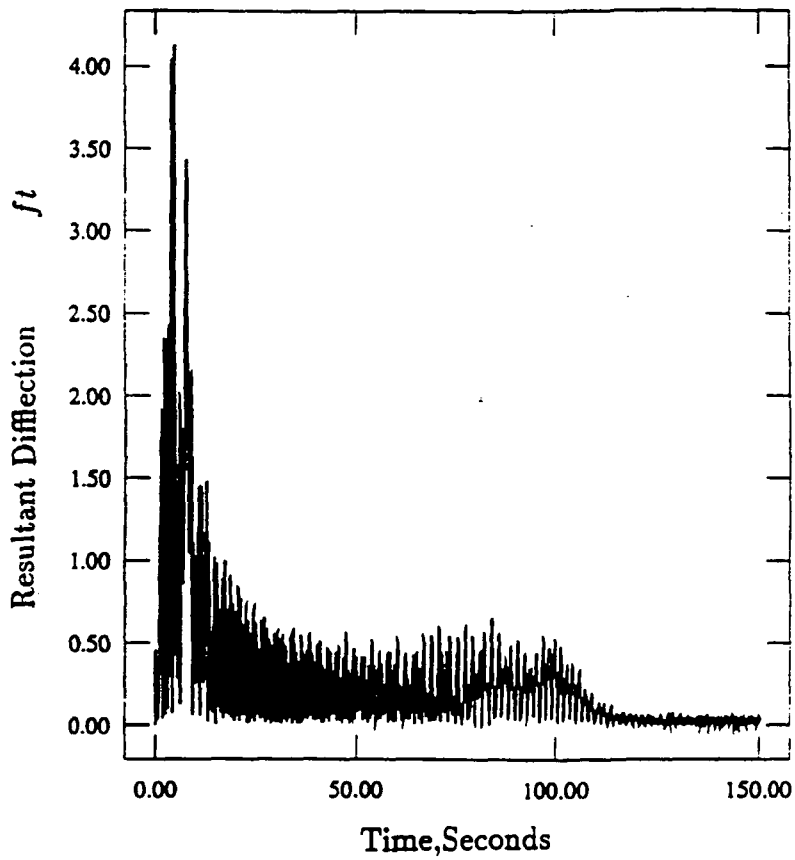

Resultant Diffection ft
4.00
3.50
3.00
2.50
2.00
1.50
1.00
0.50
0.00
0.00
50.00
100.00
150.00
Time,Seconds

Fig. 5(c)